Estrogen signaling interacts with Sirt1 in adipocyte autophagy

By

Zhipeng Tao

Dissertation submitted to the faculty of the Virginia Polytechnic Institute and State University

in partial fulfillment of the requirements for the degree of

DOCTOR OF PHILOSOPHY

In

Human Nutrition, Foods, and Exercise

Zhiyong Cheng (chair)

Dongmin Liu (co-chair)

Benjamin Corl

Young Ju

May 03, 2019

Blacksburg, Virginia

Keywords: ERα, Sirt1, adipogenesis, obesity, autophagy, gender difference, mTOR, ULK1, white adipose tissue

Estrogen signaling interacts with Sirt1 in adipocyte autophagy

Zhipeng Tao

ABSTRACT

ACADEMIC ABSTRACT

Obesity is a rapidly growing epidemic. It is associated with preventable chronic disease and vast healthcare cost in the United States (about 200 billion per year). Therefore, dissecting pathogenic mechanisms of obesity would provide effective strategies to prevent its development and reduce related cost. Obesity is characterized by excessive expansion of white adipose tissue (WAT). Autophagy, a cellular self-digestive process, is associated with WAT expansion and may be a promising target for combating obesity. Both hormone signaling (e.g., ERα) and energy sensing factors (e.g., Sirt1) control metabolism and prevent adiposity, and in which they have been shown to play collaborate roles. However, how autophagy is involved in ERα and Sirt1's inhibitory roles on adiposity is unknown. These questions have been addressed in my dissertation studies.

To address this fundamental questions, I have established a method to monitor autophagy flux during adipocyte differentiation, which better reflected the dynamic process of autophagy. Compared with preadipocytes, autophagy flux activity was increased in mature adipocytes after differentiation. And then, my thesis project has addressed three main questions.

Firstly, the gender difference in visceral fat distribution (Males have higher deposit of visceral fat than females) is controlled by an estradiol (E2)-autophagy axis. In C57BL/6J and wild type control mice, a higher visceral fat mass was detected in the males than in the females, which was associated with lower expression of estrogen receptor α (ERα) and more active autophagy in

males vs. females. ERα knockout normalized this difference. Mechanistically, E2-ERα- mTOR-ULK1-autophagy signaling contributed to the gender difference in visceral fat distribution.

Secondly, *in vitro* and *in vivo* studies demonstrated that Sirt1 suppressed autophagy and reduced adipogenesis and adiposity via inducing mTOR-ULK1 signaling. Specific activation and overexpression of Sirt1 induced mTOR-ULK1 signaling to suppress autophagy and adipogenesis. And knockdown of Sirt1 exhibited opposite effects. The first and second studies revealed that ERα and Sirt1 acted on mTOR-ULK1 signaling pathway, underlying the importance of their interaction in inhibiting autophagy and adipogenesis.

As such, the third study was conducted and it unraveled that ERα acted as upstream of Sirt1, possibly through its direct binding to Sirt1 promoter. Specifically, E2 signaling suppressed autophagy and adipogenesis. But when Sirt1 was knockdown, the effects of E2 on autophagy and adipogenesis were abolished.

Taken together, my dissertation project underscores the importance for future research to consider gender difference and how E2-ERα-autophagy axis contributes to this difference in other metabolic diseases. Also, the unraveled interaction between ERα and Sirt1 might lead to new therapeutic approach to adiposity and metabolic dysfunction in post-menopausal women or individuals with abnormal estrogen secretion. For example, dietary intervention or exercise challenge to activate Sirt1 may partially compensate estrogen deficiency.

PUBLIC ABSTRACT

Obesity is a rapidly growing epidemic, which is associated with chronic disease and vast healthcare cost in the United States. Understanding the pathogenic mechanism of obesity is of critical importance. Recent studies have implicated autophagy, a cellular self-digestive process, in WAT development and expansion. It was also shown that hormone (e.g., via estrogen receptor ERα) and energy (e.g., via Sirt1) signaling control metabolism and adiposity. However, it is unclear whether and how autophagy interacts with ERα and Sirt1 in the regulation of adiposity. My dissertation project unraveled the mechanism of how hormone signaling (e.g., ERα) and energy sensing factors (e.g., Sirt1) interacted with autophagy to control adipogenesis and adiposity.

My thesis project has addressed three main questions. Firstly, the gender difference in visceral fat distribution (Males have higher deposit of visceral fat than females) is controlled by an estradiol (E2)-autophagy axis, ERα knockout normalized this difference. Mechanistically, E2-ERα- mTOR-ULK1-autophagy signaling contributed to the gender difference in visceral fat distribution. Secondly, *in vitro* and *in vivo* studies demonstrated that Sirt1 induced mTOR-ULK1 signaling, suppressed autophagy and reduced adipogenesis and adiposity (ERα similar effects). As such, the third study was conducted and it unraveled that ERα acted as upstream of Sirt1, possibly through its direct binding to Sirt1 promoter.

Taken together, my dissertation study has explored how hormone signaling (ERα) and energy signaling (Sirt1) interact with autophagy to control adipogenesis and adiposity individually and collaboratively, which may provide new therapeutical approach to control obesity.

ACKNOWLEDGEMENTS

As the end of my student life approaches closely, I am so thankful for the grace and support from people in life, including my teachers, friends and family members. Without any of them, finishing my PhD program wouldn't be possible. I owe all of my accomplishment to all of you and could not be more grateful for your support.

First, my greatest thanks would go to my advisor, Dr. Zhiyong Cheng. His patient guidance guides me step by step to scientific research. Also, he cares about my life and gives abundant of encouragement during my life.

Then, I would like to thank Louise Zheng for her help with experiments in the lab. Also, she offered me greatly spiritual encouragement when I am in the valley of my life.

I also want to thank my lab mates, including Longhua Liu, Sarah Donnelly, Cayleen Smith, Joseph Brooke, Alex Robinson. Without help of them, I cannot accomplish all of my research work. And we enjoyed happy time in the lab.

I am greatly thankful for all of my other committee members, including Dr. Corl, Dr. Liu and Dr. Ju. They support me a lot during my scientific journey here. They always lead me to think and grow as a future scientist.

I want to thank Ms. Michele Lewis for every grace she had on me during my work as her TA. Her spirit as a teacher encourages me to know how to become a teacher.

I want to thank all members in Liu lab, including Wei Zhen, Dr. Wang, Yao Wang and Jing Luo. They are generous to lend experimental reagent to me when I need.

I want to thank my Family members, my father and mother for their support all these years. And I want to thank my brothers and sisters, Xiuping for all of their support during my hard time.

At last, I want to thank god for leading me in this way and put all these people in my life. And I want to thank him for all of his grace on me and cast the real truth on me.

ATTRIBUTIONS

In this dissertation, each listed author has contributed to the chapters extensively. And all authors have responsibilities for all of the published data and contents.

In chapter 3, Zhipeng Tao and Longhua Liu conducted the experiments and were both involved in designing the study, collecting and analyzing data, writing and revising manuscript. Zhiyong Cheng was engaged in designing study, analyzing data, preparing and polishing manuscript. Louise Zheng conducted experiments, went through and polished the manuscript. All authors went through and approved the final version of manuscript.

In chapter 4, Zhipeng Tao and Louise D. Zheng conducted the experiments and were both involved in designing study, collecting and analyzing data, and preparing manuscript. Zhiyong Cheng and Dongmin Liu conducted study design, data analysis and manuscript preparation. Cayleen Smith, Jing Luo and Alex Robinson conducted experiments. Fabio A. Almeida, Zongwei Wang and Aria F. Olumi polished the manuscript. All authors went through and agreed to publish the manuscript.

In chapter 5, Zhipeng Tao conducted the experiments and designed study, collected and analyzed data, and wrote this chapter. Louise D. Zheng helped with animal breeding. Zhiyong Cheng conducted study design, participated in data analysis and polished the writing. This chapter has not been published.

Table of Contents

LIST OF ABBREVIATIONS

A

AD: Alzheimer disease

Akt: protein kinase B

ALT: Alanine aminotransferase

AMPK: AMP-activated protein kinase

AS: Atherosclerosis

Atg5: autophagy related 5

Atg7: autophagy related 7

Atg12: autophagy related 12

B

BAT: brown adipose tissue

BDL: bile duct ligation

BDNF: brain-derived neurotrophic factor

BL: bafilomycin-A1 and leupeptin

BMI: body mass index

C

CCI: cortical impact

CMs: cardiomyocytes

CREB: cAMP response binding protein

CQ: chloroquine

CVDs: cardiovascular diseases

D

DI: differentiation induction

DOX: doxorubicin

E

E2: estradiol

4E-BP1: eIF4E-binding protein 1

ER: endoplasmic reticulum

ERα: estrogen receptor α

ERβ: estrogen receptor β

ERR: estrogen-related receptors

ESCC: esophageal squamous cell carcinoma

EX527: 6-Chloro-2,3,4,9-tetrahydro-1H-Carbazole-1-carboxamide

F

FBPase: fructose-1,6-bisphosphatase

FBS: fetal bovine serum

FoxO1: forkhead box O transcription factor 1

FoxOs: forkhead box O transcription factors

G

G6pase: glucose-6-phosphatase

GAPDH: glyceraldehyde 3-phosphate dehydrogenase

GBM: glioblastoma

GD: glucose deprivation

GFP: green fluorescent protein

GTT: glucose tolerance test

H

HCAECs: human coronary and iliac artery endothelial cells

HTT: huntingtin protein

I

IL-1β: interleukin 1 beta

IL-6: interleukin 6

ITT: insulin tolerance test

J

JNK1: C-Jun N-terminal kinase 1

L

LC3: microtubule-associated protein 1A/1B-light chain 3-phosphatidylethanolamine conjugate

M

MAPK: mitogen-activated protein kinase

3-MA: 3-methyladenine

MCD: methionine/choline-deficient

MeCP2: methyl-CpG binding protein 2

Mef2: myocyte enhancer factor 2

mESCs: murine embryonic stem cells

mTOR: mammalian target of rapamycin

mTORC1: mammalian target of rapamycin complex 1

mTORC2: mammalian target of rapamycin complex 2

N

NAD: Nicotinamide adenine dinucleotide

NAFLD: non-alcoholic fatty liver disease

NAM: nicotinamide

NASH: non-alcoholic steatohepatitis

NCoR: nuclear receptor co-repressor

NF-κB: inflammatory nuclear factor-κB

NSCLC: non-small-cell lung cancer

O

OPCs: oligodendrocyte progenitor cells

P

p62: sequestosome 1 (SQSTM1)

PC: preconditioning

PE: phenylephrine

Pepck: phosphoenolpyruvate carboxykinase

PGC-1α: peroxisome proliferator-activated receptor gamma coactivator 1-alpha

PPARα: peroxisome proliferator-activated receptor alpha

PPARγ: peroxisome proliferator-activated receptor gamma

Prdm16: PR domain containing 16

PRKA: Serine/threonine protein kinase

PTCs: primary renal proximal tubular cells

R

ROCK1: serine/threonine Rho kinase

RSV: resveratrol

S

S6K1: p70 S6 kinase

shRNA: small hairpin RNA.

siRNA: Small (or short) interfering RNA

Sirts: sirtuins

Sir2: silent information regulator 2

Sirt1: Sirtuin 1

SMRT: silencing mediator of retinoid and thyroid hormone receptors

STAT3: signal transducer and activator of transcription 3

SVF: stromal vascular fraction

sWAT: subcutaneous white adipose tissue

T

T2DM: type 2 diabetes mellitus

TBARS: thiobarbituric acid reactive substances

TBI: traumatic brain injury

T-ALL: T-cell acute lymphoblastic leukemia

TFEB: transcription factor EB

TG: triglyceride

TLR4: toll-like receptor 4

TNFα: tumor necrosis factor alpha

TSA: trichostatin A

U

UCP1: uncoupling protein 1

ULK: Unc-51-like kinase

V

vWAT: visceral white adipose tissue

W

WAT: white adipose tissue

Chapter 1 Literature Review

Resveratrol in autophagy – a "tale" of Sirt1 activator

Abstract

Resveratrol (RSV) is a natural polyphenol and abundant in foods such as grapes, berries, peanuts and other dietary plants. It has shown preventive effects on various metabolic diseases, including obesity, type 2 diabetes, cardiovascular disease and cancer. RSV may also improve immune defense, aging and neurological disease. Mounting evidence suggests that RSV exerts the beneficial effects through regulating autophagy, a conserved cellular degradative pathway to break down and recycle dysfunctional macromolecules and organelles. This review discusses the molecular targets and signaling pathways by which RSV regulates autophagy to improve health or potentially treat diseases.

1. Introduction

Sirt1 is widely involved in metabolic diseases, including liver diseases (Zhang et al., 2015), kidney diseases (Kitada & Koya, 2013), aging and neurodegenerative disease (Rubinsztein et al., 2011). Therefore, abundant numbers of Sirt1 activator have been developed to modulate Sirt1 activity, thus preventing or treating metabolic diseases (Kumar & Chauhan, 2016). In this literature review, the most commonly used and discussed Sirt1 activator resveratrol will be reviewed.

Resveratrol (3,5,4′-trihydroxystilbene) is a natural polyphenol. It has attracted vast attention since 1992, when it was postulated to explain the "French paradox" effect, i.e., red wine consumption reducing the incidence of coronary artery disease (Frankel, German, Kinsella, Parks, & Kanner, 1993). Resveratrol (RSV) is primarily found in grapes, berries, peanuts and some other dietary plants, as well as associated processed foods (**Figure 1**) (Marques, Markus, & Morris, 2009). The content of RSV in these foods may vary during storage or processing procedures (Cheng, Schmelz, Liu, & Hulver, 2014), and the beneficial effects of RSV have been reported on obesity (Szkudelska & Szkudelski, 2010), immune defense (Falchetti, Fuggetta, Lanzilli, Tricarico, & Ravagnan, 2001), cardiovascular disease, type 2 diabetes, neurological disease, and cancer (Markus & Morris, 2008; Yu et al., 2012). RSV can mimic caloric restriction to improve metabolism and it also acts as an antioxidant, anti-inflammatory, anti-cell proliferation, or anti-invasive agent (Markus & Morris, 2008; Yu et al., 2012). At the cellular level, RSV may regulate autophagy, apoptosis, and cell cycle arrest (Yu et al., 2012). This review will focus on RSV regulating autophagy in health and diseases.

The term "autophagy" is derived from the Latin words "αὐτόφαγος" or "autóphagos", where "auto" refers to "oneself" and "phagy" is "to eat". Autophagy involves physiological pathways

that deliver intracellular components to the lysosome for degradation (Singh & Cuervo, 2011). There are three forms of autophagy, i.e., chaperone-mediated autophagy, microautophagy and macroautophagy (Levine & Kroemer, 2008). RSV has been implicated mainly in the regulation of macroautophagy (hereafter as autophagy). Figure 2 shows the major steps of autophagy, including induction, nucleation, expansion, fusion and cargo degradation (Tanida, 2011). Initial processes include vesicle nucleation and vesicle elongation of an isolation membrane, which is referred to as phagophore. Then, the edges of the phagophore fuse (vesicle completion) to develop a double membrane vesicle (or autophagosome) to sequester the cellular materials such as misfolded proteins and dysfunctional mitochondria (Tanida, 2011). Autophagosome fuses with lysosomal compartment to form an autolysosome where the dysfunctional molecules and organelles are degraded (**Figure 2**) (Levine & Kroemer, 2008; Singh & Cuervo, 2011). Thus, autophagy is critical for cellular remodeling and organelle quality control (Levine & Kroemer, 2008). During nutrients and energy deprivation, autophagy can degrade cellular components and provide nutrients to fuel basic cell function (Levine & Kroemer, 2008). However, autophagy may be induced during adipogenesis (Goldman et al., 2010), and under some pathogenic stimuli such as oxidative stress, infection, and protein aggregate accumulation (Levine & Kroemer, 2008). To this end, targeting dysregulated autophagy may lead to new therapeutics for the related diseases (Aggarwal et al., 2004; Levine, Mizushima, & Virgin, 2011; Rubinsztein, Mariño, & Kroemer, 2011; Konings et al., 2014; Ma et al., 2016).

Among the targets identified for RSV in the regulation of autophagy, Sirtuin1 (Sirt1) (a mammalian homolog of Sir2 (silent information regulator 2)) is an NAD-dependent deacetylase, which was previously found to mimic caloric restriction in aging and neurodegenerative disease (Rubinsztein et al., 2011), as well as liver (Zhang et al., 2015) and kidney diseases (Kitada &

Koya, 2013). In addition, AMPK (adenosine monophosphate-activated protein kinase) (Kitada & Koya, 2013; Zhang et al., 2015), FoxOs (forkhead box O transcription factors) (Ni, Du, You, & Ding, 2013), and mTOR (mammalian target of rapamycin) (Lang et al., 2015) are targets of RSV in response to various cellular states. RSV mediated autophagy has been shown to regulate cell apoptosis (Hsu et al., 2009), inflammatory nuclear factor-κB (NF-κB) signaling (Feng et al., 2016), and oxidative stress (Miki et al., 2012). As such, RSV has been examined, as an autophagy regulator, to combat obesity (Konings et al., 2014), diabetes (Ma et al., 2016), cancer (Aggarwal et al., 2004), immune dysfunction (Levine, Mizushima, & Virgin, 2011), aging and neurodegenerative disease (Rubinsztein, Mariño, & Kroemer, 2011). In the following sections, I will discuss mechanisms and pathways by which RSV regulates autophagy and the potential to prevent or treat diseases.

2. RSV slows down aging via autophagy

Accompanied by a decline in the health condition, aging will lead to increase in the incidence and mortality of multiple organ diseases, such as neurodegenerative disease, cancer and cardiovascular disease (Haigis & Sinclair, 2010). As has been widely discussed, caloric restriction exhibits anti-aging effect and prolongs life span in various organisms and even delays disease onset (Colman et al., 2009). One of the machineries favored by caloric restriction is autophagy, which is vital for maintaining the healthy status of organisms (Pallauf & Rimbach, 2013). In nematode *Caenorhabditis elegans* insulin signaling pathway negatively regulates life span, among which autophagy showed absolute necessity in life-span extension (Meléndez et al., 2003). In contrast, suppression of autophagy shortened lifespan in the fruit fly *Drosophila melanogaster* (Bjedov et al., 2010). In older organisms, autophagy activity decreased (Del Roso et al., 2003), mainly because autophagy related (Atg) proteins or those indispensable molecules

for autophagy induction, such as Sirt1, have decreased their protein expressions in aged cells or tissues and that reduced autophagy has been associated with accelerated aging (Rubinsztein, Mariño, & Kroemer, 2011). There is an increasing interest in stimulation of autophagy to promote anti-aging effects, including genetic manipulation or pharmacological activation of autophagy to mimic nutrient starvation or caloric restriction (Madeo, Tavernarakis, & Kroemer, 2010; Petrovski & Das, 2010).

RSV is widely used as an anti-aging agent (Eugenia Morselli et al., 2010). In nematodes with autophagy-proficiency, RSV induces autophagy and extends lifespan through indirect activation Sirt1, whose effect can be abolished by knockdown or pharmacological inhibition of Sirt1 (E Morselli et al., 2010). In cultured granulosa cell complex and oocytes from aged cows' early antral follicles, RSV increased Sirt1 protein expression and promoted autophagy, as demonstrated by increased Beclin-1 and LC3-II levels and decreased p62 (a protein is selectively degraded by autophagy). Through this, RSV improved cell growth and upregulated mitochondria biogenesis and degradation (**Figure 3**) (Sugiyama et al., 2015). The promoted effect of RSV on autophagy was abolished by co-treatment with Sirt1 inhibitor EX527, suggesting RSV's role on autophagy is Sirt1 dependent (Sugiyama et al., 2015). Dependent on the Sirt1-AMPK signaling pathway, RSV exhibited neuroprotective role in rat with spinal cord injury, which is a devastating condition of aging related neurodegenerative disease (Zhao et al., 2017). Furthermore, activation of Sirt1's deacetylase activity by RSV was required for autophagy induction in human cells, *Saccharomyces cerevisiae,* and *C. elegans* (Mariño et al., 2011). At the level of acetylproteome, RSV provoked decrease in the acetylation of 560 lysine-containing motifs from 375 specific proteins, among which 170 proteins overlap with recently identified entire human autophagy protein network (Mariño et al., 2011).

The role of RSV on aging via autophagy has been confirmed by specific knockdown of essential autophagy proteins. In nematodes, silencing Beclin-1, which is an essential autophagic modulator, abrogated RSV's beneficial effect on longevity (E Morselli et al., 2010). In addition, deletion of Beclin-1/Atg6 prevented the induction of autophagy by RSV's activation of Sirt1 (E Morselli et al., 2010).

3. RSV protects heart health via autophagy

Cardiovascular diseases (CVDs) contribute to crucial morbidity and mortality in the developed countries, including the United States (Murray & Lopez, 1997). Therefore, it is urgent to develop preventive measures to lower the incidence of heart issues. Autophagy plays a vital role in myocardium, among which it is active in basal cells to maintain contractile function of heart. In ischaemia-reperfusion (IR) injury, autophagy plays a protective role in myocardium and cardiac cells (Gurusamy et al., 2009). Any fault or mutation of autophagic machinery gives rise to cardiac dysfunction that ultimately leads to heart failure (Fu, 2015). It is presumably believed that the cardioprotection effects of RSV is not because of its direct action on the diseased heart, rather, it potentiates a preconditioning (PC)-like effect, a state-of-the art for cardioprotection (Petrovski, Gurusamy, & Das, 2011).

After hypoxia-reoxygenation or ischaemia-reperfusion of H9c2 cardiac myoblast cell, RSV (0.1 μM and 1.0 μM) induced cardiac autophagy (Gurusamy et al., 2009). Involving the activation of mTORC2 pathway, RSV induced autophagy, which was correlated with improved cell survival and mitigated apoptosis (**Figure 4**). Likewise, RSV and gama-tocotrienol acted synergistically to induce autophagy, providing greater cardioprotection effects through the activation of Akt-Bec-2 pathway (Lekli et al., 2010). In left coronary artery ligation mice, high dosage (50 mg/kg/day for 2 weeks) but not low dose (5 mg/kg/day) of RSV ameliorated left ventricular dilation and

significantly improved cardiac function with augmentation of autophagy, which is dependent on activating AMPK (**Figure 4**) (Kanamori et al., 2013). However, how RSV regulates autophagy to combat doxorubicin (DOX, a powerful antibiotic generally used in clinical cancer chemotherapy)-induced damage to hearts of mice is controversial. On one hand, study showed that RSV (5.0 μM or 50.0 μM) or caloric restriction could induce autophagy to combat DOX-induced damage to hearts of mice, as shown by the protein expression levels of Atg5, p62 and LC3-II/LC3I ratio (Dutta, Xu, Dirain, & Leeuwenburgh, 2014). On the other hand, Xu et al showed that RSV (> 15.0 μM) inhibited DOX-induced autophagy to reduce cardiomyocyte cell death (Xu, Chen, Kobayashi, Timm, & Liang, 2012). As to the opposite effects of RSV on DOX-induced autophagy, the measurement of autophagy maybe problematic. For autophagy activity measurement, the autophagy related proteins expression at a given time point does not reflect the flux of autophagy, and may cause misinterpretation of autophagy activity. Therefore, it is important to block the degradation of autophagic vacuoles, leading to a time-dependent accumulation of autophagosomes in the cells or tissues to measure autophagic flux (Chen-Scarabelli et al., 2014).

To confirm the role of RSV in heart improvement via induction of autophagy, specific autophagy inhibitor and silencing autophagy gene treatments have been applied. In H9c2 cardiac myoblast cell, the beneficial effects of RSV on improved cell survival and mitigated apoptosis were significantly attenuated by autophagy inhibitors, wortmannin and 3-methyladenine (3-MA, an inhibitor of autophagy's early steps) (Gurusamy et al., 2009). Similarly, chloroquine (CQ, an autophagy inhibitor) elicited opposite effects as RSV, including exacerbation of cardiac remodeling associated with inhibition of autophagy (Kanamori et al., 2013). However, the

inhibitory effect of RSV on DOX-induced autophagy was abolished by Beclin-1 overexpression (Xu, Chen, Kobayashi, Timm, & Liang, 2012).

4. RSV reduces adiposity through autophagy

Obesity, a rapidly growing epidemic (Liu et al., 2015), originates from an imbalance between energy intake and energy expenditure. In humans and other mammals, obesity is characterized by excessive accumulation of white adipose tissue (WAT) mass, which functions as a major energy reservoir to store redundant energy in the form of triglyceride (TG) (Zhang et al., 2009). In obese persons, assays of protein and mRNA levels of essential autophagy genes indicated that autophagy significantly enhanced compared with their lean counterpart and is positively related with degree of obesity (Kovsan et al., 2010). In cellular and mice models, specific deletion of an essential protein (Atg5) for autophagy abolished adipogenesis and developed less subcutaneous mature adipocytes (Baerga, Zhang, Chen, Goldman, & Jin, 2009). In mice adipose tissue, deletion of autophagy gene Atg7 improved metabolism, leading to a leanness phenotype and protection from diet-induced obesity (Zhang et al., 2009; Singh et al., 2009).

Further, in obese men study 30 days of RSV supplementation (150 mg per day) increased adipogenesis and prominently reduced the percentage of large adipocytes, resulting in contractible mean adipocyte size and improved insulin sensitivity (Konings et al., 2014). Microarray analysis revealed that RSV administration induced signaling of lysosomal/phagosomal pathway and transcription factor EB (TFEB), suggesting an alternative approach of lipid droplets breakdown by autophagy (**Figure 5**) (Konings et al., 2014). TFEB is an essential regulator of autophagy and subjects lysosomal biogenesis to autophagy (Liu et al., 2016; Settembre & Ballabio, 2011). During adipocyte differentiation, TFEB expression was simultaneously increased with autophagic activity (Liu et al., 2016). Autophagy has implicated

in lipid droplets breakdown, which may explain the decreased adipocyte size by RSV (Singh et al., 2009). However, previous *in vitro* study on 3T3L1 preadipocytes indicated that RSV (12.5 μM to 50.0 μM) gradually decreased adipogenesis and lipid accumulation (Rayalam, Yang, Ambati, Della-Fera, & Baile, 2008). In differentiated 3T3L1 mature adipocytes, (0 μM to 100.0 μM) RSV dose-dependently reduced lipid accumulation, which is dependent on Sirt1 (Picard et al., 2004). However, opposite effect was observed in differentiating cells when the concentrations of RSV were 1.0 μM and 10.0 μM, RSV increased adipogenic marker PPARγ expression and lipid accumulation (Hu, Zhao, & Chen, 2015). All these discrepancies might be explained by differences of the dosage, duration and stages of differentiation of RSV treatment. Further studies regarding how RSV regulates adipose autophagy at different dosage, duration and stages of differentiation should be done to validate the effects of autophagy on adipose differentiation *in vitro* and *in vivo*.

Functionally and morphologically distinct from white adipose tissue, brown adipose tissue (BAT) is characterized by dense mitochondrial, innervation, and vascular content, which is responsible for non-shivering thermogenesis, dissipating energy as heat (Qiang et al., 2012). Promoting BAT function is considered as a promising therapeutic approach to combat obesity (Farmer, 2009). The anti-obesity effect of RSV partially contributes to its induction of browning of white adipose tissue (Wang et al., 2015).

On high fat diet induced obesity, RSV administration reduced body weight and fat percentage in C57BL/6J wild-type and AMPKα2−/− mice, but not in AMPKα1−/− mice. However, resveratrol failed to increase insulin sensitivity, glucose tolerance, mitochondrial biogenesis, and physical endurance in either AMPKα1 or -α2 knockout mice, suggesting the vital role of AMPK for the metabolic effects of RSV (Um et al., 2010). Likewise, In 5-month old CD1 female mice with

HFD challenge, 0.1% RSV supplementation induced beige adipogenesis in vivo, which is characterized by induced beiging of white adipocytes, increased UCP1 expression and increased fatty acid oxidation, as well as elevated AMPK phosphrylation (Wang et al., 2015). In differentiated iWAT stromal vascular cells, RSV induced brown-like adipocyte formation as shown by overexpression of brown adipocyte markers, such as UCP1, Prdm16, PGC1α, cytochrome c and etc. (Wang et al., 2015). This phenomenon is absent in stromal vascular cells with AMPKα1 defects and AMPKα1 knockout mice (Wang et al., 2017), demonstrating that AMPKα1 is a critical mediator of RSV action. AMPK induces autophagy by phophorylation of Ulk1 to activate its activity (Accili & Arden, 2004). Therefore, future studies regarding how resveratrol regulates autophagy in obesity through AMPK-Ulk1 cascade is of great value.

5. RSV regulates liver health through autophagy

Over the years, extensive investigations of hepatic autophagy indicated that autophagy machinery is not only important for maintaining liver homeostasis in physiologically normal conditions, but also for response to pathological state, such as metabolic dysregulation, infection, proteotoxicity, and even carcinogenesis. Dysfunction of autophagy has been implicated in the pathogenesis of several liver diseases, such as non-alcoholic fatty liver disease (NAFLD), non-alcoholic steatohepatitis (NASH), viral hepatitis, liver cancer and *etc.* (**Figure 6**) (Schneider & Cuervo, 2014). In NAFLD, hepatic steatosis was accompanied by decreased autophagy (Zhang et al., 2015). NASH could primarily progress into chronic liver disease and result in liver cirrhosis, fibrosis and eventually hepatocellular carcinoma, which were accompanied by decreased autophagy (Ji, Wang, Deng, Li, & Jiang, 2015). Previous study showed that acute ethanol consumption is advantageous to liver health, which ascribed to its induction of autophagy to reduce ethanol-induced liver injury (Ni, Du, You, & Ding, 2013). All of these

evidence suggests that pharmaceutical manipulation of autophagy might possess vast therapeutic meaning in liver diseases.

RSV has the competence to alleviate NAFLD, in which autophagy plays a protective role against NAFLD development (Zhang et al., 2015). In hepatocytes, RSV induced autophagy to ameliorate hepatic steatosis. Moreover, RSV increased the expression of Sirt1 in hepatocytes, as well as in HepG2 cells (Zhang et al., 2015). Incubation with Sirt1 inhibitor EX-527 or Sirt1 siRNA abrogated RSV-mediated autophagy. The *in vivo* study in mice with hepatic steatosis obtained parallel results (Zhang et al., 2015). In addition, RSV's role in NAFLD partially contributed to its action on the deacetylation activity of Sirt1 (**Figure 6**) (Colak et al., 2014). In methionine/choline-deficient (MCD) diet induced NASH animal model or medium-induced hepatic steatosis cell model, the phenotype of elevated levels of triglyceride (TG), inflammatory factors TNF-α (tumor necrosis factor alpha), IL-1β (interleukin 1 beta), IL-6 (interleukin 6), ALT (Alanine aminotransferase) and TBARS (thiobarbituric acid reactive substances) was ameliorated by RSV administration and accompanied by uplifted expressions of autophagy proteins, both *in vitro* and *in vivo* (Ji, Wang, Deng, Li, & Jiang, 2015). As to the beneficial effect of ethanol on liver, in cultured primary mouse hepatocytes and in liver ethanol significantly increased both mRNA and protein levels of many autophagy-related molecules (Ni, Du, You, & Ding, 2013). At the same time, ethanol increased the nuclear translocation of FoxO3a and its target gene's expression. These effects were diminished by overexpression of a dominant negative form of FoxO3a, indicating FoxO3a's positive role in regulating ethanol-induced autophagy and cell survival (Ni, Du, You, & Ding, 2013). RSV, acting as Sirt1 agonist, further promoted ethanol-induced autophagy-related genes expressions through Sirt1's deacetylation of FoxO3a to increase its nuclear translocation (**Figure 6**) (Ni, Du, You, & Ding, 2013). GRX is an

activated hepatic stellate cells model and widely used to study development and resolution of liver fibrosis. RSV (1.0-50.0 μM) treatment promoted cell death signals of GRX, along with improved mitochondrial dynamics and function. Accompanied with this, RSV treatment promoted autophagy/mitophagy, indicating that the cytotoxic effect of RSV on GRX maybe due to the simultaneous induction of apoptosis, autophagy/mitophagy and mitochondrial biogenesis in GRX (Martins et al., 2015). Mitochondria have reported to be involved in cholestatic liver injury. In a rat model of cholestasis developed by bile duct ligation (BDL) surgery, RSV administration upregulated LC3-II levels, and reversed the decline in mitochondrial DNA copy number and downregulated Caspase 3 expression. In addition, RSV significantly decreased the numbers of apoptotic liver cells, indicating that early RSV treatment reverses impaired liver function, which maybe partially through autophagy (Lin et al., 2012).

To confirm the protective role of RSV on liver health via autophagy, pharmaceutical inhibition of autophagy proteins or genetic knockdown of autophagy genes has been done. In hepatocytes, the protective role of RSV on hepatic steatosis was abolished by 3-MA (Zhang et al., 2015). Similarly, CQ significantly mitigated RSV's protection against liver injury and inflammation, suggesting the indispensable role of autophagy through which RSV mitigated hepatic steatosis and inflammation in MCD-induced NASH (Ji, Wang, Deng, Li, & Jiang, 2015). *In vivo*, in wild-type and autophagic mediator ULK1 (mammalian autophagy-initiating kinase 1) heterozygous knockout mice, 8 weeks high-fat diet induced NAFLD. RSV (50 mg/kg daily for 4 weeks) ameliorated all measured features of NAFLD in wild-type mice such as hepatic histology, fibrosis, oxidative status, inflammation. However, in ULK1 heterozygous knockout mice the ameliorative effects were abrogated, indicating that the effects of RSV on NAFLD-caused hepatic injury improvement partially relies on regulating autophagic pathway (Li et al., 2014).

6. RSV regulates kidney health via autophagy

In kidney, plentiful studies suggest the vital role of autophagy in organ maintenance, diseases and aging. Hypoxia, ischemic, toxic, immunological, and oxidative insults would affect autophagy in renal epithelial cells to regulate the course of various kidney diseases (Huber et al., 2012). In aged kidney, caloric restriction induced mitochondrial autophagy was essential for cell survival under hypoxia (Kume et al., 2010). Therefore, elucidating the essential role of autophagy in kidney physiology and diseases propose unique strategies to kidney disease prevention and treatment.

RSV has protective effects against age-related or other types of renal diseases, including sepsis-related injury, drug-induced injury, diabetic nephropathy, ischemia-reperfusion injury, aldosterone-induced injury, and unilateral ureteral obstruction through its activation of Sirt1 (Kitada & Koya, 2013). In those renal diseases, Sirt1 regulates several cellular events, including mitochondrial biogenesis, glucose/lipid metabolism, inflammation, apoptosis, autophagy, and adaptations to cellular stress, via its deacetylation of target proteins (Kitada & Koya, 2013). In aged kidney, long-term caloric restriction increased Sirt1 protein expression and attenuated mitochondrial and renal damage by hypoxia, which was regulated by Sirt1-mediated forkhead box O3 (Foxo3) deacetylation and it was vital for Bnip3 expression and for subsequent regulation of autophagy in primary renal proximal tubular cells (PTCs) (**Figure 7**). However, caloric restriction could not induce autophagy and followed improvement of damaged mitochondria in the kidneys of aged $Sirt1^{-/-}$ mice, highlighting the crucial role of Sirt1-FoxO3 cascade in cellular response to hypoxia (Kume et al., 2010).

7. RSV regulates inflammation through autophagy

Autophagy signaling pathway is committed to the operations of immunity and inflammation. They equilibrate the advantageous and disadvantageous aspects of immunity and inflammation, and therefore would protect organisms against infectious, autoimmune and inflammatory diseases (Levine, Mizushima, & Virgin, 2011). The NLRP3 inflammasome is a caspase-1-containing multi-protein complex, which regulates inflammatory cytokine IL-1 secretion and promotes development of inflammatory disease (Wu et al., 2016), which was activated by autophagy and subsequent IL-1β secretion (Wu et al., 2016). Atherosclerosis (AS), an inflammatory disease characterized by overexpression of the adhesion molecules, begins with inflammatory changes in the endothelium in which inflammation centrally participates in all stages of pathogenesis (Chen et al., 2013). Autophagy has implicated its protective role during AS development (Liao et al., 2012). Otherwise, autophagy is involved in pathophysiological responses following inflammatory diseases, such as Traumatic brain injury (TBI), which is an extremely complicated type of neurological trauma and involved a series of inflammatory response. In mechanism, this injury would profoundly activate autophagy subsequent neuroinflammatory signaling that induces dramatic neuronal damage and behavioral impairment, in which Toll-like receptor 4 (TLR4) acts as a vital administrator of this cascade (Feng et al., 2016). RSV has been proposed to regulate or collaborate multiple inflammation and immunity related molecular targets (Švajger & Jeras, 2012), among which autophagy's role will be reviewed.

In murine macrophage cell line J774A, RSV induced autophagy by activating p38 to inhibit NLRP3 inflammasome-derived IL-1 secretion (**Figure 8**) (Chang et al., 2015). In peritoneal inflammatory injury of peritoneal mesothelial cells (PMCs), NLRP3 activation leads to IL-1β

secretion, which was promoted by Beclin-1 and Atg5 siRNAs interference or autophagy inhibitor 3-MA treatment. Furthermore, Beclin-1 and Atg5 knockdown sensitized cells to IL-Iβ release induced by NLRP3 inflammasome activator. To the contrary, RSV treatment attenuated these effects by induction of mitophagy and autophagy dependent on AMPK activation (Wu et al., 2016). In AS development, RSV attenuated endothelial inflammation characterized by reduction of tumor necrosis factor α (TNF/TNFα)-induced inflammation, and increased autophagy in a concentration-dependent manner (**Figure 8**). Mechanistically, the promotive effects of RSV on autophagy were dependent on cAMP, PRKA (Serine/threonine protein kinase), AMPK and Sirt1 (Chen et al., 2013). In adult male Sprague Dawley rats subjected to cortical impact (CCI) injury, RSV administration significantly diminished brain edema, motor deficit, and neuronal loss, and ameliorated spatial cognitive function. RSV decreased Beclin-1 and LC3 expressions and significantly decreased the number of TLR4-positive neuron-specific nuclear protein (NeuN) cells following TBI (Feng et al., 2016). Furthermore, RSV treatment reduced the levels of TLR4 and its downstream signaling molecules, including nuclear factor-κB (NF-κB), IL-1β and TNF-α (**Figure 8**) (Feng et al., 2016), potentiating a role of autophagy in RSV's protective effects in TBI.

The role of RSV in mediating inflammation via autophagy was confirmed by autophagy inhibitor co-treatment with RSV. The inhibition effect of RSV on NLRP3 inflammasome-derived IL-1 secretion in macrophages was abolished by an autophagy inhibitor 3-MA *in vitro* and *in vivo* (Chang et al., 2015). In AS development, autophagy inhibitors 3-MA and CQ treatments as well as silencing Atg5 and Beclin-1 significantly mitigated RSV-induced autophagy, which subsequently reversed RSV-induced downregulation of inflammatory factors (Chen et al., 2013).

8. RSV regulates cancer biology via autophagy

Autophagy plays bifacial roles in cancer, either as guardian or as executioner, depending on the stage of cancer initiation and progression, or surrounding cellular environment (**Figure 9**) (S.-y. Wang, Yu, Zhang, & Liu, 2011). On one hand, under extreme conditions autophagy is an essential machinery for cell survival by degradation of intracellular macromolecules or organelles to provide energy for maintaining minimal cell functioning when nutrients are limited or even deprived (Dalby, Tekedereli, Lopez-Berestein, & Ozpolat, 2010). At the same time, elimination of aggregated proteins or damaged organelles in cytosol by autophagy prevents cells from further damages, domenstrating that autophagy is protective to cancer cells in early stages of cancer (Levine & Klionsky, 2004). On the other hand, autophagy promotes cell death or apoptosis, as a bona fide tumor suppressor in cancer development (Thorburn, 2008). RSV has been shown to possess anti-cancer characteristics, including suppression of proliferation, cell cycle arrest, and potentiation of apoptotic effect (Aggarwal et al., 2004).

In T-cell acute lymphoblastic leukemia (T-ALL) cells, RSV induced autophagy, cell cycle arrest at G0/G1 phase and remarkably reduced phosphorylation of Akt, mTOR, p70S6K, and 4E-BP1, but induced phosphorylation of p38-MAPK which was blocked by SB203580, a MAPK inhibitor, indicating that RSV induces autophagy in T-ALL cells via blocking Akt/mTOR/p70S6K/4E-BP1 signaling cascades and stimulating p38-MAPK signaling (**Figure 9**) (Jiao et al., 2013). However, in human esophageal squamous cell carcinoma (ESCC) cells, RSV induced cell cycle arrest at the sub-G1 stage and promoted subsequent apoptosis, and RSV-induced autophagy in the ESCC cells is independent of AMPK/mTOR signaling pathway (Tang et al., 2013). In human glioma cells Glioma cells, RSV induced autophagy and the effect was promoted by P38 and the ERK1/2 pathway, but independent of Akt/mTOR signaling pathway

(Yamamoto, Suzuki, & Himeno, 2010). In PC12 cells, in a dose-dependent manner RSV-induced AMPK activation and suppression, possibly through the modulation of Sirt1 activity (**Figure 9**) (Hayakawa et al., 2013). This may thus be related to the promotion or inhibition of mitochondrial functions and autophagy activity, resulting in cell death and survival in both undifferentiated and differentiated cells, respectively (Hayakawa et al., 2013). In cultured human non-small-cell lung cancer (NSCLC) cells, treatment with an analogue of RSV 3,4,4'-THS (10-80 μM) induced cell apoptosis, inhibited autophagy through the mTOR-dependent pathway in concentration-dependent manner, did not impair autophagic flux (L. Zhang et al., 2015). In Melanoma B16 cells, RSV induced apoptosis and autophagy, which might come up through ceramide accumulation and Akt/mTOR pathway inhibition (M. Wang et al., 2014). Besides the canonical (Beclin-1 dependent) autophagy, RSV can trigger autophagy-associated cell death (type II PCD) via various mechanisms through non-canonical (Beclin-1 independent) autophagy (Hasima & Ozpolat, 2014). In human breast cancer MCF-7 cells, RSV treatment induced apoptotic cell death devoid of caspase-3 activity. Belin-1 and hVPS34 (human vacuolar protein sorting 34) small interfering RNAs treatment indicated that RSV activates Beclin-1-independent autophagy in this cell line, suggesting that RSV can induce non-canonical autophagy to regulate a caspase-independent cell death mechanism in breast cancer cells (Scarlatti, Maffei, Beau, Codogno, & Ghidoni, 2008).

To confirm the role of autophagy in RSV's regulation on cancer, genetic or pharmaceutical manipulation of autophagy was applied to co-treat with RSV. In OVCAR-3 human ovarian cancer cells, both pharmacological and genetic inhibition of autophagy, including autophagy inhibitor CQ and Atg5 siRNA treatments abolished the apoptotic cell death induced by RSV (Lang et al., 2015). In non-small lung adenocarcinoma A549 cells, knockdown Beclin-1 by

siRNA acquired same effects as CQ and Atg5, to block RSV-induced apoptosis, demonstrating a dependence of apoptosis on autophagy, as confirmed by autophagy inhibitor 3-MA treatment (J. Zhang et al., 2015). In three human glioblastoma (GBM) cell lines, silencing RSV-induced autophagy abolished cell cycle arrest (Chiela, Villodre, Zamin, & Lenz, 2011). In A549 human lung adnocarcinoma cells, 3-MA suppressed RSV-induced autophagic cell death, and silencing of autophagy-related genes Atg5 and Beclin-1 with siRNAs reversed RSV-induced cell death (J. Zhang et al., 2013).

Even though RSV can regulate autophagy to inhibit cell proliferation, induce apoptosis and cell cycle arrest, some studies showed that autophagy inhibitor did not abolish the effects of RSV, but promoted it. In cultured human non-small-cell lung cancer (NSCLC) cells *in vitro*, an RSV analogue 3,4,4'-THS-induced apoptosis was further promoted by treatment with autophagy inhibitors 3-MA (5.0 mM) or Wortmannin (2.0 μM) (L. Zhang et al., 2015). In B16 cells, RSV induced autophagy. Both inhibition of autophagy by an autophagic inhibitor 3-MA and knockdown of Beclin-1 by siRNA enhanced RSV-induced cytotoxicity and apoptosis (M. Wang et al., 2014). In GH3 cells, pre-treatment with bafilomycin A1 or 3-MA, inhibitors of autophagy, furtherly promoted the RSV-mediated caspase activation and cell death. Furthermore, the inhibition of autophagy increased the cytotoxicity of RSV to GH3 cells (X. Zhang et al., 2014). The same effects were observed in T-cell acute lymphoblastic leukemia (T-ALL) cells (Jiao et al., 2013) and human esophageal squamous cell carcinoma (ESCC) (Tang et al., 2013). In these cases, autophagy might play a role as a self-defense mechanism in cells treated by RSV, so combination of autophagy inhibitor and RSV will provide a new strategy for cancer treatment.

9. Sirt1-the molecular link between RSV and autophagy

Sirt1 is one of the most important targets of RSV, which plays an important role in liver homeostasis (Zhang et al., 2015), kidney diseases (Kitada & Koya, 2013), aging and neurodegenerative disease (Rubinsztein et al., 2011). Sirt1 plays a vital role in the regulation of gene expression and protein posttranslational modification (acetylation) (Jeong, Moon, Lee, Seol, & Park, 2013). In energy deprivation and some extreme conditions, deacetylation of essential autophagy proteins and transcriptional factors by Sirt1 has involved in regulating autophagy (Hariharan et al., 2010).

Deacetylase activity of Sirt1 is indispensable for stimulating basal rates of autophagy in the HCT116 colon cancer cell line (Lee et al., 2008). In mouse embryonic fibroblasts deletion of Sirt1 attenuated autophagy under starved conditions. Reconstitution active but not a deacetylase-inactive mutant of Sirt1 recovered autophagy in these cells (Lee et al., 2008). Mechanistically, Sirt1 binds with several important proteins for autophagy machinery, including Atg5, Atg7, and LC3 and directly deacetylases these proteins in an NAD-dependent fashion (**Figure 10**). Sirt1 silencing results in markedly increased acetylation of Atg5 and Atg7 and abolished autophagy as highly accumulated p62 in embryonic and neonatal tissues (Lee et al., 2008). LC3 is a key initiator of autophagy that can translocate across nucleus and cytoplasm. During starvation, LC3 was deacetylated by nuclear Sirt1 to be selectively activated in the nucleus (Huang et al., 2015). After deacetylation at K49 and K51 residues, LC3 would interact with the nuclear protein DOR (The diabetes- and obesity-regulated nuclear factor) and jointly transport to the cytoplasm, where it would bind with Atg7 and other autophagy factors and undergo phosphatidylethanolamine conjugation to preautophagic membranes (**Figure 10**). Thus, during starvation the deacetylation process of LC3 by Sirt1 in the nucleus would promote the downstream of autophagy to adapt the

cell to energy deprivation (Huang et al., 2015). Regulation of autophagy by Sirt1 is important for spermiogenesis in germ cells (Liu et al., 2016). Germ cell-specific Sirt1 knockout mice were almost completely infertile, accompanied by disruption of LC3 and Atg7 deacetylation, which affected the relocation of LC3 from the nucleus to the cytoplasm and its subsequent activation of autophagy. Furthermore, Sirt1 depletion failed to recruit LC3 to Golgi apparatus-derived vesicles and recruit GOPC and PICK1 to nucleus-associated acrosomal vesicles (Liu et al., 2016). In addition to acetylation of Atg5, Atg7 and LC3, acetylation of Beclin-1 plays a vital role in autophagy (Sun et al., 2015). Beclin-1 positively or negatively regulates autophagy by interacting with Vps34 and other cofactors to form the Beclin-1 complex under various conditions (Backer, 2008; Matsunaga et al., 2009; Zhong et al., 2009). Deacetylase inhibitors TSA and NAM treatment significantly elevated the acetylation level of Beclin-1 and co-immunoprecipitation of Beclin-1 and Rubicon, which is a negative cofactor of Beclin complex and autophagy (Zhong et al., 2009). In addition, Beclin-1 acetylation and further recruitment of Rubicon inhibit autophagosome maturation. Structurally, Beclin-1 was acetylated by p300 and deacetylated by Sirt1 at lysine residues 430 and 437. In 293T cells and MCF7 cells, K430 or K437 mutation ameliorated the binding of Beclin-1 to Ribicon, when both sites were mutated the binding was completed abrogated. In tumour xenografts, the expression of double mutated lysine residue for Beclin-1 (substitution of K430 and K437 to arginines) resulted in elevation of both autophagosome maturation and tumour growth suppression (Sun et al., 2015).

FoxO (Forkhead box-containing protein, O subfamily) transcriptional factors are a subunit of the large forkhead family of transcriptional factors. They regulate various cellular functions, including cell cycle, differentiation, metabolism, proliferation, cell survival and autophagy (Accili & Arden, 2004; Burgering & Kops, 2002; Ferdous, Battiprolu, Ni, Rothermel, & Hill,

2010). Several studies have demonstrated that FoxOs promote several autophagic genes expression at transcriptional levels (Ferdous et al., 2010; Mammucari et al., 2007; Sengupta, Molkentin, & Yutzey, 2009). Moreover, these promoted effects were affected by posttranslational modification of FoxOs. Acetylation, a rapier in FoxOs modification, would positively or negatively affect autophagy (**Figure 10**) (Gu et al., 2016; Hariharan et al., 2010; Y. Zhao et al., 2010). In cardiomyocytes (CMs), glucose deprivation (GD) increased autophagy flux, which was concurrently accompanied by induction Sirt1 and FoxO1 expressions. Overexpression of either Sirt1 or FoxO1 was sufficient to induce autophagy flux activity, whereas simultaneous deletions of Sirt1 and FoxO1 failed to induce GD-induced autophagy (Hariharan et al., 2010). GD increased deacetylation of FoxO1, which was dependent on Sirt1's deacetylation activity to function on FoxO1. Overexpression of FoxO1(3A/LXXAA), which was a deacetylation defect form of FoxO1 and cannot interact with Sirt1, significantly elevated acetylation level of FoxO1 and blocked GD-induced autophagy and further abolished FoxO1's induction of its downstream Rab7, a small GTP-binding protein that mediates late autophagosome-lysosome fusion in vitro and *in vivo*. Therefore, Sirt1-mediated deacetylation of FoxO1 and upregulation of Rab7 play significant roles in mediating induction of autophagy followed starvation (Hariharan et al., 2010). The prolonging of lifespan has been closely associated with efficient maintenance of autophagic degradation, which declines dramatically during aging (Salminen & Kaarniranta, 2009). Sirt1 has been reported to interact with FoxO and p53 signaling, and regulated the autophagic degradation and lifespan extension, suggesting the important role of the Sirt1-FoxO cascade in the regulation of lifespan (Salminen & Kaarniranta, 2009). Fluorine contributes to damage of teeth, bones and other body tissues, which is a serious public health issue.

In addition, some other signaling pathways studies have involved Sirt1 in regulating autophagy. During oxidative stress, autophagy was induced with an increase expression of Sirt1 (Ou, Lee, Huang, Messina-Graham, & Broxmeyer, 2014; H. Zhao, Yang, & Cui, 2015). In parthenogenetic haploid embryonic stem cells (ph ESCs), exogenous H_2O_2 challenge induced SIRT1 expression and promoted autophagy via mTOR node (H. Zhao et al., 2015). In murine embryonic stem cells (mESCs), Sirt1 knockout decreased induction of autophagy dependent on at least in part by the class III PI3K/Beclin-1 and mTOR pathways (Ou et al., 2014).

10. Conclusion

Autophagy is important to maintain mammalian health. Dysregulated autophagy has been involved in pathogenesis of various diseases (Pallauf & Rimbach, 2013; Fu, 2015; Kovsan et al., 2010; Schneider & Cuervo, 2014; Huber et al., 2012; Levine, Mizushima, & Virgin, 2011; S.-y. Wang, Yu, Zhang, & Liu, 2011). Targeting dysregulated autophagy may lead to new therapeutics for the related diseases. In this review, I have discussed the evidence that RSV may reverse the dysregulation of autophagy in different cell types and diseases. Mechanistically, RSV mainly acts on the deacetylase Sirt1, which in turn activates autophagy proteins, including Atg7, Atg5, LC3, Beclin-1, and transcriptional factors like FoxO1 and FoxO3 that induces autophagy genes. These findings have revealed the great potential of RSV to ameliorate human diseases, such as metabolic disorders, neurodegenerative diseases, and cancer. As the evidence was primarily derived from cell culture or animal studies, it is of critical importance for future investigations to validate physiological relevance *in vivo* and human studies. To this end, parameters like the safe and effective dosage, duration and timing of treatment have to be established before RSV

supplements in the market can be recommended as an autophagy-mediated treatment of human diseases.

List of abbreviations

A

Akt: protein kinase B

ALT: Alanine aminotransferase

AMPK: AMP-activated protein kinase

AS: Atherosclerosis

Atg5: autophagy related 5

Atg7: autophagy related 7

B

BDL: bile duct ligation

C

CCI: cortical impact

CMs: cardiomyocytes

CQ: chloroquine

CVDs: cardiovascular diseases

D

DOX: doxorubicin

E

4E-BP1: eIF4E-binding protein 1

ESCC: esophageal squamous cell carcinoma

EX527: 6-Chloro-2,3,4,9-tetrahydro-1H-Carbazole-1-carboxamide

F

FoxOs: forkhead box O transcription factors

G

GBM: glioblastoma

GD: glucose deprivation

H

HCAECs: human coronary and iliac artery endothelial cells

I

IL-1β: interleukin 1 beta

IL-6: interleukin 6

L

LC3: microtubule-associated protein 1A/1B-light chain 3-phosphatidylethanolamine conjugate

M

MAPK: mitogen-activated protein kinase

3-MA: 3-methyladenine

MCD: methionine/choline-deficient

mESCs: murine embryonic stem cells

mTOR: mammalian target of rapamycin

mTORC1: mammalian target of rapamycin complex 1

mTORC2: mammalian target of rapamycin complex 2

N

NAD: Nicotinamide adenine dinucleotide

NAFLD: non-alcoholic fatty liver disease

NAM: nicotinamide

NASH: non-alcoholic steatohepatitis

NF-κB: inflammatory nuclear factor-κB

NSCLC: non-small-cell lung cancer

P

p62: sequestosome 1 (SQSTM1)

PC: preconditioning

PPARγ: peroxisome proliferator-activated receptor gamma

PRKA: Serine/threonine protein kinase

PTCs: primary renal proximal tubular cells

R

RSV: resveratrol

S

S6K1: p70 S6 kinase

siRNA: Small (or short) interfering RNA

Sir2: silent information regulator 2

Sirt1: Sirtuin 1

T

TBARS: thiobarbituric acid reactive substances

TBI: traumatic brain injury

T-ALL: T-cell acute lymphoblastic leukemia

TFEB: transcription factor EB

TG: triglyceride

TLR4: toll-like receptor 4

TNFα: tumor necrosis factor alpha

TSA: trichostatin A

U

ULK: Unc-51-like kinase

W

WAT: white adipose tissue

References

Accili, D., & Arden, K. C. (2004). FoxOs at the crossroads of cellular metabolism, differentiation, and transformation. *Cell, 117*(4), 421-426.

Aggarwal, B. B., Bhardwaj, A., Aggarwal, R. S., Seeram, N. P., Shishodia, S., & Takada, Y. (2004). Role of resveratrol in prevention and therapy of cancer: preclinical and clinical studies. *Anticancer Research, 24*(5A), 2783-2840.

Backer, J. M. (2008). The regulation and function of Class III PI3Ks: novel roles for Vps34. *Biochemical Journal, 410*(1), 1-17.

Baerga, R., Zhang, Y., Chen, P.-H., Goldman, S., & Jin, S. V. (2009). Targeted deletion of autophagy-related 5 (atg5) impairs adipogenesis in a cellular model and in mice. *Autophagy, 5*(8), 1118-1130.

Bjedov, I., Toivonen, J. M., Kerr, F., Slack, C., Jacobson, J., Foley, A., & Partridge, L. (2010). Mechanisms of life span extension by rapamycin in the fruit fly Drosophila melanogaster. *Cell Metabolism,* 11(1), 35-46.

Burgering, B. M., & Kops, G. J. (2002). Cell cycle and death control: long live Forkheads. *Trends in Biochemical Sciences, 27*(7), 352-360.

Chang, Y. P., Ka, S. M., Hsu, W. H., Chen, A., Chao, L. K., Lin, C. C., & Ho, C. L. (2015). Resveratrol inhibits NLRP3 inflammasome activation by preserving mitochondrial integrity and augmenting autophagy. *Journal of Cellular Physiology, 230*(7), 1567-1579.

Chen, M.-l., Yi, L., Jin, X., Liang, X.-y., Zhou, Y., Zhang, T., & Fu, Y.-j. (2013). Resveratrol attenuates vascular endothelial inflammation by inducing autophagy through the cAMP signaling pathway. *Autophagy, 9*(12), 2033-2045.

Chen-Scarabelli, C., Agrawal, P. R., Saravolatz, L., Abuniat, C., Scarabelli, G., Stephanou, A., & Knight, R. (2014). The role and modulation of autophagy in experimental models of myocardial ischemia-reperfusion injury. *Journal of Geriatric Cardiology: JGC, 11*(4), 338.

Cheng, Z., Schmelz, E. M., Liu, D., & Hulver, M. W. (2014). Targeting mitochondrial alterations to prevent type 2 diabetes—Evidence from studies of dietary redox-active compounds. *Molecular Nutrition & Food Research, 58*(8), 1739-1749.

Chiela, E. C. F., Villodre, E. S., Zamin, L. L., & Lenz, G. (2011). Autophagy interplay with apoptosis and cell cycle regulation in the growth inhibiting effect of resveratrol in glioma cells. *PLoS ONE, 6* (6), e20849, p. 1-13.

Colak, Y., Yesil, A., Mutlu, H. H., Caklili, O. T., Ulasoglu, C., Senates, E., & Yilmaz Enc, F. (2014). A potential treatment of non-alcoholic fatty liver disease with SIRT1 activators. *Journal of Gastrointestinal and Liver Disease, 23*(3), 311-319.

Colman, R. J., Anderson, R. M., Johnson, S. C., Kastman, E. K., Kosmatka, K. J., Beasley, T. M., & Kemnitz, J. W. (2009). Caloric restriction delays disease onset and mortality in rhesus monkeys. *Science, 325*(5937), 201-204.

Dalby, K., Tekedereli, I., Lopez-Berestein, G., & Ozpolat, B. (2010). Targeting the pro-death and pro-survival functions of autophagy as novel therapeutic strategies in cancer. *Autophagy, 6*(3), 322-329.

Del Roso, A., Vittorini, S., Cavallini, G., Donati, A., Gori, Z., Masini, M., & Bergamini, E. (2003). Ageing-related changes in the *in vivo* function of rat liver macroautophagy and proteolysis. *Experimental Gerontology, 38*(5), 519-527.

Dutta, D., Xu, J., Dirain, M. L., & Leeuwenburgh, C. (2014). Calorie restriction combined with resveratrol induces autophagy and protects 26-month-old rat hearts from doxorubicin-induced toxicity. *Free Radical Biology and Medicine, 74*, 252-262.

Falchetti, R., Fuggetta, M. P., Lanzilli, G., Tricarico, M., & Ravagnan, G. (2001). Effects of resveratrol on human immune cell function. *Life sciences, 70*(1), 81-96.

Farmer, S. R. (2009). Obesity: Be cool, lose weight. *Nature, 458*(7240), 839-840.

Feng, Y., Cui, Y., Gao, J.-L., Li, M.-H., Li, R., Jiang, X.-H., & Cui, J.-Z. (2016). Resveratrol attenuates neuronal autophagy and inflammatory injury by inhibiting the TLR4/NF-κB signaling pathway in experimental traumatic brain injury. *International Journal of Molecular Medicine, 37*(4), 921-930.

Ferdous, A., Battiprolu, P. K., Ni, Y. G., Rothermel, B. A., & Hill, J. A. (2010). FoxO, autophagy, and cardiac remodeling. *Journal of Cardiovascular Translational Research, 3*(4), 355-364.

Frankel, E., German, J. B., Kinsella, J., Parks, E., & Kanner, J. (1993). Inhibition of oxidation of human low-density lipoprotein by phenolic substances in red wine. *The Lancet, 341*(8843), 454-457.

Fu, D. (2015). Regulation of redox signalling and autophagy during cardiovascular diseases-role of resveratrol. *European Review for Medical and Pharmacological Sciences, 19*(8), 1530-1536.

Goldman, S., Zhang, Y., & Jin, S. V. (2010). Autophagy and adipogenesis: implications in obesity and type II diabetes. *Autophagy, 6*(1), 179-181.

Gurusamy, N., Lekli, I., Gorbunov, N. V., Gherghiceanu, M., Popescu, L. M., & Das, D. K. (2009). Cardioprotection by adaptation to ischaemia augments autophagy in association with BAG-1 protein. *Journal of Cellular and Molecular Medicine, 13*(2), 373-387.

Gurusamy, N., Lekli, I., Mukherjee, S., Ray, D., Ahsan, M. K., Gherghiceanu, M., & Das, D. K. (2009). Cardioprotection by resveratrol: a novel mechanism via autophagy involving the mTORC2 pathway. *Cardiovascular Research, 86*(1), 103-112.

Haigis, M. C., & Sinclair, D. A. (2010). Mammalian sirtuins: biological insights and disease relevance. *Annual Review of Pathological Mechanical Disease, 5*, 253-295.

Hariharan, N., Maejima, Y., Nakae, J., Paik, J., DePinho, R. A., & Sadoshima, J. (2010). Deacetylation of FoxO by Sirt1 Plays an Essential Role in Mediating Starvation-Induced Autophagy in Cardiac MyocytesNovelty and Significance. *Circulation Research, 107*(12), 1470-1482.

Hasima, N., & Ozpolat, B. (2014). Regulation of autophagy by polyphenolic compounds as a potential therapeutic strategy for cancer. *Cell Death & Disease, 5*(11), e1509.

Hayakawa, N., Shiozaki, M., Shibata, M., Koike, M., Uchiyama, Y., Matsuura, N., & Gotow, T. (2013). Resveratrol affects undifferentiated and differentiated PC12 cells differently, particularly with respect to possible differences in mitochondrial and autophagic functions. *European Journal of Cell Biology, 92*(1), 30-43.

Hsu, K.-F., Wu, C.-L., Huang, S.-C., Wu, C.-M., Hsiao, J.-R., Yo, Y.-T., & Chou, C.-Y. (2009). Cathepsin L mediates resveratrol-induced autophagy and apoptotic cell death in cervical cancer cells. *Autophagy, 5*(4), 451-460.

Huang, R., Xu, Y., Wan, W., Shou, X., Qian, J., You, Z., & Lippincott-Schwartz, J. (2015). Deacetylation of nuclear LC3 drives autophagy initiation under starvation. *Molecular cell, 57*(3), 456-466.

Huber, T. B., Edelstein, C. L., Hartleben, B., Inoki, K., Jiang, M., Koya, D., & Quiroga, A. (2012). Emerging role of autophagy in kidney function, diseases and aging. *Autophagy, 8*(7), 1009-1031.

Hu, P., Zhao, L., & Chen, J. (2015). Physiologically achievable doses of resveratrol enhance 3T3-L1 adipocyte differentiation. *European Journal of Nutrition, 54*(4), 569-579.

Jiao, G., Yan, L., Qiang, L., Xia, G., Ling, G., Gui, Z., & Zhu, Y. P. (2013). Resveratrol induces apoptosis and autophagy in T-cell acute lymphoblastic leukemia cells by inhibiting Akt/mTOR and activating p38-MAPK. *Biomedical and Environmental Sciences, 26*(11), 902-911.

Ji, G., Wang, Y., Deng, Y., Li, X., & Jiang, Z. (2015). Resveratrol ameliorates hepatic steatosis and inflammation in methionine/choline-deficient diet-induced steatohepatitis through regulating autophagy. *Lipids in Health and Disease, 14*(1), 134.

Kanamori, H., Takemura, G., Goto, K., Tsujimoto, A., Ogino, A., Takeyama, T., & Kawasaki, M. (2013). Resveratrol reverses remodeling in hearts with large, old myocardial infarctions through enhanced autophagy-activating AMP kinase pathway. *The American Journal of Pathology, 182*(3), 701-713.

Kitada, M., & Koya, D. (2013). Renal protective effects of resveratrol. *Oxidative Medicine and Cellular Longevity.*

Konings, E., Timmers, S., Boekschoten, M., Goossens, G., Jocken, J., Afman, L., & Blaak, E. (2014). The effects of 30 days resveratrol supplementation on adipose tissue morphology and gene expression patterns in obese men. *International Journal of Obesity, 38*(3), 470-473.

Kovsan, J., Blüher, M., Tarnovscki, T., Klöting, N., Kirshtein, B., Madar, L., & Schön, M. R. (2010). Altered autophagy in human adipose tissues in obesity. *The Journal of Clinical Endocrinology & Metabolism, 96*(2), 268-277.

Kumar, A., & Chauhan, S. (2016). How much successful are the medicinal chemists in modulation of SIRT1: A critical review. *European Journal of Medicinal Chemistry*, 119, 45-69.

Kume, S., Uzu, T., Horiike, K., Chin-Kanasaki, M., Isshiki, K., Araki, S.-i., & Koya, D. (2010). Calorie restriction enhances cell adaptation to hypoxia through Sirt1-dependent mitochondrial autophagy in mouse aged kidney. *The Journal of Clinical Investigation, 120*(4), 1043-1055.

Lang, F., Qin, Z., Li, F., Zhang, H., Fang, Z., & Hao, E. (2015). Apoptotic cell death induced by resveratrol is partially mediated by the autophagy pathway in human ovarian cancer cells. *PloS one, 10*(6), e0129196.

Lee, I. H., Cao, L., Mostoslavsky, R., Lombard, D. B., Liu, J., Bruns, N. E., & Finkel, T. (2008). A role for the NAD-dependent deacetylase Sirt1 in the regulation of autophagy. *Proceedings of the National Academy of Sciences, 105*(9), 3374-3379.

Lekli, I., Ray, D., Mukherjee, S., Gurusamy, N., Ahsan, M., Juhasz, B., & Popescu, L. M. (2010). Co-ordinated autophagy with resveratrol and γ-tocotrienol confers synergetic cardioprotection. *Journal of Cellular and Molecular Medicine, 14*(10), 2506-2518.

Levine, B., & Klionsky, D. J. (2004). Development by self-digestion: molecular mechanisms and biological functions of autophagy. *Developmental Cell, 6*(4), 463-477.

Levine, B., & Kroemer, G. (2008). Autophagy in the pathogenesis of disease. *Cell, 132*(1), 27-42.

Levine, B., Mizushima, N., & Virgin, H. W. (2011). Autophagy in immunity and inflammation. *Nature, 469*(7330), 323-335.

Li, L., Hai, J., Li, Z., Zhang, Y., Peng, H., Li, K., & Weng, X. (2014). Resveratrol modulates autophagy and NF-κB activity in a murine model for treating non-alcoholic fatty liver disease. *Food and Chemical Toxicology, 63*, 166-173.

Liao, X., Sluimer, J. C., Wang, Y., Subramanian, M., Brown, K., Pattison, J. S., & Tabas, I. (2012). Macrophage autophagy plays a protective role in advanced atherosclerosis. *Cell Metabolism, 15*(4), 545-553.

Lin, T.-K., Huang, L.-T., Huang, Y.-H., Tiao, M.-M., Tang, K.-S., & Liou, C.-W. (2012). The effect of the red wine polyphenol resveratrol on a rat model of biliary obstructed cholestasis: involvement of anti-apoptotic signalling, mitochondrial biogenesis and the induction of autophagy. *Apoptosis, 17*(8), 871-879.

Liu, C., Song, Z., Wang, L., Yu, H., Liu, W., Shang, Y., & Wen, J. (2016). Sirt1 regulates acrosome biogenesis by modulating autophagic flux during spermiogenesis in mice. *Development, 144*(3), 441-451.

Liu, L., Tao, Z., Zheng, L. D., Brooke, J. P., Smith, C. M., Liu, D., & Cheng, Z. (2016). FoxO1 interacts with transcription factor EB and differentially regulates mitochondrial uncoupling proteins via autophagy in adipocytes. *Cell Death Discovery, 2*, 16066.

Liu, L., Zou, P., Zheng, L., Linarelli, L. E., Amarell, S., Passaro, A., & Cheng, Z. (2015). Tamoxifen reduces fat mass by boosting reactive oxygen species. *Cell Death & Disease, 6*(1), e1586.

Madeo, F., Tavernarakis, N., & Kroemer, G. (2010). Can autophagy promote longevity? *Nature Cell Biology, 12*(9), 842-846.

Ma, L., Fu, R., Duan, Z., Lu, J., Gao, J., Tian, L., & Jia, L. (2016). Sirt1 is essential for resveratrol enhancement of hypoxia-induced autophagy in the type 2 diabetic nephropathy rat. *Pathology-Research and Practice, 212*(4), 310-318.

Mammucari, C., Milan, G., Romanello, V., Masiero, E., Rudolf, R., Del Piccolo, P., & Zhao, J. (2007). FoxO3 controls autophagy in skeletal muscle *in vivo*. *Cell Metabolism, 6*(6), 458-471.

Mariño, G., Morselli, E., Bennetzen, M. V., Eisenberg, T., Megalou, E., Schroeder, S., & Criollo, A. (2011). Longevity-relevant regulation of autophagy at the level of the acetylproteome. *Autophagy, 7*(6), 647-649.

Markus, M. A., & Morris, B. J. (2008). Resveratrol in prevention and treatment of common clinical conditions of aging. *Clinical Interventions in Aging, 3*(2), 331.

Marques, F. Z., Markus, M. A., & Morris, B. J. (2009). Resveratrol: cellular actions of a potent natural chemical that confers a diversity of health benefits. *The International Journal of Biochemistry & Cell Biology, 41*(11), 2125-2128.

Martins, L. A. M., Vieira, M. Q., Ilha, M., de Vasconcelos, M., Biehl, H. B., Lima, D. B., & Guma, F. C. R. (2015). The interplay between apoptosis, mitophagy and mitochondrial biogenesis induced by resveratrol can determine activated hepatic stellate cells death or survival. *Cell Biochemistry and Biophysics, 71*(2), 657-672.

Matsunaga, K., Saitoh, T., Tabata, K., Omori, H., Satoh, T., Kurotori, N., & Isobe, T. (2009). Two Beclin 1-binding proteins, Atg14L and Rubicon, reciprocally regulate autophagy at different stages. *Nature Cell Biology, 11*(4), 385-396.

Meléndez, A., Talloczy, Z., Seaman, M., Eskelinen, E.-L., Hall, D. H., & Levine, B. (2003). Autophagy genes are essential for dauer development and life-span extension in *C. elegans*. *Science, 301*(5638), 1387-1391.

Miki, H., Uehara, N., Kimura, A., Sasaki, T., Yuri, T., Yoshizawa, K., & Tsubura, A. (2012). Resveratrol induces apoptosis via ROS-triggered autophagy in human colon cancer cells. *International Journal of Oncology, 40*(4), 1020-1028.

Morselli, E., Maiuri, M., Markaki, M., Megalou, E., Pasparaki, A., Palikaras, K., & Vitale, I. (2010). Caloric restriction and resveratrol promote longevity through the Sirtuin-1-dependent induction of autophagy. *Cell Death & Disease, 1*(1), e10.

Morselli, E., Maiuri, M. C., Markaki, M., Megalou, E., Pasparaki, A., Palikaras, K., & Vitale, I. (2010). The life span-prolonging effect of sirtuin-1 is mediated by autophagy. *Autophagy, 6*(1), 186-188.

Murray, C. J., & Lopez, A. D. (1997). Global mortality, disability, and the contribution of risk factors: Global Burden of Disease Study. *The Lancet, 349*(9063), 1436-1442.

Ni, H.-M., Du, K., You, M., & Ding, W.-X. (2013). Critical role of FoxO3a in alcohol-induced autophagy and hepatotoxicity. *The American Journal of Pathology, 183*(6), 1815-1825.

Ou, X., Lee, M. R., Huang, X., Messina-Graham, S., & Broxmeyer, H. E. (2014). SIRT1 positively regulates autophagy and mitochondria function in embryonic stem cells under oxidative stress. *Stem Cells, 32*(5), 1183-1194.

Pallauf, K., & Rimbach, G. (2013). Autophagy, polyphenols and healthy ageing. *Ageing Research Reviews, 12*(1), 237-252.

Petrovski, G., & Das, D. K. (2010). Does autophagy take a front seat in lifespan extension? *Journal of Cellular and Molecular Medicine, 14*(11), 2543-2551.

Petrovski, G., Gurusamy, N., & Das, D. K. (2011). Resveratrol in cardiovascular health and disease. *Annals of the New York Academy of Sciences, 1215*(1), 22-33.

Picard, F., Kurtev, M., Chung, N., Topark-Ngarm, A., Senawong, T., De Oliveira, R. M., & Guarente, L. (2004). Sirt1 promotes fat mobilization in white adipocytes by repressing PPAR-γ. *Nature, 429*(6993), 771-776.

Qiang, L., Wang, L., Kon, N., Zhao, W., Lee, S., Zhang, Y., &Farmer, S. R. (2012). Brown remodeling of white adipose tissue by SirT1-dependent deacetylation of Pparγ. *Cell, 150*(3), 620-632.

Rayalam, S., Yang, J. Y., Ambati, S., Della-Fera, M. A., & Baile, C. A. (2008). Resveratrol induces apoptosis and inhibits adipogenesis in 3T3-L1 adipocytes. *Phytotherapy Research, 22*(10), 1367-1371.

Rubinsztein, D. C., Mariño, G., & Kroemer, G. (2011). Autophagy and aging. *Cell, 146*(5), 682-695.

Salminen, A., & Kaarniranta, K. (2009). SIRT1: regulation of longevity via autophagy. *Cellular Signalling, 21*(9), 1356-1360.

Sato, M., Maulik, N., & Das, D. K. (2002). Cardioprotection with alcohol. *Annals of the New York Academy of Sciences, 957*(1), 122-135.

Scarlatti, F., Maffei, R., Beau, I., Codogno, P., & Ghidoni, R. (2008). Role of non-canonical Beclin 1-independent autophagy in cell death induced by resveratrol in human breast cancer cells. *Cell Death & Differentiation, 15*(8), 1318-1329.

Schneider, J. L., & Cuervo, A. M. (2014). Liver autophagy: much more than just taking out the trash. *Nature Reviews Gastroenterology & Hepatology, 11*(3), 187-200.

Sengupta, A., Molkentin, J. D., & Yutzey, K. E. (2009). FoxO transcription factors promote autophagy in cardiomyocytes. *Journal of Biological Chemistry, 284*(41), 28319-28331.

Settembre, C., & Ballabio, A. (2011). TFEB regulates autophagy: an integrated coordination of cellular degradation and recycling processes. *Autophagy, 7*(11), 1379-1381.

Singh, R., & Cuervo, A. M. (2011). Autophagy in the cellular energetic balance. *Cell Metabolism, 13*(5), 495-504.

Singh, R., Kaushik, S., Wang, Y., Xiang, Y., Novak, I., Komatsu, M., & Czaja, M. J. (2009). Autophagy regulates lipid metabolism. *Nature, 458*(7242), 1131-1135.

Singh, R., Xiang, Y., Wang, Y., Baikati, K., Cuervo, A. M., Luu, Y. K., & Czaja, M. J. (2009). Autophagy regulates adipose mass and differentiation in mice. *The Journal of Clinical Investigation, 119*(11), 3329-3339.

Sugiyama, M., KAWAHARA-MIKI, R., Kawana, H., Shirasuna, K., Kuwayama, T., & Iwata, H. (2015). Resveratrol-induced mitochondrial synthesis and autophagy in oocytes derived from early antral follicles of aged cows. *Journal of Reproduction and Development, 61*(4), 251-259.

Sun, T., Li, X., Zhang, P., Chen, W.-D., Zhang, H.-l., Li, D.-D., & Ji, J. (2015). Acetylation of Beclin 1 inhibits autophagosome maturation and promotes tumour growth. *Nature Communications, 6*.

Švajger, U., & Jeras, M. (2012). Anti-inflammatory effects of resveratrol and its potential use in therapy of immune-mediated diseases. *International Reviews of Immunology, 31*(3), 202-222.

Szkudelska, K., & Szkudelski, T. (2010). Resveratrol, obesity and diabetes. *European Journal of Pharmacology, 635*(1), 1-8.

Tang, Q., Li, G., Wei, X., Zhang, J., Chiu, J.-F., Hasenmayer, D., & Zhang, H. (2013). Resveratrol-induced apoptosis is enhanced by inhibition of autophagy in esophageal squamous cell carcinoma. *Cancer Letters, 336*(2), 325-337.

Tanida, I. (2011). Autophagosome formation and molecular mechanism of autophagy. *Antioxidants & Redox Signaling, 14*(11), 2201-2214.

Thorburn, A. (2008). Apoptosis and autophagy: regulatory connections between two supposedly different processes. *Apoptosis, 13*(1), 1-9.

Um, J.-H., Park, S.-J., Kang, H., Yang, S., Foretz, M., McBurney, M. W., & Chung, J. H. (2010). AMP-activated protein kinase–deficient mice are resistant to the metabolic effects of resveratrol. *Diabetes, 59*(3), 554-563.

Wang, M., Yu, T., Zhu, C., Sun, H., Qiu, Y., Zhu, X., & Li, J. (2014). Resveratrol triggers protective autophagy through the ceramide/Akt/mTOR pathway in melanoma B16 cells. *Nutrition and Cancer, 66*(3), 435-440.

Wu, J., Li, X., Zhu, G., Zhang, Y., He, M., & Zhang, J. (2016). The role of Resveratrol-induced mitophagy/autophagy in peritoneal mesothelial cells inflammatory injury via NLRP3 inflammasome activation triggered by mitochondrial ROS. *Experimental Cell Research, 341*(1), 42-53.

Wang, S., Liang, X., Yang, Q., Fu, X., Rogers, C. J., Zhu, M., & Du, M. (2015). Resveratrol induces brown-like adipocyte formation in white fat through activation of AMP-activated protein kinase (AMPK) α1. *International Journal of Obesity, 39*(6), 967-976.

Wang, S., Liang, X., Yang, Q., Fu, X., Zhu, M., Rodgers, B., & Du, M. (2017). Resveratrol enhances brown adipocyte formation and function by activating AMP-activated protein kinase (AMPK) α1 in mice fed high-fat diet. *Molecular Nutrition & Food Research*.

Wang, S.-y., Yu, Q.-j., Zhang, R.-d., & Liu, B. (2011). Core signaling pathways of survival/death in autophagy-related cancer networks. *The International Journal of Biochemistry & Cell Biology, 43*(9), 1263-1266.

Xu, X., Chen, K., Kobayashi, S., Timm, D., & Liang, Q. (2012). Resveratrol attenuates doxorubicin-induced cardiomyocyte death via inhibition of p70 S6 kinase 1-mediated autophagy. *Journal of Pharmacology and Experimental Therapeutics, 341*(1), 183-195.

Yamamoto, M., Suzuki, S. O., & Himeno, M. (2010). Resveratrol-induced autophagy in human U373 glioma cells. *Oncology Letters, 1*(3), 489-493.

Yu, W., Fu, Y. C., & Wang, W. (2012). Cellular and molecular effects of resveratrol in health and disease. *Journal of Cellular Biochemistry, 113*(3), 752-759.

Zhang, J., Chiu, J., Zhang, H., Qi, T., Tang, Q., Ma, K., & Li, G. (2013). Autophagic cell death induced by resveratrol depends on the Ca 2+/AMPK/mTOR pathway in A549 cells. *Biochemical pharmacology, 86*(2), 317-328.

Zhang, J., Ma, K., Qi, T., Wei, X., Zhang, Q., Li, G., & Chiu, J.-F. (2015). P62 regulates resveratrol-mediated Fas/Cav-1 complex formation and transition from autophagy to apoptosis. *Oncotarget, 6*(2), 789-801.

Zhang, L., Dai, F., Sheng, P.-l., Chen, Z.-Q., Xu, Q.-P., & Guo, Y.-Q. (2015). Resveratrol analogue 3, 4, 4′-trihydroxy-trans-stilbene induces apoptosis and autophagy in human non-small-cell lung cancer cells in vitro. *Acta Pharmacologica Sinica, 36*(10), 1256-1265.

Zhang, X., Xu, W., Su, J., Chu, M., Jin, H., Li, G., & Wang, C. (2014). The prosurvival role of autophagy in resveratrol-induced cytotoxicity in GH3 cells. *International Journal of Molecular Medicine*, 33(4), 987-993.

Zhang, Y., Chen, M. l., Zhou, Y., Yi, L., Gao, Y. x., Ran, L., & Zou, D. (2015). Resveratrol improves hepatic steatosis by inducing autophagy through the cAMP signaling pathway. *Molecular Nutrition & Food Research, 59*(8), 1443-1457.

Zhang, Y., Goldman, S., Baerga, R., Zhao, Y., Komatsu, M., & Jin, S. (2009). Adipose-specific deletion of autophagy-related gene 7 (atg7) in mice reveals a role in adipogenesis. *Proceedings of the National Academy of Sciences, 106*(47), 19860-19865.

Zhao, H., Chen, S., Gao, K., Zhou, Z., Wang, C., Shen, Z., & Liu, C. (2017). Resveratrol protects against spinal cord injury by activating autophagy and inhibiting apoptosis mediated by the SIRT1/AMPK signaling pathway. *Neuroscience, 348*, 241-251.

Zhao, H., Yang, L., & Cui, H. (2015). SIRT1 regulates autophagy and diploidization in parthenogenetic haploid embryonic stem cells. *Biochemical and Biophysical Research Communications, 464*(4), 1163-1170.

Zhao, Y., Yang, J., Liao, W., Liu, X., Zhang, H., Wang, S., & Zhu, W.-G. (2010). Cytosolic FoxO1 is essential for the induction of autophagy and tumour suppressor activity. *Nature Cell Biology, 12*(7), 665-675.

Zhong, Y., Wang, Q. J., Li, X., Yan, Y., Backer, J. M., Chait, B. T., & Yue, Z. (2009). Distinct regulation of autophagic activity by Atg14L and Rubicon associated with Beclin 1–phosphatidylinositol-3-kinase complex. *Nature Cell Biology, 11*(4), 468-476.

Zhu, Y., He, W., Gao, X., Li, B., Mei, C., Xu, R., & Chen, H. (2015). Resveratrol overcomes gefitinib resistance by increasing the intracellular gefitinib concentration and triggering apoptosis, autophagy and senescence in PC9/G NSCLC cells. *Scientific Reports, 5*, 17730.

Figure legends

Figure 1

Structure and major dietary sources of resveratrol (RSV). A. Structure of RSV (3,5,4′-trihydroxystilbene); B. Major dietary sources of RSV in foods and associated processed items, i.e., grapes, berries, peanuts, other dietary plants, jam and red wine.

Figure 2

The autophagy machinery. Major steps of autophagy include initiation, elongation, maturation, fusion and degradation. Initiation step involves Atg14-Beclin-1-Vps34 complex. Atg12-Atg5 complex and LC3-II are involved in the elongation and maturation of autophagy. At last, autophagosome forms and fuse with lysosome to form autolysosome. In the autolysosome, the engulfed dysfunctional organelles (i.e., mitochondria) and molecules (i.e., protein aggregates, cytosolic proteins, and pathogen) are degraded by lysosomal proteinases.

Figure 3

RSV regulates autophagy in aging and related metabolic diseases. Sirt1 (Sirtuin 1) is the major target of RSV in aging and related metabolic diseases. During inhibiting aging and prolonging life span, Sirt1 promotes autophagy dependent on Beclin-1. During inhibiting neurodegenerative disease, RSV promotes autophagy dependent on Sirt1-AMPK (5' AMP-activated protein kinase) signaling pathway.

Figure 4

RSV regulates autophagy in heart disease. RSV promotes autophagy dependent on mTORC2 (mammalian target of rapamycin complex 2) and AMPK molecules to promote cardiomyocyte cell survival under hypoxia.

Figure 5

RSV regulates autophagy in adipocytes and obesity. RSV administration decreases the adipocyte size, increases adipogenesis and improves the profile of insulin resistance in adipocytes, which probably involve TFEB, a major transcriptional factor of autophagy in the nucleus. In the nucleus, TFEB may regulate ATG9, LC3 and p62 gene expressions that relate to autophagy.

Figure 6

RSV regulates autophagy in liver disease. RSV activates Sirt1 to induce the deacetylation of FoxOs to induce autophagy and mitophagy. The induced autophagy plays a protective role from nonalcoholic fatty liver disease (NAFLD) and Non-alcoholic steatohepatitis (NASH). The induced mitophagy plays a protective role from liver fibrosis.

Figure 7

RSV regulates autophagy in kidney disease. Under hypoxia condition, RSV induces Sirt1 to deacetylase FoxO3, which induces autophagy and Bnip3 (BCL2/adenovirus E1B 19-kDa interacting protein 3)-dependent mitophagy to improve renal proximal tubular cells (PTCs) cell survival. Under starvation condition, RSV inhibits autophagy dependent on S6K1, which inhibits HEK293 Kidney cell lysosomal clearance.

Figure 8

RSV regulates autophagy in inflammation. RSV induces autophagy to inhibit NLRP3 (NACHT, LRR and PYD domains-containing protein 3) inflammasome and NLRP3 inflammasome induced IL-1 (interleukin-1) secretion; and RSV ameliorates autophagy induced TLR4 (Toll-like receptor 4) and its downstream inflammatory factors IL-1, NF-κB (nuclear factor kappa-light-chain-enhancer of activated B cells) and TNF-α (tumor necrosis factor alpha) secretion. The inhibition of inflammation will prevent the pathogenesis of Atherosclerosis and Traumatic brain injury.

Figure 9

RSV regulates autophagy in cancer. RSV regulates autophagy to promote or inhibit cancer development, which is dependent on Raptor (Regulatory-associated protein of mTOR) phosphorylation, AMPK phosphorylation and Sirt1 activity. RSV regulates autophagy to promote cancer cell growth to induce cancer (skin cancer, pituitary tumor, lymph cancer, esophageal cancer) promotion. RSV regulates autophagy to promote apoptosis to induce cancer (ovarian cancer, lung cancer and glioblastoma) inhibition.

Figure 10

The signaling pathways of how Sirt1 regulates autophagy in metabolic diseases. In the nucleus, Sirt1 deacetylases FoxO1 to promote FoxO1 activity and its target genes in autophagy. Also in the nucleus, Sirt1 deacetylases LC3 to promote its binding with the nuclear protein DOR (The diabetes- and obesity-regulated nuclear factor) and translocation to cytosol and downstream autophagy steps. In the cytosol, Sirt1 deacetylases Atg7 and Atg5 to induce autophagy.

Figure 1

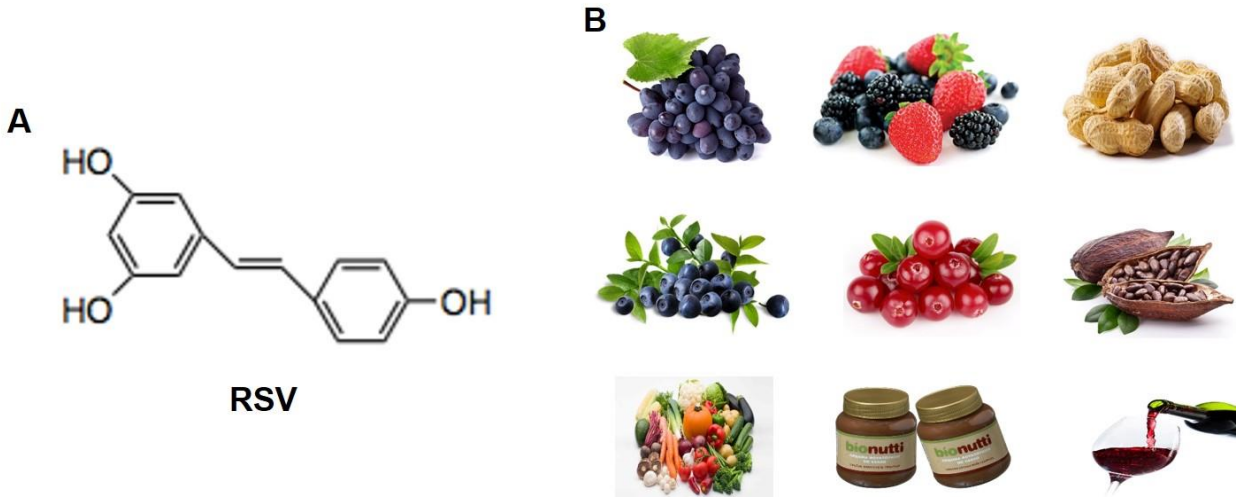

Figure 2

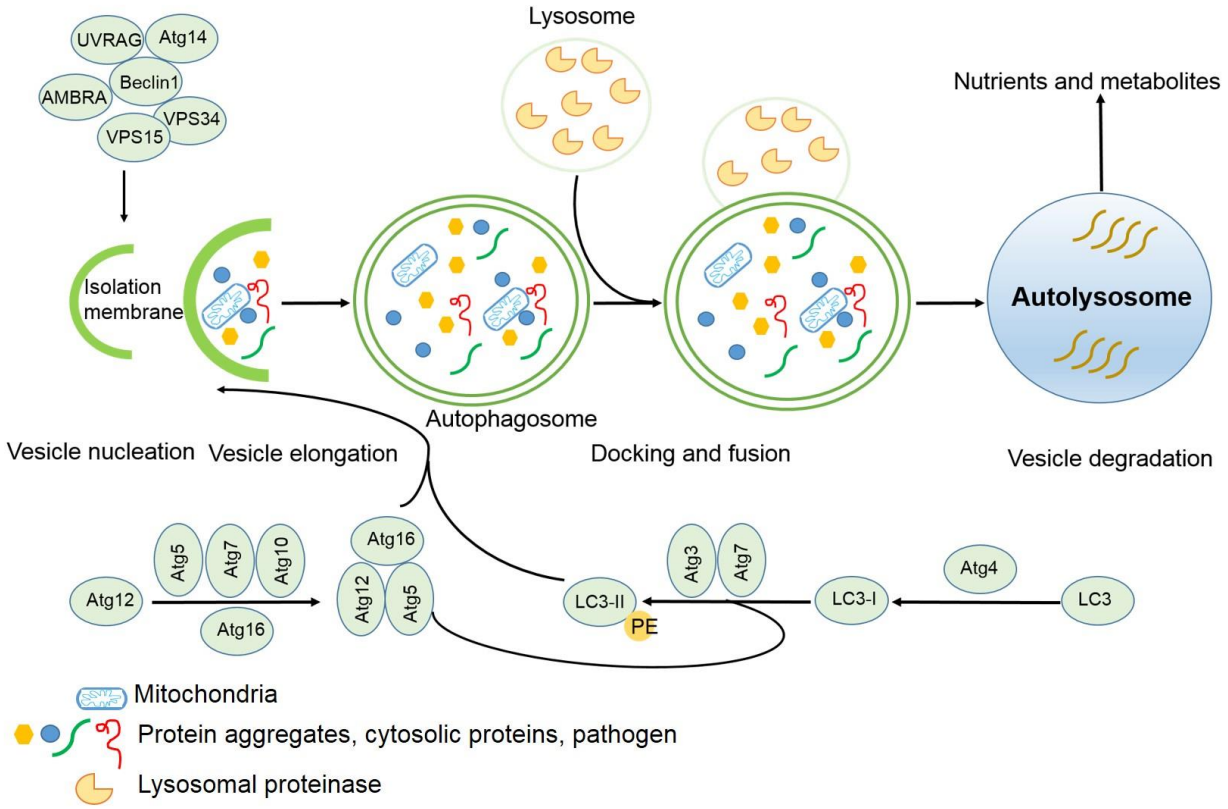
UVRAG
Atg14
Beclin1
AMBRA
VPS34
VPS15
Lysosome
Nutrients and metabolites
Isolation membrane
Autolysosome
Autophagosome
Vesicle nucleation
Vesicle elongation
Docking and fusion
Vesicle degradation
Atg5
Atg7
Atg10
Atg12
Atg16
Atg16
Atg12
Atg5
LC3-II
PE
Atg3
Atg7
LC3-I
Atg4
LC3
Mitochondria
Protein aggregates, cytosolic proteins, pathogen
Lysosomal proteinase

Figure 3

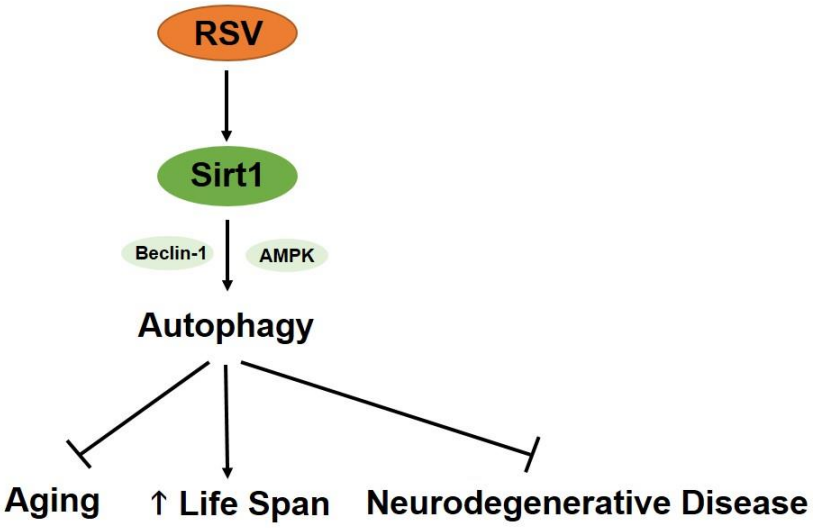
RSV
Sirt1
Beclin-1
AMPK
Autophagy
Aging
↑ Life Span
Neurodegenerative Disease

Figure 4

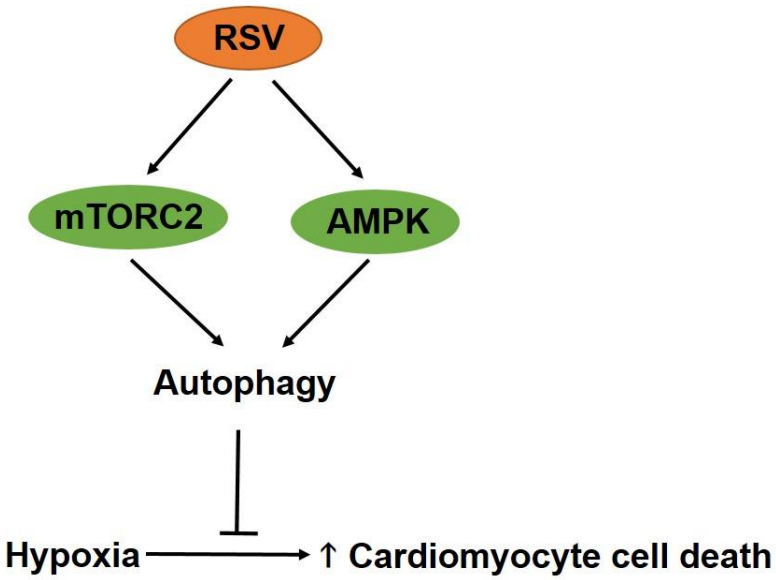
RSV
mTORC2
AMPK
Autophagy
Hypoxia
↑ Cardiomyocyte cell death

Figure 5

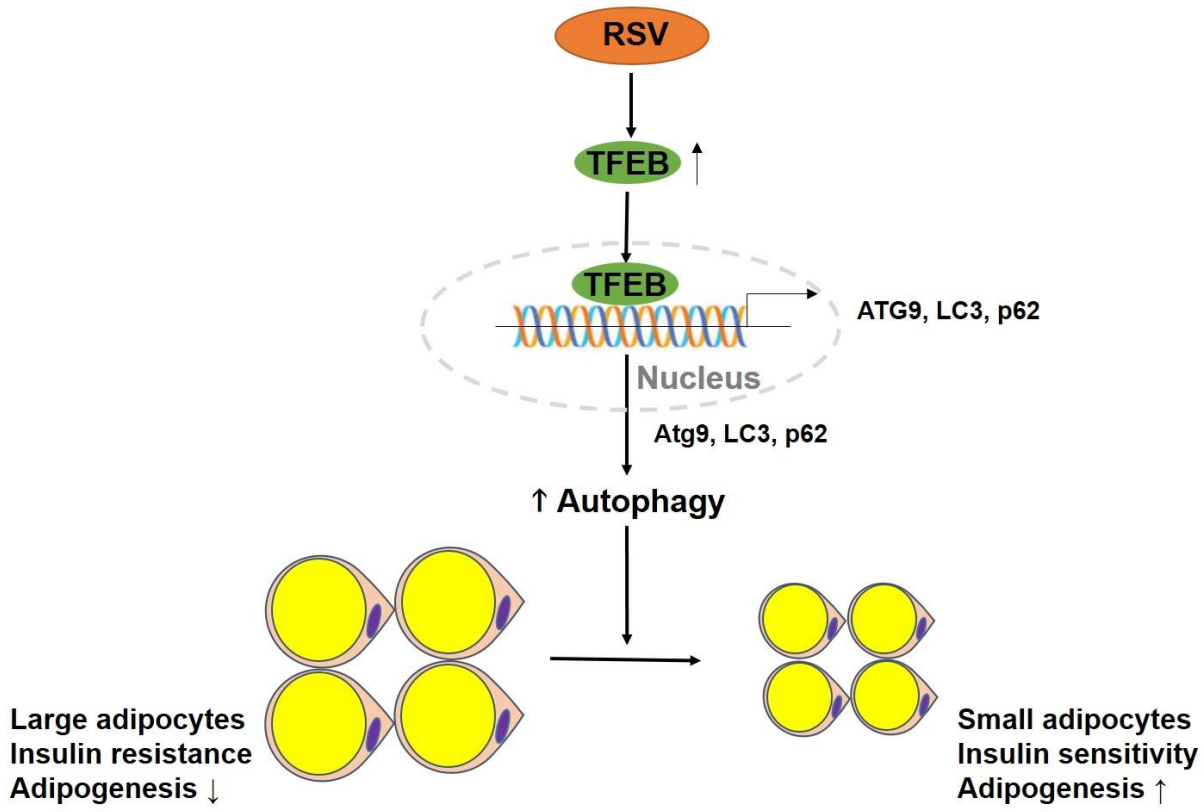
RSV
TFEB
TFEB
ATG9, LC3, p62
Nucleus
Atg9, LC3, p62
↑ Autophagy
Large adipocytes
Insulin resistance
Adipogenesis ↓
Small adipocytes
Insulin sensitivity
Adipogenesis ↑

Figure 6

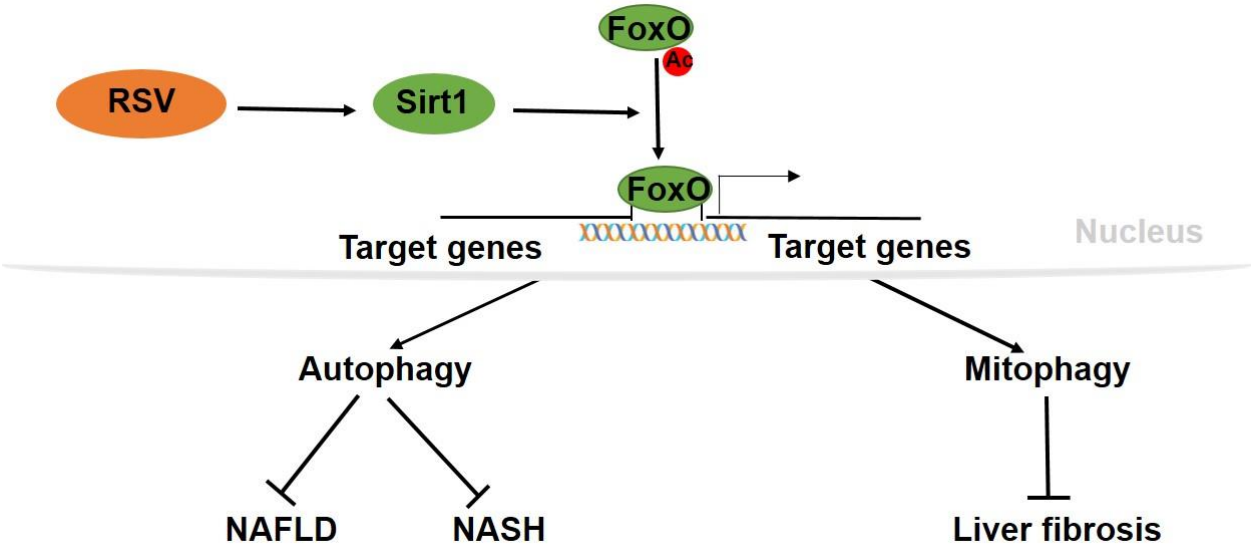
FoxO
Ac
RSV
Sirt1
FoxO
Target genes
Target genes
Nucleus
Autophagy
Mitophagy
NAFLD
NASH
Liver fibrosis

Figure 7

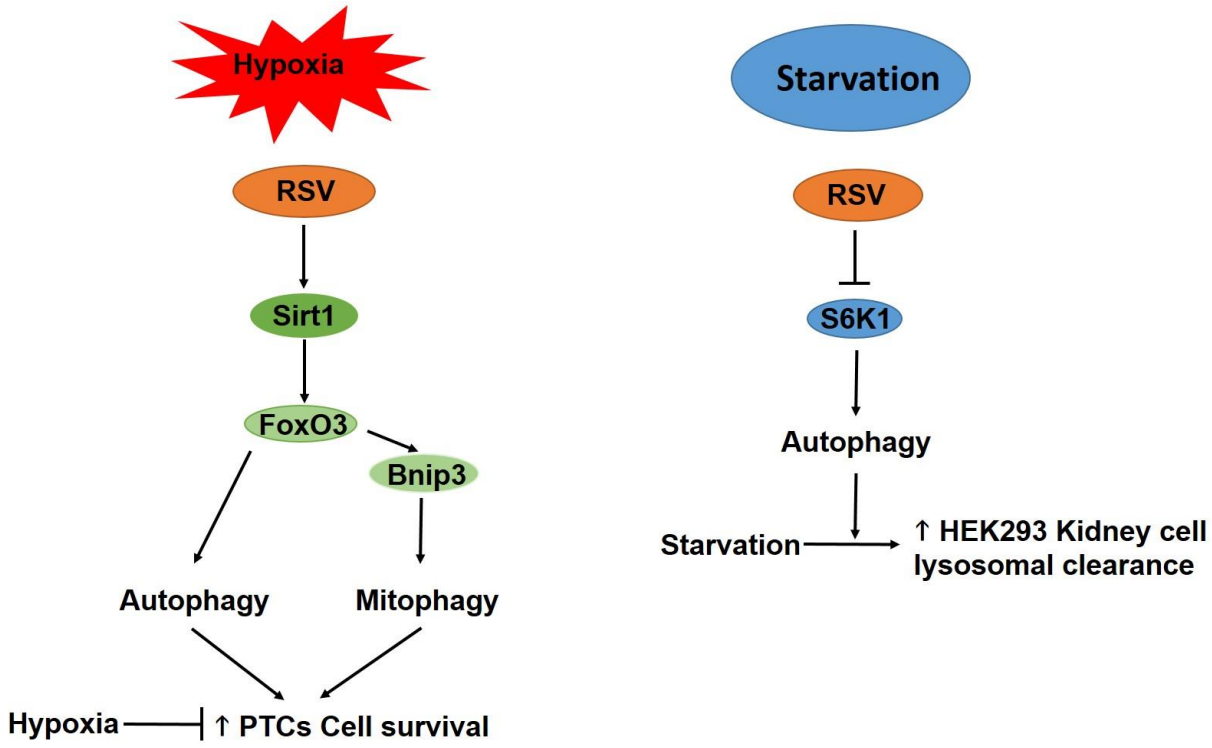
Hypoxia
RSV
Sirt1
FoxO3
Bnip3
Autophagy
Mitophagy
Hypoxia
↑ PTCs Cell survival
Starvation
RSV
S6K1
Autophagy
Starvation
↑ HEK293 Kidney cell lysosomal clearance

Figure 8

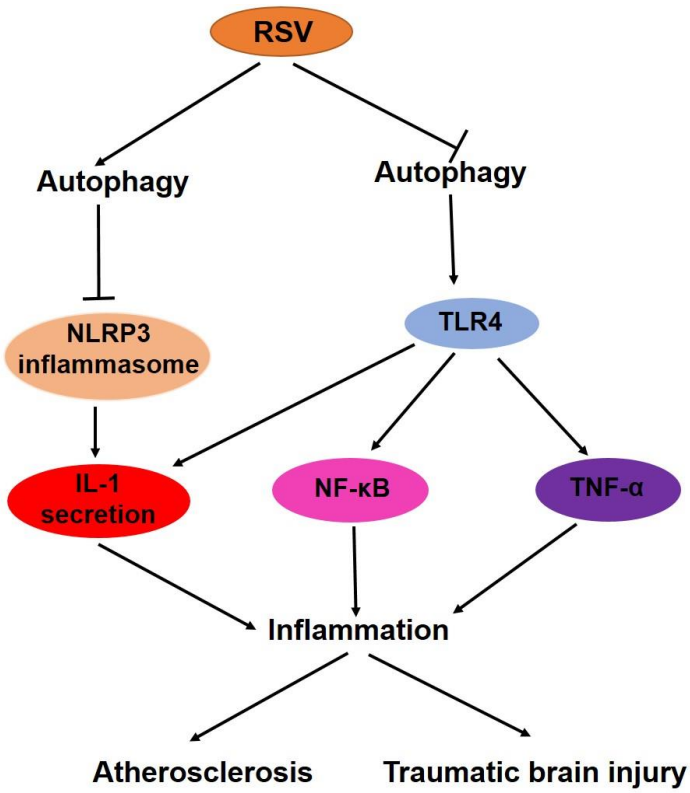
RSV
Autophagy
Autophagy
NLRP3 inflammasome
TLR4
IL-1 secretion
NF-κB
TNF-α
Inflammation
Atherosclerosis
Traumatic brain injury

Figure 9

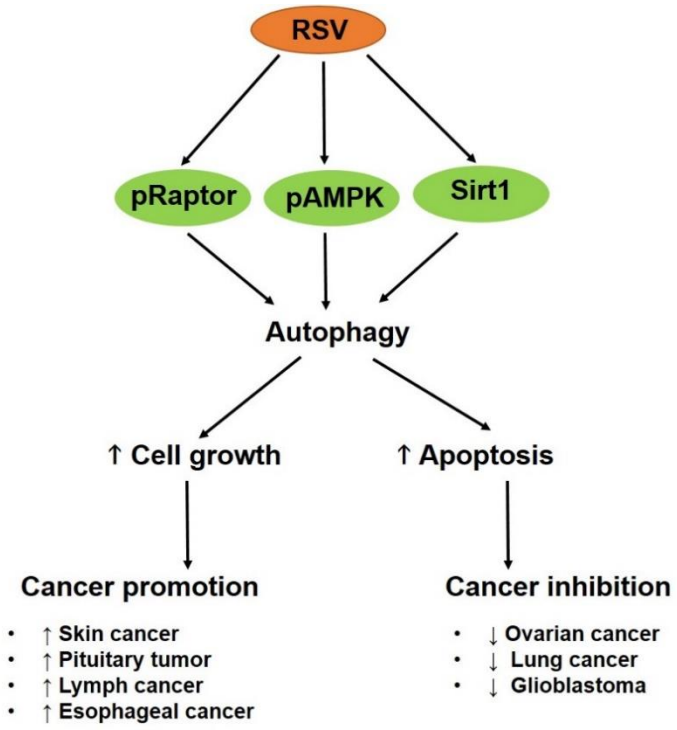
RSV
pRaptor
pAMPK
Sirt1
Autophagy
↑ Cell growth
↑ Apoptosis
Cancer promotion
• ↑ Skin cancer
• ↑ Pituitary tumor
• ↑ Lymph cancer
• ↑ Esophageal cancer
Cancer inhibition
• ↓ Ovarian cancer
• ↓ Lung cancer
• ↓ Glioblastoma

Figure 10

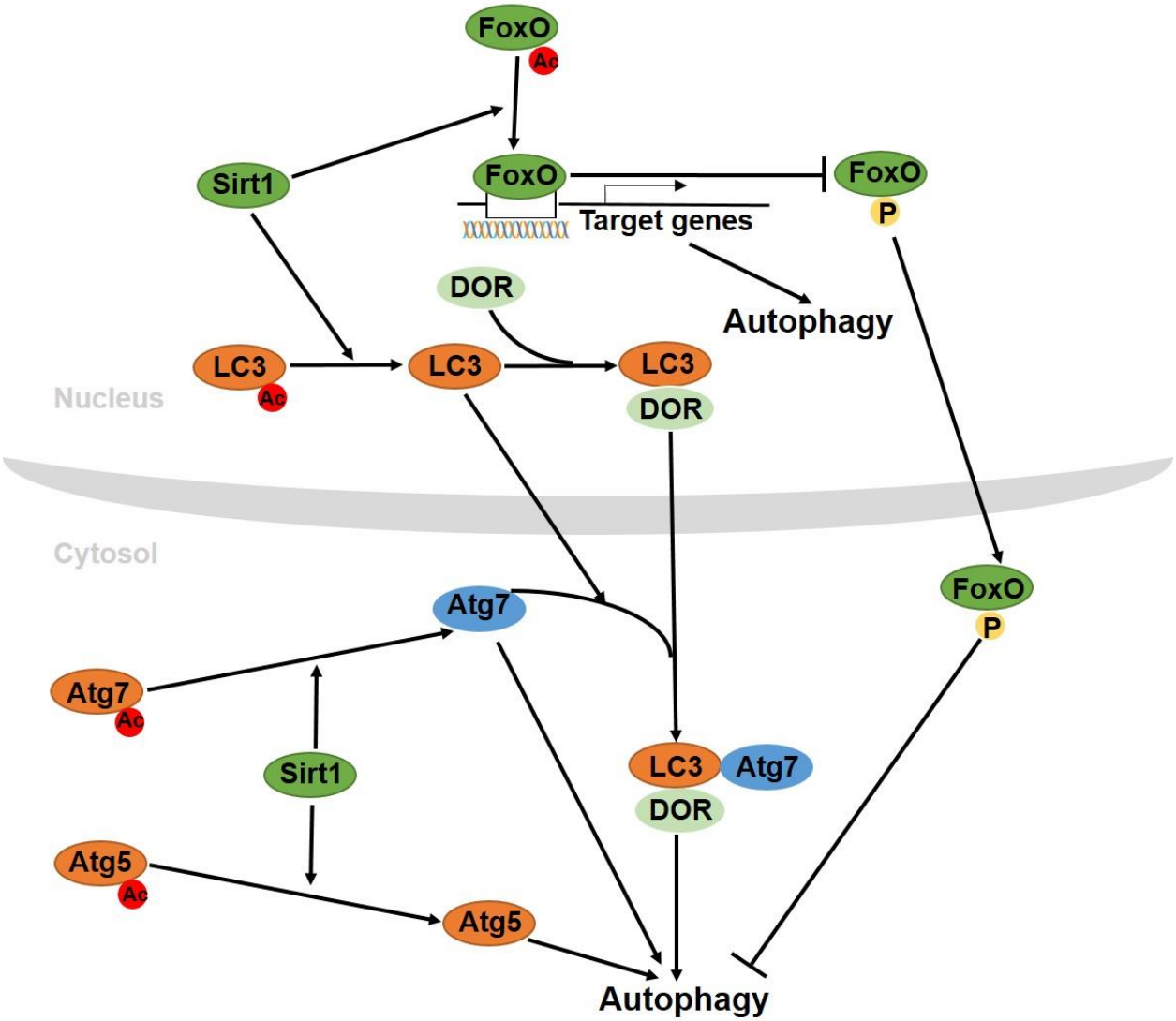
FoxO
Ac
Sirt1
FoxO
Target genes
FoxO
P
DOR
Autophagy
LC3
Ac
LC3
LC3
DOR
Nucleus
Cytosol
Atg7
FoxO
P
Atg7
Ac
Sirt1
LC3
Atg7
DOR
Atg5
Ac
Atg5
Autophagy

Chapter 2 Introduction

1. The Sirtuin family

The sirtuins (Sirts), a family of nicotinamide adenine dinucleotide (NAD+)-dependent deacetylases, include Sirt1-Sirt7 and are involved in the regulation of various cellular metabolisms and metabolic diseases [1, 2, 3, 4], in which Sirt1 is most abundantly studied. Sirt1 play its role in metabolism through its deacetylating effects on histones and non-histone proteins that are participated in different organ metabolisms and diseases, including adipose tissue [5, 6], muscle [7, 8, 9], liver [10, 11, 12], heart [13, 14, 15], brain [16, 17, 18, 19, 20] and *etc*.

2. The role of Sirt1 in metabolism

2.1 Sirt1 in adipose tissue

Obesity is a rapidly growing epidemic. It may arise from increased energy intake and/or reduced energy expenditure [21]. White adipose tissue (WAT) is the major energy reservoir to store redundant energy in the form of triglyceride [22]. Morphologically and functionally distinct from WAT, brown adipose tissue (BAT) is composed of brown adipocytes with multilocular morphology, dense mitochondrial and the ability to activate thermogenesis upon cold treatment [23]. Recent studies indicated that activation of BAT promotes lipid metabolism in rodents [24] and humans [25], proposing its anti-obesity potential.

In WAT, as an energy sensor, Sirt1 is downregulated in obesity [5]. In high fat diet-induced and genetic obesity mice, full length of Sirt1 was cleaved by caspase 1 into inactive form in adipose tissue [26]. Furthermore, gene expression in high fat diet fed mice were greatly recapitulated in adipose tissue Sirt1 knockout mice [26]. Specific activation or gain function of Sirt1 protected rodents from diet-induced obesity and insulin resistance [27, 28]. The potent Sirt1 activator

SRT1720 administration protected mice from diet-induced obesity through elevating fatty acid oxidation by deacetylation of PGC-1α, FoxO1 and stimulation of AMPK signaling [27]. However, on normal chow diet transgenic mice overexpression of Sirt1 showed normal insulin sensitivity as wild type mice [28]. Only on high fat diet challenge or db/db background, Sirt1 overexpression improved glucose tolerance [28]. Sirt1 knockout female mice showed higher body weight and fat percentage than wild type, but shared similar GTT and ITT profile on normal chow diet [26]. After high fat diet challenge, Sirt1 knockout mice deteriorated GTT and ITT profile with lower adiponectin in plasma [26]. Consistently, Sirt1 knockout males has higher body weight and fat percentage on normal chow diet [29]. However, Sirt1 knockout showed low-grade inflammation but glucose intolerance and insulin resistance, which was similarly exhibited during short-term (5 weeks) high fat diet challenge. In contrast to short-term high fat diet, on chronic (15 weeks) high fat diet feeding Sirt1 knockout mice improved glucose intolerance, insulin resistance and inflammation [29].

In cellular level, Sirt1 suppressed preadipocyte proliferation [30], preadipocyte differentiation [5] and promoted browning of white adipocyte [6]. During 3T3L1 preadipocyte proliferation, Srit1 knockdown resulted in hyperplastic and inflamed adipocytes that were dysfunctional through hyperacetylation and activation of c-Myc, which is a transcriptional factor responsible for cell proliferation [30]. During 3T3L1 preadipocyte differentiation, Sirt1 docked with PPARγ's cofactors NCoR (nuclear receptor co-repressor) and SMRT (silencing mediator of retinoid and thyroid hormone receptors) to suppress PPARγ [5]. Overexpression of Sirt1 suppressed PPARγ expression and adipogenesis, while silencing Sirt1 increased PPARγ expression and adipogenesis [5]. In WAT, Sirt1 promoted the release of free fatty acid from adipocyte by repressing PPARγ during energy restriction, indicating Sirt1's inhibitory role in WAT

development [5]. In addition, Sirt1 promoted browning of subcutaneous WAT following acute cold exposure [6]. After 4 °C overnight cold treatment, Sirt1 overexpression induced browning of subcutaneous as increased numbers of UCP1-immunoreactive paucilocular adipocytes [6].

Other than direct targeting on adipocyte of WAT, gain or loss function of Sirt1 in adipocyte had effects on recruitment of macrophage into WAT [31]. Adipose tissue specific knockout of Sirt1 in mice had increased WAT expression of macrophage and inflammatory factor TNF-α and NF-κB nuclear translocation and gene expression by reducing H3K9 deacetylation [31].

In brown adipocyte, UCP1 expression is controlled by Sirt1 and is reduced under inflammation, which could be rescued by Sirt1 activation through resveratrol treatment [32]. *In vivo*, gain function of Sirt1 enhanced insulin sensitivity through induction of glucose uptake in BAT and improved body temperature maintenance upon cold challenge [33]. Mechanistically, Sirt1 showed no effect on differentiation of BAT, but promoted metabolic transcriptional response to β3-adrenergic stimuli in differentiated adipocytes [33].

In conclusion, Sirt1 ameliorated adipocyte hyperplasticity, inflammation through inhibiting preadipocyte proliferation and differentiation, and promoted adipocyte browning. However, in adipose tissue Sirt1 may physiologically play distinct roles due to variations of dietary challenge, gender and genetic background.

2.2 Sirt1 in muscle

Skeletal muscle is able to induce mitochondrial biogenesis in response to metabolic stress, such as fasting and exercise [34]. During these physical and physiological challenge, Sirt1 is widely investigated in muscular mitochondrial biogenesis both in rodents and humans [35, 36]. Under these conditions of metabolic stress, Sirt1 is known to regulate a number of protein targets, including

peroxisome proliferator-activated receptor-γ coactivator 1α (PGC1α), 5' AMP-activated protein kinase (AMPK), p53 and *etc.*, which are potential signaling nodes participating in mitochondrial biogenesis [37]. Among which, PGC1α is the most well studied linkage between Sirt1 and mitochondrial biogenesis in muscle.

Most of *in vitro* studies pointed that Sirt1 positively regulates PGC1α transcriptionally or post transcriptionally to induce mitochondrial biogenesis [38, 39]. Transcriptionally, in C2C12 myotubes Sirt1 bound to the proximal promoter region of the PGC1α gene, which promoted a positive auto-regulatory PGC1α expression loop [38]. Posttranscriptionally, Sirt1 deacetylated PGC1α to activate its activity and downstream mitochondrial biogenesis [39]. Also, during fasting and low glucose concentrations Sirt1 was responsible for deacetylating PGC1α, accompanied by activation of fatty acid oxidation and increased expression of mitochondrial genes, as shown by gene expression of PDK4, ERRα, cytochrome c in C2C12 muscle cells [9]. However, *in vivo* studies may not be consistent with *in vitro* studies and even contradict with observations found *in vitro*. For example, in skeletal muscle subject to voluntary wheel running and electric stimulation, PGC1α level was not closely associated with Sirt1 expression and enzymatic deacetylase activity [40]. Further, lacking Sirt1 deacetylase activity in skeletal muscle did not impair wheel running-induced PGC1α expression and mitochondrial biogenesis [41], suggesting Sirt1 may not be required for PGC1α expression and mitochondrial biogenesis. Another study even proposed that Sirt1 overexpression in rodent muscle downregulated PGC1α and mtTFA and COX IV [42].

Taken all these observations together, discrepancies existed between *in vitro* and *in vivo* studies probably due to the fact that cell culture medium system and physiological conditions are quite different. Further studies are warranted to compare the experimental conditions and relativeness

of *in vitro* and *in vivo* studies before translating observations acquired from cell culture to animal and human studies.

2.3 Sirt1 in liver

Sirt1 plays important roles in the regulation of lipid metabolism in liver, the dysfunction of which may result in the development of alcoholic liver disease [43] and nonalcoholic fatty liver disease (NAFLD), including hepatic steatosis, inflammation, insulin resistance and liver damage [12, 44, 45].

In alcoholic liver disease, liver samples from patients with alcohol hepatitis had reduced levels of Sirt1 than healthy counterparts [44]. Hepatic deletion of Sirt1 promoted lipid accumulation and inflammatory cytokines, whereas overexpression of Sirt1 reversed ethanol induced fat accumulation and metabolic dysfunction in liver [44]. Phamathetical administration of rosiglitazone, a peroxisomal proliferator-activated receptor-γ (PPAR- γ), ameliorated alcoholic fatty liver in mice through enhanced hepatic adiponectin-Sirt1-AMPK signaling [43].

NAFLD is characterized by hepatic endoplasmic reticulum (ER) stress [12], insulin resistance [46] and inflammation [47]. Also, the expression of Sirt1 is reduced by genetic and high fat diet induced NAFLD [12, 48]. The reduction of Sirt1 may due to phosphorylation by C-Jun N-terminal kinase 1 (JNK1) and casein kinase 2, which promoted its subsequent degradation by proteasome and inhibited its nuclear localization [49, 50]. Lack of Sirt1 activity contributed to liver steatosis in response to high fat diet feeding, which may result from increased lipogenesis and reduce lipid export [47]. In low-density lipoprotein receptor-deficient mice with diet-induced insulin-resistance and genetically obese mice, overexpression of Sirt1 in liver attenuated hepatic steatosis and insulin resistance through inhibition of ER stress, enhanced insulin receptor and mTORC1

signaling [12]. In liver, Sirt1 promoted insulin sensitivity through transcriptional promotion of the gene encoding Rictor, and its activation on phosphorylation of Akt and forkhead box O1 (FoxO1) [51], leading to reduced transcription of the gluconeogenic genes glucose-6-phosphatase (G6pase) and phosphoenolpyruvate carboxykinase (Pepck) [52]. Liver specific knockdown of Sirt1 contributed to hepatic glucose over-production and hyperglycemia [52]. However, discrepancies raised in the study that Sirt1 knockdown in type 2 diabetes mellitus (T2DM) mice model increased insulin sensitivity and reduced glucose production through decreased Pepck, fructose-1,6-bisphosphatase (FBPase) and G6pase due to increased acetylation of signal transducer and activator of transcription 3 (STAT3), FoxO1 and PGC1α [53]. The controversial effects of Sirt1 knockout may explain by the fact that Sirt1 is involved in multiple signaling pathways and plays distinct roles in different disease condition.

2.4 Sirt1 in heart

Hear failure results from aging, mechanical load and drug-caused cardiotoxicity [54, 55, 56]. Sirt1 played protective roles in preventing heart from aging [13, 57], mechanical and physiological pressure [58, 59], and cardiotoxicity [15]. However, detrimental roles of over-activation of Sirt1 in heart are role documented [13, 60].

Compared with healthy cardiomyocytes, Sirt1 was downregulated in cardiomyocytes from advanced heart failure human patients [61]. Both *in vitro* and *in vivo,* Sirt1 inhibition or deficiency increased endoplasmic reticulum (ER) stress-induced cardiac injury [62]. Activation of Sirt1 by chemical is protective from cardiac injury and ameliorated ER stress induced cardiomyocyte apoptosis by attenuating PERK/elF2α pathway activation [62]. *In vitro,* Sirt1 reduced acetylation of FoxO1 and downstream Rab7 (a small GTP-binding protein that mediates late autophagosome-

lysosome fusion), which is essential for maintaining cardiomyocyte function during starvation [63]. In neonatal cardiomyocyte, Sirt1 coordinated with PPARα to suppress hypertrophy *in vitro* as shown by the evidence that activation of Sirt1 by resveratrol or overexpression of Sirt1 inhibited phenylephrine (PE)-induced hypertrophy and inhibited PE-induced down-regulation of fatty acid oxidation genes [59].

In vivo, knockdown of Sirt1 led to dilated cardiomyopathy and reduced cardiomyocyte size, which was accompanied by reduced mitochondrial genes (Tfam, cytochrome b, ND1) [64]. This phenotype was due to increased acetylation level of the myocyte enhancer factor 2 (Mef2) transcription factor, which is essential for normal heart development and mitochondrial integrity [64]. In dystrophin-deficient mdx mice, Sirt1 suppresses cardiac hypertrophy and fibrosis through its deacetylation of lysine residues for ubiquitination of p300, a pro-hypertrophic co-activator, to promote its subsequent degradation by ubiquitin-proteasome [65]. As to protective effects against drug-induced cardiotoxicity, resveratrol ameliorated doxorubicin induced cardiomyocyte apoptosis through activating Sirt1 and its deacetylation effects on p53 *in vivo* [66]. *In vivo*, low or moderate (2.5 fold or 7.5 fold) overexpression of Sirt1 in the heart attenuated age-dependent increases in cardiac hypertrophy, apoptosis/fibrosis, and cardiac dysfunction. However, a high level of Sirt1 overexpression showed opposite effects [13].

Nevertheless, Sirt1 was upregulated by pressure overload in the heart, and knockdown of Sirt1 attenuated pressure overload induced cardiac hypertrophy and failure [55]. Sirt1 was shown to coordinate with PPARα to suppress genes in mitochondrial function that are regulated by estrogen-related receptors (ERRs), which leads to cardiac dysfunction. Similarly, cardiac specific overexpression of Sirt1 impaired cardiac function associated with reduced mitochondrial function genes (like cytochrome b, cytochrome c and Cox5a) and respiration [60].

2.5 Sirt1 in brain

In brain, Sirt1 is highly expressed in metabolically active sites, including hypothalamic arcuate, dorsomedial, ventromedial, and paraventricular nuclei and the area postrema and the nucleus of the solitary tract in the hindbrain [67]. Like adipose tissue, muscle and heart, Sirt1 expression increased in the brain during nutrient deprivation [67, 68, 69]. Physiologically, Sirt1 regulates neural development [17], energy balance and glucose metabolism in neurons [70], and neural diseases [18, 20, 71, 72, 73]. In cellular level, Sirt1 mediates neuronal cell differentiation [74], cell expansion [75], and cell death [76].

Hypothalamic Sirt1 regulated energy balance as shown by the evidence that pharmacological or genetic silencing of Sirt1 in hypothalamus decreased food intake and body weight gain [16]. Neural Sirt1 negatively regulated systemic and hypothalamic insulin signaling through directly deacetylating and repressing IRS-1 function [70]. Specifically, Sirt1 knockout in neurons promoted insulin sensitivity and had lower fasting insulin levels, improved glucose tolerance and insulin tolerance in systemic and hypothalamic level as shown by increased PI3K signaling, pAkt and pFoxO1 [70].

Alzheimer disease (AD) onset and progression is characterized by accumulation of aggregated β-amyloid [19]. Overexpression or activation of Sirt1 mimicked the effects of caloric restriction that it attenuated β-amyloid content in the brain and amyloid neuropathology through repressing serine/threonine Rho kinase (ROCK1) and promoting its downstream non-amyloidogenic α-secretase's cleavage of the amyloid precursor protein [20]. In an inherited neurodegenerative disorder caused by glutamine repeat expansion in huntingtin protein (HTT), mutant HTT interfered with Sirt1 to repress the TORC1-CREB interaction to suppress brain-derived neurotrophic factor (BDNF) transcription. Sirt1 overexpression would deacetylate TORC1 to

induce the effects of TORC1-CREB on BDNF to rescue the defects in this type of neurodegenerative disorder [18]. In addition, Sirt1 could deacetylate methyl-CpG binding protein 2 (MeCP2), an epigenetic regulator, and activate its DNA binding activity to BDNF promoter to induce its expression in brain [77].

In cellular level, nuclear translocalization of Sirt1 was indispensable for neural precursor cells differentiation upon differentiation stimuli, which was through its binding with nuclear receptor corepressor (N-CoR) and synergistically increased the number of $Tuj1^+$ neurons [74]. Sirt1 was reported to be negatively involved in oligodendrocytes regeneration during adulthood. Lack of active Sirt1 in neural stem cells increased the production of new oligodendrocyte progenitor cells (OPCs) and its expansion into oligodendrocyte [75]. In neuronal cells, Sirt1 overexpression promoted neurite outgrowth and enhances tolerance to cell death or degeneration induced by amyloid-β1-42 oligomers probably by its inhibition on mTOR signaling [76]. Other than its cell survival effects, Sirt1 directly modulated synaptic plasticity and memory formation by microRNA. It was shown by the results that activation of Sirt1 promoted synaptic function through repressing the expression of miR-134 by a repressor complex containing the transcription factor YY1, and consequent translational induction of cAMP response binding protein (CREB) and brain-derived neurotrophic factor (BDNF) [78].

3. Gender difference in metabolism

As to body composition, women have higher fat percentage but lower lean tissue percentage than men [79, 80]. Because of the difference in body composition, men have higher glycolytic capacity and higher basal metabolic rate than women [81, 82]. It has been reported that insulin sensitivity is

inversely correlated with fat percentage [83]. Other than fat percentage, regional difference of adipose tissue distribution would also affect glucose metabolism and insulin sensitivity [84]. Visceral fat accumulation is thought to develop insulin resistance, but not subcutaneous fat [85, 86]. Women have higher level of subcutaneous fat [87], while men have higher level of visceral fat [88]. Estrogen-autophagy-adipogenesis axis maybe account for this gender difference [89]. The prevalence of insulin resistance is higher in men than in women, which in partially could be explained by estrogen [88].

In skeletal muscle, females have lower overall capacity for aerobic oxidation and for anaerobic glycolysis than males, but have a higher capacity for β-oxidation [90], which may explain why females have advantages on the fatigability of skeletal muscle [81]. In heart, females rely more on fatty acid β-oxidation as energetics than males [91, 92]. Estrogen would promote fatty acid oxidation and decrease glucose metabolism in oxygen sufficient condition, thus estrogen exhibited cardio-protective effect and explained lower incidence of cardiovascular disease in females [93]. In non-alcoholic fatty liver disease (NAFLD), males have a more severe metabolic phenotype with high glucose level, lower plasma adiponectin and high-density lipoprotein cholesterol levels [94]. However, concerning what factor in liver contributes to this gender difference it is still little known. In brain, gender difference exists in every brain lobe, such as hippocampus, amygdala and neocortex, which affects brain development, function and disease predisposition [95, 96]. For example, in Alzheimer's disease related pathology men showed high level of phosphorylated tau protein in hypothalamus region, while women shower higher in the nucleus basalis of Meynert [97]. Therefore, understanding molecular mechanism of gender difference in brain will better the development of specific treatment of neural disease in both genders.

4. Proposal

As mentioned above, Obesity is a rapidly growing epidemic and accompanied by other metabolic diseases [21]. In humans and other mammals, obesity is characterized by excessive accumulation of white adipose tissue (WAT), which functions as a major energy reservoir to store redundant energy in the form of triglyceride [22]. Autophagy, a cellular self-digestive process, is involved in cell differentiation, survival, development and remodeling[98]. Blockage of autophagy suppressed adipogenesis and adiposity and prevented rodent from diet induce obesity[22, 99]. Thus, targeting autophagy may be a promising strategy to combat obesity and related metabolic disease.

Estrogen signaling plays an important role in adiposity. In rodents, ovariectomy increases WAT weight and estrogen replacement lowers WAT weight [100]. In postmenopausal women, WAT mass was increased but estrogen therapy could reverse it [101]. A mechanistic study showed that estradiol (E2) negatively regulated PPARγ and blocked adipogenesis through estrogen receptors ERα and ERβ both *in vitro and in vivo* [102]. Moreover, estrogen receptor α (ERα) knockout mice developed more WAT mass, larger and more adipocytes, accompanied by insulin resistance and impaired metabolism [103]. However, it is unknown whether autophagy is involved in the estrogen-mediated adipogenesis.

As an energy sensor, Sirt1 (a NAD-dependent deacetylase) is downregulated in obesity, and its role in WAT development has been reported [5]. Importantly, specific Sirt1 activator protects rodents from diet-induced obesity and insulin resistance [27]. It was shown that Sirt1 promoted the release of free fatty acid from adipocyte by repressing PPARγ in WAT during energy restriction [5]. In addition, Sirt1 promotes browning of subcutaneous WAT following acute cold exposure [6]. Given the regulatory role of both autophagy and Sirt1 in adiposity, we ask whether Sirt1 may suppress adipogenesis through autophagy.

As discussed above, both energy sensing factors (e.g., Sirt1) and hormone signaling (e.g., ERα) control metabolism and energy balance [104, 105, 106]. Emerging evidence of the interaction of ERα with Sirt1 suggests that, in breast cancer MCF-7 cells Sirt1 deacetylase activity is responsible for promoting ERα expression [107]. In hepatocyte and fibroblast, however, Sirt1 deacetylates ERα resulting in elevation of its DNA-binding activity [108]. Currently, little is known in adipocytes on how Sirt1 interacts with ERα and how the interaction affects autophagy and adipogenesis.

The dissertation project was aiming to answer these questions. Firstly, a protocol to monitor autophagy flux activity during adipocyte differentiation was developed. Then, this project investigated how Sirt1 and ERα individually and collaboratively interacted with autophagy to suppress adipogenesis and adiposity. Lastly, the regulating order of Sirt1 and ERα in these regulatory events was determined by using cell and mouse models.

Reference

1. Fang J, Ianni A, Smolka C, Vakhrusheva O, Nolte H, Krüger M, *et al.* Sirt7 promotes adipogenesis in the mouse by inhibiting autocatalytic activation of Sirt1. *Proceedings of the National Academy of Sciences* 2017, **114**(40)**:** E8352-E8361.

2. Lemos V, De Oliveira RM, Naia L, Szegö É, Ramos E, Pinho S, *et al.* The NAD+-dependent deacetylase SIRT2 attenuates oxidative stress and mitochondrial dysfunction and improves insulin sensitivity in hepatocytes. *Human molecular genetics* 2017, **26**(21)**:** 4105-4117.

3. Jing E, Gesta S, Kahn CR. SIRT2 regulates adipocyte differentiation through FoxO1 acetylation/deacetylation. *Cell metabolism* 2007, **6**(2)**:** 105-114.

4. Shi T, Wang F, Stieren E, Tong Q. SIRT3, a mitochondrial sirtuin deacetylase, regulates mitochondrial function and thermogenesis in brown adipocytes. *Journal of Biological Chemistry* 2005.

5. Picard F, Kurtev M, Chung N, Topark-Ngarm A, Senawong T, De Oliveira RM, *et al.* Sirt1 promotes fat mobilization in white adipocytes by repressing PPAR-γ. *Nature* 2004, **429**(6993)**:** 771.

6. Qiang L, Wang L, Kon N, Zhao W, Lee S, Zhang Y, *et al.* Brown remodeling of white adipose tissue by SirT1-dependent deacetylation of Pparγ. *Cell* 2012, **150**(3)**:** 620-632.

7. Cantó C, Jiang LQ, Deshmukh AS, Mataki C, Coste A, Lagouge M, *et al.* Interdependence of AMPK and SIRT1 for metabolic adaptation to fasting and exercise in skeletal muscle. *Cell metabolism* 2010, **11**(3)**:** 213-219.

8. Gao P, Xu T-T, Lu J, Li L, Xu J, Hao D-L, *et al.* Overexpression of SIRT1 in vascular smooth muscle cells attenuates angiotensin II-induced vascular remodeling and hypertension in mice. *Journal of molecular medicine* 2014, **92**(4)**:** 347-357.

9. Gerhart-Hines Z, Rodgers JT, Bare O, Lerin C, Kim SH, Mostoslavsky R, *et al.* Metabolic control of muscle mitochondrial function and fatty acid oxidation through SIRT1/PGC-1α. *The EMBO journal* 2007, **26**(7)**:** 1913-1923.

10. Cao Y, Xue Y, Xue L, Jiang X, Wang X, Zhang Z, *et al.* Hepatic menin recruits SIRT1 to control liver steatosis through histone deacetylation. *Journal of hepatology* 2013, **59**(6)**:** 1299-1306.

11. Kim H-S, Xiao C, Wang R-H, Lahusen T, Xu X, Vassilopoulos A, *et al.* Hepatic-specific disruption of SIRT6 in mice results in fatty liver formation due to enhanced glycolysis and triglyceride synthesis. *Cell metabolism* 2010, **12**(3)**:** 224-236.

12. Li Y, Xu S, Giles A, Nakamura K, Lee JW, Hou X, *et al.* Hepatic overexpression of SIRT1 in mice attenuates endoplasmic reticulum stress and insulin resistance in the liver. *The FASEB Journal* 2011, **25**(5)**:** 1664-1679.

13. Alcendor RR, Gao S, Zhai P, Zablocki D, Holle E, Yu X, *et al.* Sirt1 regulates aging and resistance to oxidative stress in the heart. *Circulation research* 2007, **100**(10)**:** 1512-1521.

14. Hsu C-P, Odewale I, Alcendor RR, Sadoshima J. Sirt1 protects the heart from aging and stress. *Biological chemistry* 2008, **389**(3)**:** 221-231.

15. Ruan Y, Dong C, Patel J, Duan C, Wang X, Wu X, *et al.* SIRT1 suppresses doxorubicin-induced cardiotoxicity by regulating the oxidative stress and p38MAPK pathways. *Cellular Physiology and Biochemistry* 2015, **35**(3)**:** 1116-1124.

16. Çakir I, Perello M, Lansari O, Messier NJ, Vaslet CA, Nillni EA. Hypothalamic Sirt1 regulates food intake in a rodent model system. *PloS one* 2009, **4**(12)**:** e8322.

17. Herskovits AZ, Guarente L. SIRT1 in neurodevelopment and brain senescence. *Neuron* 2014, **81**(3)**:** 471-483.

18. Jeong H, Cohen DE, Cui L, Supinski A, Savas JN, Mazzulli JR, *et al.* Sirt1 mediates neuroprotection from mutant huntingtin by activation of the TORC1 and CREB transcriptional pathway. *Nature medicine* 2012, **18**(1)**:** 159.

19. Selkoe DJ. Amyloid β-protein and the genetics of Alzheimer's disease. *Journal of Biological Chemistry* 1996, **271**(31)**:** 18295-18298.

20. Qin W, Yang T, Ho L, Zhao Z, Wang J, Chen L, *et al.* Neuronal SIRT1 activation as a novel mechanism underlying the prevention of Alzheimer disease amyloid neuropathology by calorie restriction. *Journal of Biological Chemistry* 2006, **281**(31)**:** 21745-21754.

21. Liu L, Zou P, Zheng L, Linarelli LE, Amarell S, Passaro A, *et al.* Tamoxifen reduces fat mass by boosting reactive oxygen species. *Cell death & disease* 2015, **6**(1)**:** e1586.

22. Singh R, Xiang Y, Wang Y, Baikati K, Cuervo AM, Luu YK, *et al.* Autophagy regulates adipose mass and differentiation in mice. *The Journal of clinical investigation* 2009, **119**(11)**:** 3329-3339.

23. Kajimura S, Spiegelman BM, Seale P. Brown and beige fat: physiological roles beyond heat generation. *Cell metabolism* 2015, **22**(4)**:** 546-559.

24. Liu X, Wang S, You Y, Meng M, Zheng Z, Dong M, *et al.* Brown adipose tissue transplantation reverses obesity in Ob/Ob mice. *Endocrinology* 2015, **156**(7)**:** 2461-2469.

25. Chondronikola M, Volpi E, Børsheim E, Porter C, Saraf MK, Annamalai P, *et al.* Brown adipose tissue activation is linked to distinct systemic effects on lipid metabolism in humans. *Cell metabolism* 2016, **23**(6)**:** 1200-1206.

26. Chalkiadaki A, Guarente L. High-fat diet triggers inflammation-induced cleavage of SIRT1 in adipose tissue to promote metabolic dysfunction. *Cell metabolism* 2012, **16**(2)**:** 180-188.

27. Feige JN, Lagouge M, Canto C, Strehle A, Houten SM, Milne JC, *et al.* Specific SIRT1 activation mimics low energy levels and protects against diet-induced metabolic disorders by enhancing fat oxidation. *Cell metabolism* 2008, **8**(5)**:** 347-358.

28. Banks AS, Kon N, Knight C, Matsumoto M, Gutiérrez-Juárez R, Rossetti L, *et al.* SirT1 gain of function increases energy efficiency and prevents diabetes in mice. *Cell metabolism* 2008, **8**(4)**:** 333-341.

29. Mayoral R, Osborn O, McNelis J, Johnson AM, Izquierdo CL, Chung H, *et al.* Adipocyte SIRT1 knockout promotes PPARγ activity, adipogenesis and insulin sensitivity in chronic-HFD and obesity. *Molecular metabolism* 2015, **4**(5)**:** 378-391.

30. Abdesselem H, Madani A, Hani A, Al-Noubi M, Goswami N, Hamidane HB, *et al.* SIRT1 limits adipocyte hyperplasia through c-Myc inhibition. *Journal of Biological Chemistry* 2016, **291**(5)**:** 2119-2135.

31. Gillum MP, Kotas ME, Erion DM, Kursawe R, Chatterjee P, Nead KT, *et al.* SirT1 regulates adipose tissue inflammation. *Diabetes* 2011, **60**(12)**:** 3235-3245.

32. Nøhr MK, Bobba N, Richelsen B, Lund S, Pedersen SB. Inflammation Downregulates UCP1 expression in brown adipocytes potentially via SIRT1 and DBC1 interaction. *International journal of molecular sciences* 2017, **18**(5)**:** 1006.

33. Boutant M, Joffraud M, Kulkarni SS, García-Casarrubios E, García-Roves PM, Ratajczak J, *et al.* SIRT1 enhances glucose tolerance by potentiating brown adipose tissue function. *Molecular metabolism* 2015, **4**(2)**:** 118-131.

34. Gurd BJ. Deacetylation of PGC-1α by SIRT1: importance for skeletal muscle function and exercise-induced mitochondrial biogenesis. *Applied Physiology, Nutrition, and Metabolism* 2011, **36**(5)**:** 589-597.

35. Suwa M, Nakano H, Radak Z, Kumagai S. Endurance exercise increases the SIRT1 and peroxisome proliferator-activated receptor γ coactivator-1α protein expressions in rat skeletal muscle. *Metabolism-Clinical and Experimental* 2008, **57**(7)**:** 986-998.

36. Gurd BJ, Perry CG, Heigenhauser GJ, Spriet LL, Bonen A. High-intensity interval training increases SIRT1 activity in human skeletal muscle. *Applied Physiology, Nutrition, and Metabolism* 2010, **35**(3)**:** 350-357.

37. Philp A, Schenk S. Unraveling the complexities of SIRT1-mediated mitochondrial regulation in skeletal muscle. *Exercise and sport sciences reviews* 2013, **41**(3)**:** 174.

38. Amat R, Planavila A, Chen SL, Iglesias R, Giralt M, Villarroya F. SIRT1 controls the transcription of the peroxisome proliferator-activated receptor-γ co-activator-1α (PGC-1α) gene in skeletal muscle through the PGC-1α autoregulatory loop and interaction with MyoD. *Journal of biological chemistry* 2009, **284**(33)**:** 21872-21880.

39. Nemoto S, Fergusson MM, Finkel T. SIRT1 functionally interacts with the metabolic regulator and transcriptional coactivator PGC-1α. *Journal of Biological Chemistry* 2005, **280**(16)**:** 16456-16460.

40. Chabi B, Adhihetty PJ, O'Leary MF, Menzies KJ, Hood DA. Relationship between Sirt1 expression and mitochondrial proteins during conditions of chronic muscle use and disuse. *Journal of applied physiology* 2009, **107**(6)**:** 1730-1735.

41. Philp A, Chen A, Lan D, Meyer GA, Murphy AN, Knapp AE, *et al.* Sirtuin 1 (SIRT1) deacetylase activity is not required for mitochondrial biogenesis or peroxisome proliferator-activated receptor-γ coactivator-1α (PGC-1α) deacetylation following endurance exercise. *Journal of Biological Chemistry* 2011, **286**(35)**:** 30561-30570.

42. Gurd BJ, Yoshida Y, Lally J, Holloway GP, Bonen A. The deacetylase enzyme SIRT1 is not associated with oxidative capacity in rat heart and skeletal muscle and its

overexpression reduces mitochondrial biogenesis. *The Journal of physiology* 2009, **587**(8)**:** 1817-1828.

43. Shen Z, Liang X, Rogers CQ, Rideout D, You M. Involvement of adiponectin-SIRT1-AMPK signaling in the protective action of rosiglitazone against alcoholic fatty liver in mice. *American Journal of Physiology-Gastrointestinal and Liver Physiology* 2009, **298**(3)**:** G364-G374.

44. Yin H, Hu M, Liang X, Ajmo JM, Li X, Bataller R, *et al.* Deletion of SIRT1 from hepatocytes in mice disrupts lipin-1 signaling and aggravates alcoholic fatty liver. *Gastroenterology* 2014, **146**(3)**:** 801-811.

45. Purushotham A, Schug TT, Xu Q, Surapureddi S, Guo X, Li X. Hepatocyte-specific deletion of SIRT1 alters fatty acid metabolism and results in hepatic steatosis and inflammation. *Cell metabolism* 2009, **9**(4)**:** 327-338.

46. Wang R-H, Li C, Deng C-X. Liver steatosis and increased ChREBP expression in mice carrying a liver specific SIRT1 null mutation under a normal feeding condition. *International journal of biological sciences* 2010, **6**(7)**:** 682.

47. Xu F, Gao Z, Zhang J, Rivera CA, Yin J, Weng J, *et al.* Lack of SIRT1 (Mammalian Sirtuin 1) activity leads to liver steatosis in the SIRT1+/− mice: a role of lipid mobilization and inflammation. *Endocrinology* 2010, **151**(6)**:** 2504-2514.

48. Deng XQ, Chen LL, Li NX. The expression of SIRT1 in nonalcoholic fatty liver disease induced by high-fat diet in rats. *Liver International* 2007, **27**(5)**:** 708-715.

49. Gao Z, Zhang J, Kheterpal I, Kennedy N, Davis RJ, Ye J. Sirtuin 1 (SIRT1) protein degradation in response to persistent c-Jun N-terminal kinase 1 (JNK1) activation contributes to hepatic steatosis in obesity. *Journal of Biological Chemistry* 2011, **286**(25)**:** 22227-22234.

50. Choi SE, Kwon S, Seok S, Xiao Z, Lee K-W, Kang Y, *et al.* Obesity-linked phosphorylation of SIRT1 by CK2 inhibits its nuclear localization and promotes fatty liver. *Molecular and cellular biology* 2017**:** MCB. 00006-00017.

51. Guertin DA, Stevens DM, Thoreen CC, Burds AA, Kalaany NY, Moffat J, *et al.* Ablation in mice of the mTORC components raptor, rictor, or mLST8 reveals that mTORC2 is required for signaling to Akt-FOXO and PKCα, but not S6K1. *Developmental cell* 2006, **11**(6)**:** 859-871.

52. Wang R-H, Kim H-S, Xiao C, Xu X, Gavrilova O, Deng C-X. Hepatic Sirt1 deficiency in mice impairs mTorc2/Akt signaling and results in hyperglycemia, oxidative damage, and insulin resistance. *The Journal of clinical investigation* 2011, **121**(11).

53. Erion DM, Yonemitsu S, Nie Y, Nagai Y, Gillum MP, Hsiao JJ, *et al.* SirT1 knockdown in liver decreases basal hepatic glucose production and increases hepatic insulin responsiveness in diabetic rats. *Proceedings of the National Academy of Sciences* 2009, **106**(27)**:** 11288-11293.

54. Danz EDB, Skramsted J, Henry N, Bennett JA, Keller RS. Resveratrol prevents doxorubicin cardiotoxicity through mitochondrial stabilization and the Sirt1 pathway. *Free Radical Biology and Medicine* 2009, **46**(12)**:** 1589-1597.

55. Oka S, Alcendor R, Zhai P, Park JY, Shao D, Cho J, *et al.* PPARα-Sirt1 complex mediates cardiac hypertrophy and failure through suppression of the ERR transcriptional pathway. *Cell metabolism* 2011, **14**(5)**:** 598-611.

56. Vinciguerra M, Santini MP, Martinez C, Pazienza V, Claycomb WC, Giuliani A, *et al.* mIGF-1/JNK1/SirT1 signaling confers protection against oxidative stress in the heart. *Aging cell* 2012, **11**(1)**:** 139-149.

57. Baur JA, Pearson KJ, Price NL, Jamieson HA, Lerin C, Kalra A, *et al.* Resveratrol improves health and survival of mice on a high-calorie diet. *Nature* 2006, **444**(7117)**:** 337.

58. Hsu C-P, Zhai P, Yamamoto T, Maejima Y, Matsushima S, Hariharan N, *et al.* Silent Information Regulator 1 Protects the Heart From Ischemia/ReperfusionClinical Perspective. *Circulation* 2010, **122**(21)**:** 2170-2182.

59. Planavila A, Iglesias R, Giralt M, Villarroya F. Sirt1 acts in association with PPARα to protect the heart from hypertrophy, metabolic dysregulation, and inflammation. *Cardiovascular research* 2010, **90**(2)**:** 276-284.

60. Kawashima T, Inuzuka Y, Okuda J, Kato T, Niizuma S, Tamaki Y, *et al.* Constitutive SIRT1 overexpression impairs mitochondria and reduces cardiac function in mice. *Journal of molecular and cellular cardiology* 2011, **51**(6)**:** 1026-1036.

61. Lu T-M, Tsai J-Y, Chen Y-C, Huang C-Y, Hsu H-L, Weng C-F, *et al.* Downregulation of Sirt1 as aging change in advanced heart failure. *Journal of biomedical science* 2014, **21**(1)**:** 57.

62. Prola A, Da Silva JP, Guilbert A, Lecru L, Piquereau J, Ribeiro M, *et al.* SIRT1 protects the heart from ER stress-induced cell death through eIF2α deacetylation. *Cell death and differentiation* 2017, **24**(2)**:** 343.

63. Hariharan N, Maejima Y, Nakae J, Paik J, DePinho RA, Sadoshima J. Deacetylation of FoxO by Sirt1 Plays an Essential Role in Mediating Starvation-Induced Autophagy in Cardiac MyocytesNovelty and Significance. *Circulation research* 2010, **107**(12)**:** 1470-1482.

64. Planavila A, Dominguez E, Navarro M, Vinciguerra M, Iglesias R, Giralt M, *et al.* Dilated cardiomyopathy and mitochondrial dysfunction in Sirt1-deficient mice: a role for Sirt1-Mef2 in adult heart. *Journal of molecular and cellular cardiology* 2012, **53**(4)**:** 521-531.

65. Kuno A, Hori YS, Hosoda R, Tanno M, Miura T, Shimamoto K, *et al.* Resveratrol improves cardiomyopathy in dystrophin-deficient mice through SIRT1 protein-mediated modulation of p300 protein. *Journal of Biological Chemistry* 2013, **288**(8)**:** 5963-5972.

66. Zhang C, Feng Y, Qu S, Wei X, Zhu H, Luo Q, *et al.* Resveratrol attenuates doxorubicin-induced cardiomyocyte apoptosis in mice through SIRT1-mediated deacetylation of p53. *Cardiovascular research* 2011, **90**(3)**:** 538-545.

67. Ramadori G, Lee CE, Bookout AL, Lee S, Williams KW, Anderson J, *et al.* Brain SIRT1: anatomical distribution and regulation by energy availability. *Journal of Neuroscience* 2008, **28**(40)**:** 9989-9996.

68. Cohen HY, Miller C, Bitterman KJ, Wall NR, Hekking B, Kessler B, *et al.* Calorie restriction promotes mammalian cell survival by inducing the SIRT1 deacetylase. *science* 2004, **305**(5682)**:** 390-392.

69. Chen D, Bruno J, Easlon E, Lin S-J, Cheng H-L, Alt FW, *et al.* Tissue-specific regulation of SIRT1 by calorie restriction. *Genes & development* 2008, **22**(13)**:** 1753-1757.

70. Lu M, Sarruf DA, Li P, Osborn O, Sanchez-Alavez M, Talukdar S, *et al.* Neuronal Sirt1 deficiency increases insulin sensitivity in both brain and peripheral tissues. *Journal of Biological Chemistry* 2013, **288**(15)**:** 10722-10735.

71. Jiang M, Wang J, Fu J, Du L, Jeong H, West T, *et al.* Neuroprotective role of Sirt1 in mammalian models of Huntington's disease through activation of multiple Sirt1 targets. *Nature medicine* 2012, **18**(1)**:** 153.

72. Kim D, Nguyen MD, Dobbin MM, Fischer A, Sananbenesi F, Rodgers JT, *et al.* SIRT1 deacetylase protects against neurodegeneration in models for Alzheimer's disease and amyotrophic lateral sclerosis. *The EMBO journal* 2007, **26**(13)**:** 3169-3179.

73. Ng F, Wijaya L, Tang BL. SIRT1 in the brain—connections with aging-associated disorders and lifespan. *Frontiers in cellular neuroscience* 2015, **9:** 64.

74. Hisahara S, Chiba S, Matsumoto H, Tanno M, Yagi H, Shimohama S, *et al.* Histone deacetylase SIRT1 modulates neuronal differentiation by its nuclear translocation. *Proceedings of the National Academy of Sciences* 2008, **105**(40)**:** 15599-15604.

75. Rafalski VA, Ho PP, Brett JO, Ucar D, Dugas JC, Pollina EA, *et al.* Expansion of oligodendrocyte progenitor cells following SIRT1 inactivation in the adult brain. *Nature cell biology* 2013, **15**(6)**:** 614.

76. Guo W, Qian L, Zhang J, Zhang W, Morrison A, Hayes P, *et al.* Sirt1 overexpression in neurons promotes neurite outgrowth and cell survival through inhibition of the mTOR signaling. *Journal of neuroscience research* 2011, **89**(11)**:** 1723-1736.

77. Zocchi L, Sassone-Corsi P. SIRT1-mediated deacetylation of MeCP2 contributes to BDNF expression. *Epigenetics* 2012, **7**(7)**:** 695-700.

78. Gao J, Wang W-Y, Mao Y-W, Gräff J, Guan J-S, Pan L, *et al.* A novel pathway regulates memory and plasticity via SIRT1 and miR-134. *Nature* 2010, **466**(7310)**:** 1105.

79. Yki-Järvinen H. Sex and insulin sensitivity. *Metabolism-Clinical and Experimental* 1984, **33**(11)**:** 1011-1015.

80. Ley CJ, Lees B, Stevenson JC. Sex-and menopause-associated changes in body-fat distribution. *The American journal of clinical nutrition* 1992, **55**(5)**:** 950-954.

81. Hicks AL, Kent-Braun J, Ditor DS. Sex differences in human skeletal muscle fatigue. *Exercise and sport sciences reviews* 2001, **29**(3)**:** 109-112.

82. Arciero PJ, Goran MI, Poehlman ET. Resting metabolic rate is lower in women than in men. *Journal of applied physiology* 1993, **75**(6)**:** 2514-2520.

83. Yki-Järvinen H, Koivisto VA. Effects of body composition on insulin sensitivity. *Diabetes* 1983, **32**(10)**:** 965-969.

84. Kissebah AH, Vydelinfum N, Murray R, Evans DJ, Hartz AJ, Kalkhoff RK, *et al.* Relation of body fat distribution to metabolic complications of obesity. *Obstetrical & gynecological survey* 1983, **38**(1)**:** 41-43.

85. Gillum RF. The association of body fat distribution with hypertension, hypertensive heart disease, coronary heart disease, diabetes and cardiovascular risk factors in men and women aged 18–79 years. *Journal of chronic diseases* 1987, **40**(5)**:** 421-428.

86. Kissebah AH, Krakower GR. Regional adiposity and morbidity. *Physiological reviews* 1994, **74**(4)**:** 761-811.

87. Camhi SM, Bray GA, Bouchard C, Greenway FL, Johnson WD, Newton RL, *et al.* The relationship of waist circumference and BMI to visceral, subcutaneous, and total body fat: sex and race differences. *Obesity* 2011, **19**(2)**:** 402-408.

88. Macotela Y, Boucher J, Tran TT, Kahn CR. Sex and depot differences in adipocyte insulin sensitivity and glucose metabolism. *Diabetes* 2009, **58**(4)**:** 803-812.

89. Tao Z, Zheng LD, Smith C, Luo J, Robinson A, Almeida FA, *et al.* Estradiol signaling mediates gender difference in visceral adiposity via autophagy. *Cell death & disease* 2018, **9**(3)**:** 309.

90. Green H, Fraser I, Ranney D. Male and female differences in enzyme activities of energy metabolism in vastus lateralis muscle. *Journal of the neurological sciences* 1984, **65**(3)**:** 323-331.

91. Stevenson JC. Mechanisms of Estrogen Action on the Cardiovascular System. *Hormonal Carcinogenesis III*. Springer, 2001, pp 365-371.

92. Peterson LR, Soto PF, Herrero P, Schechtman KB, Dence C, Gropler RJ. Sex differences in myocardial oxygen and glucose metabolism. *Journal of nuclear cardiology* 2007, **14**(4)**:** 573-581.

93. Luczak ED, Leinwand LA. Sex-based cardiac physiology. *Annual Review of Physiology* 2009, **71:** 1-18.

94. Ayonrinde OT, Olynyk JK, Beilin LJ, Mori TA, Pennell CE, de Klerk N, *et al.* Gender-specific differences in adipose distribution and adipocytokines influence adolescent nonalcoholic fatty liver disease. *Hepatology* 2011, **53**(3)**:** 800-809.

95. Juraska JM. Sex differences in "cognitive" regions of the rat brain. *Psychoneuroendocrinology* 1991, **16**(1)**:** 105-119.

96. Cahill L. Why sex matters for neuroscience. *Nature Reviews Neuroscience* 2006, **7**(6)**:** 477.

97. Barnes LL, Wilson RS, Bienias JL, Schneider JA, Evans DA, Bennett DA. Sex differences in the clinical manifestations of Alzheimer disease pathology. *Archives of general psychiatry* 2005, **62**(6)**:** 685-691.

98. Levine B, Kroemer G. Autophagy in the pathogenesis of disease. *Cell* 2008, **132**(1)**:** 27-42.

99. Zhang Y, Goldman S, Baerga R, Zhao Y, Komatsu M, Jin S. Adipose-specific deletion of autophagy-related gene 7 (atg7) in mice reveals a role in adipogenesis. *Proceedings of the National Academy of Sciences* 2009, **106**(47)**:** 19860-19865.

100. Bartness TJ, Wade GN. Photoperiodic control of seasonal body weight cycles in hamsters. *Neuroscience & Biobehavioral Reviews* 1985, **9**(4)**:** 599-612.

101. Tchernof A, Calles-Escandon J, Sites CK, Poehlman ET. Menopause, central body fatness, and insulin resistance: effects of hormone-replacement therapy. *Coronary artery disease* 1998, **9**(8)**:** 503-511.

102. Jeong S, Yoon M. 17β-Estradiol inhibition of PPARγ-induced adipogenesis and adipocyte-specific gene expression. *Acta Pharmacologica Sinica* 2011, **32**(2)**:** 230.

103. Heine P, Taylor J, Iwamoto G, Lubahn D, Cooke P. Increased adipose tissue in male and female estrogen receptor-α knockout mice. *Proceedings of the National Academy of Sciences* 2000, **97**(23)**:** 12729-12734.

104. Brown LM, Gent L, Davis K, Clegg DJ. Metabolic impact of sex hormones on obesity. *Brain research* 2010, **1350:** 77-85.

105. Cantó C, Auwerx J. PGC-1alpha, SIRT1 and AMPK, an energy sensing network that controls energy expenditure. *Current opinion in lipidology* 2009, **20**(2)**:** 98.

106. Mauvais-Jarvis F. Estrogen and androgen receptors: regulators of fuel homeostasis and emerging targets for diabetes and obesity. *Trends in Endocrinology & Metabolism* 2011, **22**(1)**:** 24-33.

107. Yao Y, Li H, Gu Y, Davidson NE, Zhou Q. Inhibition of SIRT1 deacetylase suppresses estrogen receptor signaling. *Carcinogenesis* 2009, **31**(3)**:** 382-387.

108. Wilson BJ, Tremblay AM, Deblois G, Sylvain-Drolet G, Giguere V. An acetylation switch modulates the transcriptional activity of estrogen-related receptor α. *Molecular endocrinology* 2010, **24**(7)**:** 1349-1358.

Chapter 3 Autophagy in Adipocyte Differentiation

Zhipeng Tao,[1] Longhua Liu,[1,2] Louise D. Zheng,[1] Zhiyong Cheng[1*]

[1] Department of Human Nutrition, Foods, and Exercise, Fralin Translational Obesity Research Center, College of Agriculture and Life Science, Virginia Tech, Blacksburg, VA 24061, USA

[2] Current address: Department of Pathology and Cell Biology, Naomi Berrie Diabetes Center, College of Physicians and Surgeons, Columbia University, New York, NY 10032, USA

Correspondence: Dr. Zhiyong Cheng, 1981 Kraft Drive, Blacksburg, VA 24061, USA. Phone: (540) 231 9445; Fax: (540) 231 5522; email: zcheng@vt.edu.

This chapter has been published in Methods in Molecular Biology. 2019; 1854:45-53.

Abstract: Adipose tissue regulates metabolic homeostasis by acting as an endocrine organ and energy reservoir. Adipose tissue development and functional maintenance is dependent on adipocyte differentiation, in which autophagy plays an important role. It has been shown that autophagy deficiency dampens adipocyte differentiation, compromise adipose tissue development, dysregulates adipocytekine secretion, and even causes sudden death in young animals. Therefore, accurate assessment of autophagy in adipocyte is critical for the study of adipose biology or pathology of metabolic diseases. In this paper, we describe the procedure of autophagy analysis during adipocyte differentiation, and discuss the power of steady-state autophagy protein levels versus autophagy flux to reflect autophagy activity.

Keywords: Autophagy, Adipocyte differentiation, Adipose development and function, Endocrine, Metabolism

1. Introduction

Adipose tissue has been recognized as a critical endocrine organ in mammals [1-3]. In addition to storing energy, adipose tissue can secret adipocytokines that regulate inflammation, cell signaling, and metabolism [1-3]. Positive energy balance increases adiposity, which may lead to hypoxia because of rapid expansion of adipose tissue, thereby dysregulating adipocyte function, adipocytokine secretion, and metabolic homeostasis [4, 5]. Nevertheless, heathy expansion of adipose tissue after adipocyte differentiation is critical for adipose tissue maintenance and function [4, 5]. Recently, we found that adipocyte differentiation and lipid droplet expansion was dependent on autophagy, a common mechanism that cells adapt for cellular remodeling and recycling [6-9]. Suppression of autophagy dampens adipocyte differentiation, reduce fat mass, and induces browning of white adipose tissue [10, 11]. However, embryonic deletion of autophagy genes seems to compromise adipose tissue development and function, resulting in a substantial death rate in model animals at young ages [10]. These findings suggest that autophagy is a central regulator of adipocyte differentiation, adipose tissue development, and functional maintenance.

Autophagy process consists of multiple steps, i.e., initiation, vesicle elongation, vesicle completion, fusion, and degradation [7, 12]. Among the identified autophagy proteins, beclin 1 is a critical component of the initiation complex, while LC3-II is found to participate in vesicle elongation, vesicle completion, and fusion [7, 12]. In addition, LC3II can be selectively degraded by autolysosome along with adaptor protein p62 such that the turnover of these two proteins reflects autophagy flux [7, 12]. Given the highly dynamic and multi-step process of autophagy, it has been recognized that substrate turnover (or autophagy flux) other than steady-state parameters (e.g., monitoring autophagosome number with electron microscopy and fluorescence

microscopy) can reveal autophagy activity [12, 13]. In this article, we describe the protocol to monitor autophagy flux during adipocyte differentiation.

2 Materials

2.1 Cell culture

1. Equipment and supplies: 10-cm tissue culture dishes, 6-well tissue culture plates, 50-ml sterile conical tubes, sterile tips, pipettes, light microscope, benchtop centrifuge, and biosafety cabinet.
2. 3T3-L1 cell line (CL-173) purchased from ATCC (Manassas, VA, USA).
3. SVF cells isolated freshly from subcutaneous white adipose tissue (sWAT) as described previously [14].
4. Phosphate-buffered saline.
5. Basal medium for 3T3-L1 cells: Dulbecco's modified Eagle's (DMEM) medium, 10% Fetal Bovine Serum (FBS), and 1x Pen/Strep.
6. Basal medium for SVF cells: DMEM/F12, 10% Fetal Bovine Serum (FBS), and 1x Pen/Strep.

2.2 Adipocyte differentiation

1. Equipment and supplies: 6-well tissue culture plates, sterile tips, pipettes, inverted microscope, laboratory CO_2 Water-Jacketed Incubators, and biosafety cabinet.
2. Differentiation media (DM) for 3T3-L1 cells: DMI – DMEM supplemented with 10% FBS, P/S (1 ×), IBMX (0.5 mM), dexamethasone (1 μM), insulin (1 μg/ml) and rosiglitazone (2 μM). DMII – DMEM supplemented with 10% FBS, P/S (1 ×), and insulin (1 μg/ml).
3. Differentiation medium for SVF cells: DMEM/F12 media containing 10% FBS, 1x Pen/Strep, dexamethasone (5 μM), insulin (0.5 μg/ml), IBMX (0.5mM), and rosiglitazone (1μM).

4. Maintenance medium for 3T3-L1 cells: DMEM media containing 10% FBS, 1x Pen/Strep.
5. Maintenance medium for SVF cells: DMEM/F12 media containing 10% FBS, 1x Pen/Strep, and insulin (0.5 μg/ml).

2.3 Autophagy flux assay

1. Bafilomycin A1 (inhibitor of autophagosome acidification, 0.1 mM in DMSO)
2. Leupeptin (inhibitor of lysosomal proteases, 10 mg/ml in DMSO).

2.4 Western blotting

1. Equipment and supplies: 50-ml sterile conical tubes, sterile tips, 2 ml sterile tubes, pipettes, benchtop centrifuge, microplate reader, heat block (Benchmark).
2. Phosphate buffered saline (PBS).
3. Bullet Blender® (Next Advance, Inc.).
4. DC protein assay kits (Bio-Rad).
5. PLC lysis buffer: 30 mM Hepes, pH 7.5, 150 mM NaCl, 10% glycerol, 1% Triton X-100, 1.5 mM MgCl2, 1 mM EGTA, 10 mM NaPPi, 100 mM NaF, 1 mM Na3VO4) supplemented with protease inhibitor cocktail (Roche), 1 mM PMSF (freshly added right before use).
6. Loading buffer (5X): Tris-HCl (pH 6.8) 0.25 M, glycerol 25%, 5% SDS, bromophenol blue 0.25%, 0.5 M DTT.
7. Running buffer (1X): 25 mM Tris-Base, 192 mM glycine, 0.1% SDS (pH 8.3)
8. Transfer buffer: 25 mM Tris-Base, 192 mM glycine (pH 8.3), 15-20% methanol.
9. Washing buffer: 50 mM Tris-HCl, 150 mM NaCl, 0.1% Tween 20 (pH 7.4)

10. Antibodies: Beclin 1 (Cat No: MABN16) from EMD Millipore. p62 (Cat No: 5114s) from Cell Signaling Technology; LC3 (cat No: L7543) from Sigma-Aldrich; GAPDH (Cat No: MA5-15738) from ThermoFisher Scientific.

3 Method

3.1 Differentiation of 3T3-L1 cells

1. Seed 3T3-L1 cells in 10-cm dishes and then subculture in 6-well plates with basal media.
2. Change the media every 2 days until the cells reach confluence (day 0).
3. Change the media one more time and maintain the cells in basal media till day 2.
4. At the end of day 2, replace basal media with differentiation medium I (DMI).
5. At the end of day 4, replace DMI with differentiation medium II (DMII).
6. At the end of day 6, replace DMII medium with maintenance medium.
7. Change maintenance medium every 2 days until day 12 when the cells are fully differentiated, which is confirmed by oil red O staining as described previously (Figure 1A; **see Note 1**) [8, 9, 15, 16].

3.2 Differentiation of SVF cells

1. Seed the isolate SVF cells in 10-cm dishes (collagen-coated dishes preferred) then subculture in 6-well plates (either collagen-coated or regular tissue culture plates work well) with basal media.
2. Change the media every 2 days until the cells reach confluence (day 0).
3. Change the media one more time and maintain the cells in basal media till day 2.
4. At the end of day 2, replace basal media with differentiation medium; supply fresh differentiation medium every 2 days.

5. At the end of day 6, replace differentiation medium with maintenance medium. At this point, development of lipid droplets in the cells becomes obvious.
6. Supply fresh maintenance medium every 2 days till day 10, when adipocyte differentiation and lipid accumulation is complete, which is confirmed by oil red O staining as described previously (Figure 1B; **see Note 2**) [14].

3.3 Kinetics of autophagy markers during adipocyte differentiation

1. At the indicated time points during cell differentiation (Figure 2), remove the media and wash the cells with cold PBS twice.
2. Harvest the cells in 2 ml cold PBS using cell lifters.
3. Centrifuge at 5,000 x g, 4C for 5 min to pellet the cells, and discard the supernatant.
4. Lyse the cells with a Bullet Blender according the manufacturer's instruction
5. Centrifuge at 12,000 x g, 4C for 10 min.
6. Transfer the cell lysate to a clean Eppendorf tubes, and measure total protein concentration on a microplate reader with DC protein assay kits.
7. Perform western blot analysis, using 12.5% gel for SDS-PAGE (60V for 30 min, following by 110V for 2 hr; **see Note 3**).
8. Use ECL kits and X-ray film for Western Blot Detection of the steady state level of autophagy proteins beclin 1, LC3II, and p62 on day 0 through day 12 (Figure 2; **see Note 4**).

3.4 Autophagy flux in preadipocytes and mature adipocytes

1. At day 12, 3T3L1 preadipocytes (without differentiation induction) and mature adipocytes (with differentiation induction) in basal media are treated with bafilomycin A1 (inhibitor of

autophagosome acidification, at 0.1 μM) plus leupeptin (the inhibitor of lysosomal proteases, at 10 μg/ml) for 4 hr. Cells treated with DMSO serve as the controls (**See Notes 5 and 6**).

2. Remove the media and wash the cells with cold PBS twice.
3. Harvest the cells in 2 ml cold PBS using cell lifters.
4. Centrifuge at 5,000 x g, 4C for 5 min to pellet the cells, and discard the supernatant.
5. Lyse the cells with a Bullet Blender according the manufacturer's instruction
6. Centrifuge at 12,000 x g, 4C for 10 min
7. Transfer the cell lysate to a clean Eppendorf tubes, and measure total protein concentration on a microplate reader with DC protein assay kits.
8. Proceed to western blot analysis to detect the protein levels of LC3II, and p62 in the absence and presence of autophagy inhibitors bafilomycin A1 plus leupeptin (B+L).
9. Use NIH ImageJ software to perform densitometry analyses of western blot images.
10. Autophagy flux is calculated as the difference of band density between B+L treated cells and untreated cells, for preadipocytes and differentiated (or mature) adipocytes, respectively (Figure 3; **see Notes 7 and 8)**.

4 Notes

1. The expression of PPARγ (a key adipogenic regulator) and adiponectin (adipocytokine secreted by adipocytes) can be used as molecular markers to confirm adipocyte differentiation. Our experience indicates that after day 12 there is no further increase in lipid accumulation or expression PPARγ and adiponectin.
2. Our experience indicates that after day 10 there is no further increase in lipid accumulation or expression of PPARγ and adiponectin.

3. SDS-PAGE at a lower voltage when necessary, e.g., 30V for overnight (12-14hr) to increase the separation efficiency for LC3I and LC3II.

4. The steady-state level of beclin 1 increases over time during cell differentiation, indicative of an activated autophagy. However, the steady-state level of LC3II is downregulated during cell differentiation, seemingly suggestive of inhibition of autophagy. This complexity arises from the dual role of LC3II in autophagy, i.e., (a) promoter of phagophore formation and autophagosome maturation, and (b) autophagy substrate for degradation and recycling [12]. As such, the decreased steady-state level of LC3II protein may be due to elevated autophagy degradation, or to reduced expression of LC3 or compromised conversion from LC3I into LC3II. In the former case, autophagy is upregulated, whereas in the latter, autophagy is dampened. Although the decrease in p62 protein seems to support the former case (i.e., activation of autophagy to degrade p62 and LC3II), the conclusion is insecure before it is determined whether that p62 and LC3 expression undergoes downregulation, and whether the conversion of LC3I to LC3II is compromised. The complexity and uncertainty can be solved by autophagy flux analysis.

5. For SVF cell, the B+L treatment starts on day 10. Preadipocytes (without differentiation induction) and mature adipocytes (with differentiation induction) in basal media are treated with bafilomycin A1 (0.1 μM) plus leupeptin at 10 μg/ml) for 4 hr. Cells treated with DMSO serve as the controls.

6. If it is desirable to measure autophagy flux on any specific day (e.g., day 6) during differentiation, the cells (with or without differentiation induction) will be treated with B+L on day 6 for 4 hr, and then proceed to step 2 of section 3.4.

7. The autophagy flux measurements based on LC3II and p62 both suggest a higher substrate turnover (i.e., autophagy activity) in differentiated cells than in undifferentiated cells. Therefore, determination of autophagy flux is preferred to detection of steady-state parameters for accurate assessment of autophagy activity (see Note 4).
8. Autophagy flux is upregulated in differentiated 3T3L1 and SVF cells. However, autophagy is activated to a greater extent in 3T3L1 cells than in SVF cell during differentiation, in line with the lesser potential known for differentiation in SVF cells (Figure 1). Indeed, compromised autophagy results in suppression of adipocyte differentiation [10, 11].

Acknowledgement

This work was supported in part by USDA National Institute of Food and Agriculture Hatch Project 1007334 (ZC).

References

[1] Kershaw EE, Flier JS (2004) Adipose tissue as an endocrine organ. J Clin Endocrinol Metab 89: 2548-2556

[2] Galic S, Oakhill JS, Steinberg GR (2010) Adipose tissue as an endocrine organ. Mol Cell Endocrinol 316: 129-139

[3] Slutsky N, Vatarescu M, Haim Y, et al. (2016) Decreased adiponectin links elevated adipose tissue autophagy with adipocyte endocrine dysfunction in obesity. Int J Obes (Lond) 40: 912-920

[4] Rutkowski JM, Stern JH, Scherer PE (2015) The cell biology of fat expansion. J Cell Biol 208: 501-512

[5] Crewe C, An YA, Scherer PE (2017) The ominous triad of adipose tissue dysfunction: inflammation, fibrosis, and impaired angiogenesis. J Clin Invest 127: 74-82

[6] Mizushima N, Komatsu M (2011) Autophagy: renovation of cells and tissues. Cell 147: 728-741

[7] Green DR, Levine B (2014) To be or not to be? How selective autophagy and cell death govern cell fate. Cell 157: 65-75

[8] Liu L, Tao Z, Zheng LD, et al. (2016) FoxO1 interacts with transcription factor EB and differentially regulates mitochondrial uncoupling proteins via autophagy in adipocytes. Cell death discovery 2: 16066

[9] Liu L, Zheng LD, Zou P, et al. (2016) FoxO1 antagonist suppresses autophagy and lipid droplet growth in adipocytes. Cell Cycle 15: 2033-2041

[10] Singh R, Xiang Y, Wang Y, et al. (2009) Autophagy regulates adipose mass and differentiation in mice. J Clin Invest 119: 3329-3339

[11] Zhang Y, Goldman S, Baerga R, Zhao Y, Komatsu M, Jin S (2009) Adipose-specific deletion of autophagy-related gene 7 (atg7) in mice reveals a role in adipogenesis. Proc Natl Acad Sci U S A 106: 19860-19865

[12] Mizushima N, Yoshimori T, Levine B (2010) Methods in mammalian autophagy research. Cell 140: 313-326

[13] Klionsky DJ, Abdelmohsen K, Abe A, et al. (2016) Guidelines for the use and interpretation of assays for monitoring autophagy (3rd edition). Autophagy 12: 1-222

[14] Liu L, Zheng LD, Donnelly SR, Emont MP, Wu J, Cheng Z (2017) Isolation of Mouse Stromal Vascular Cells for Monolayer Culture. Methods Mol Biol 1566: 9-16

[15] Liu L, Zou P, Zheng L, et al. (2015) Tamoxifen reduces fat mass by boosting reactive oxygen species. Cell death & disease 6: e1586

[16] Zou P, Liu L, Zheng L, et al. (2014) Targeting FoxO1 with AS1842856 suppresses adipogenesis. Cell Cycle 13: 3759-3767

Legends to the Figures

Figure 1. Differentiation of 3T3L1 cells and SVF cells. In the absence of differentiation induction (A), 3T3L1 preadipocytes have marginal lipid accumulation on day 12. In the presence of differentiation induction (B), 3T3L1 cell are fully differentiated into mature adipocytes and show drastic fat accumulation on day 12 (B). Panels C (without differentiation induction) and D (with differentiation induction) show that SVF cells have similar differentiation pattern and substantial lipid accumulation on day 10. Scale bar, 50 μm.

Figure 2. The kinetics of autophaphy protein levels during 3T3L1 adipocyte differentiation. Beclin 1, the regulator of autophagy initiation, is upregulated. By contrast, LC3II and p62, the proteins that can be selectively degraded by autolysosome, are downregulated. GAPDH serves as the loading control. The time course of autophaphy protein changes indicates activation of autophagy during adipocyte differentiation. However, note the limitation of using steady state level of autophagy proteins to assess autophagy activity (see Notes 4 and 7).

Figure 3. Measurement of autophagy activity in preadipocytes and differentiated adipocytes (or mature adipocytes). (A) 3T3L1 preadipocytes (pre-ad) and differentiated adipocytes are treated with bafilomycin A1 and leupeptin (i.e., B+L) for 4 hours, and cell lysates are prepared to probe LC3II and p62 by western blot analysis. (B) autophagy flux is calculated, (band density of LC3II with B+L) – (band density of LC3II without B+L), for

3T3-L1 cells. (C) SVF cells and differentiated SVF cells are treated with bafilomycin A1 and leupeptin (i.e., B+L) for 4 hours, and cell lysates are prepared to probe LC3II and p62 by western blot analysis. (B) autophagy flux is calculated, (band density of LC3II with B+L) – (band density of LC3II without B+L), for SVF cells. GAPDH and β-actin serve as the loading controls. n=4-6, *, $p<0.05$; *** and $p<0.001$ (comparing preadipocytes with mature adipocytes).

Figure 1

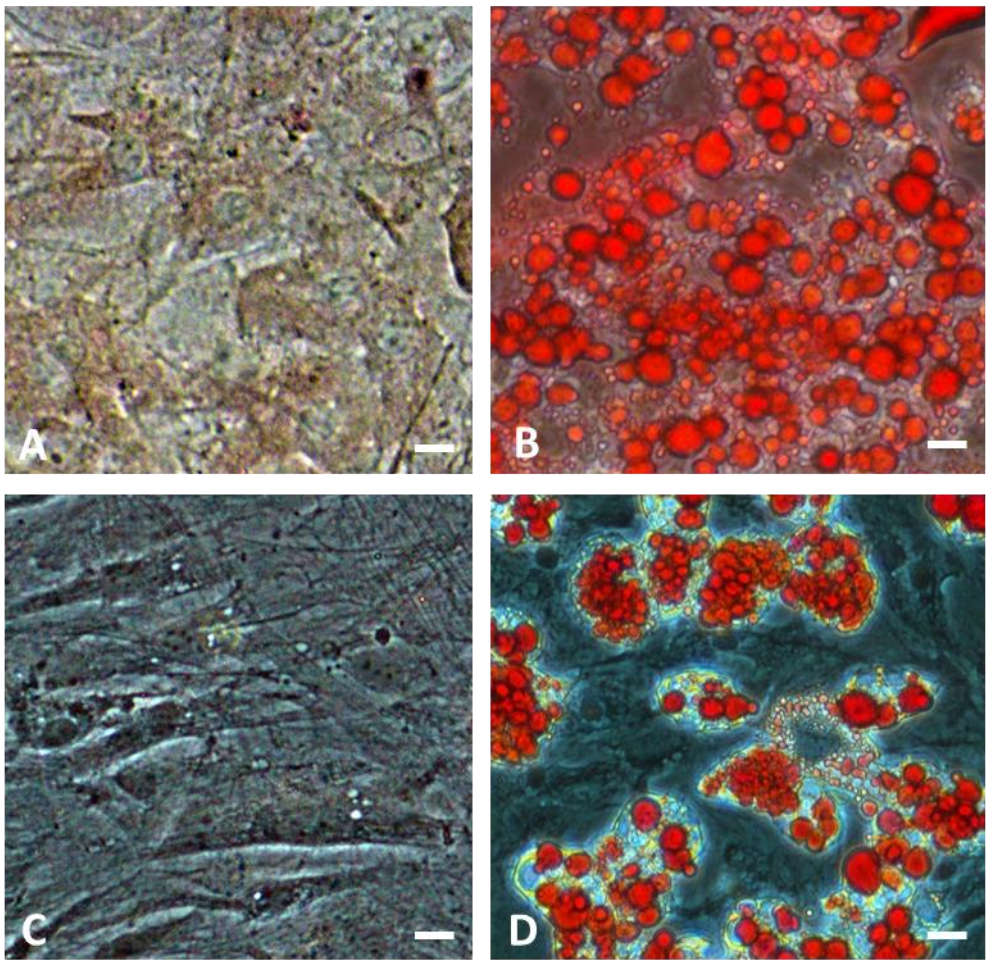

Figure 2

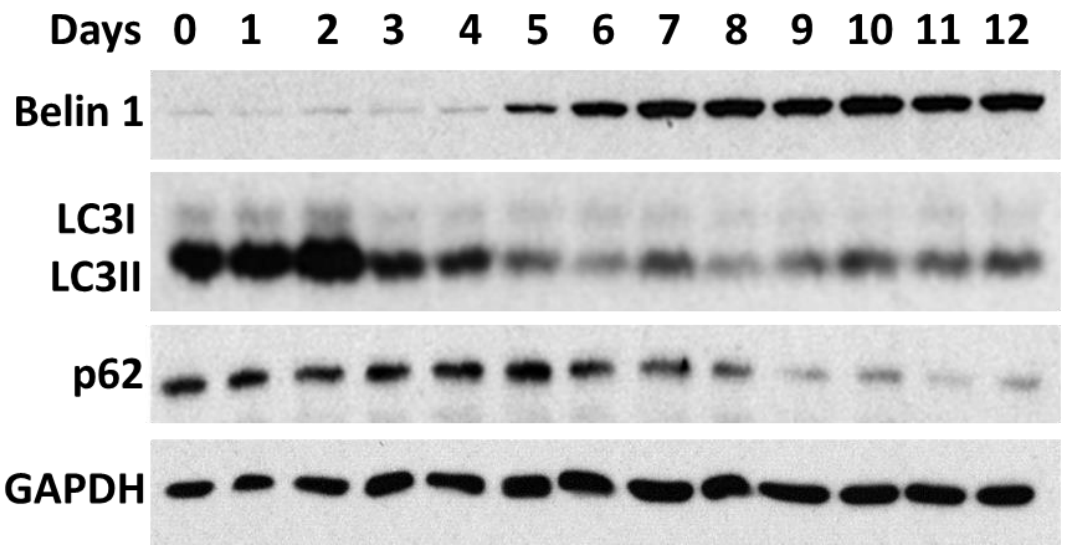

Figure 3

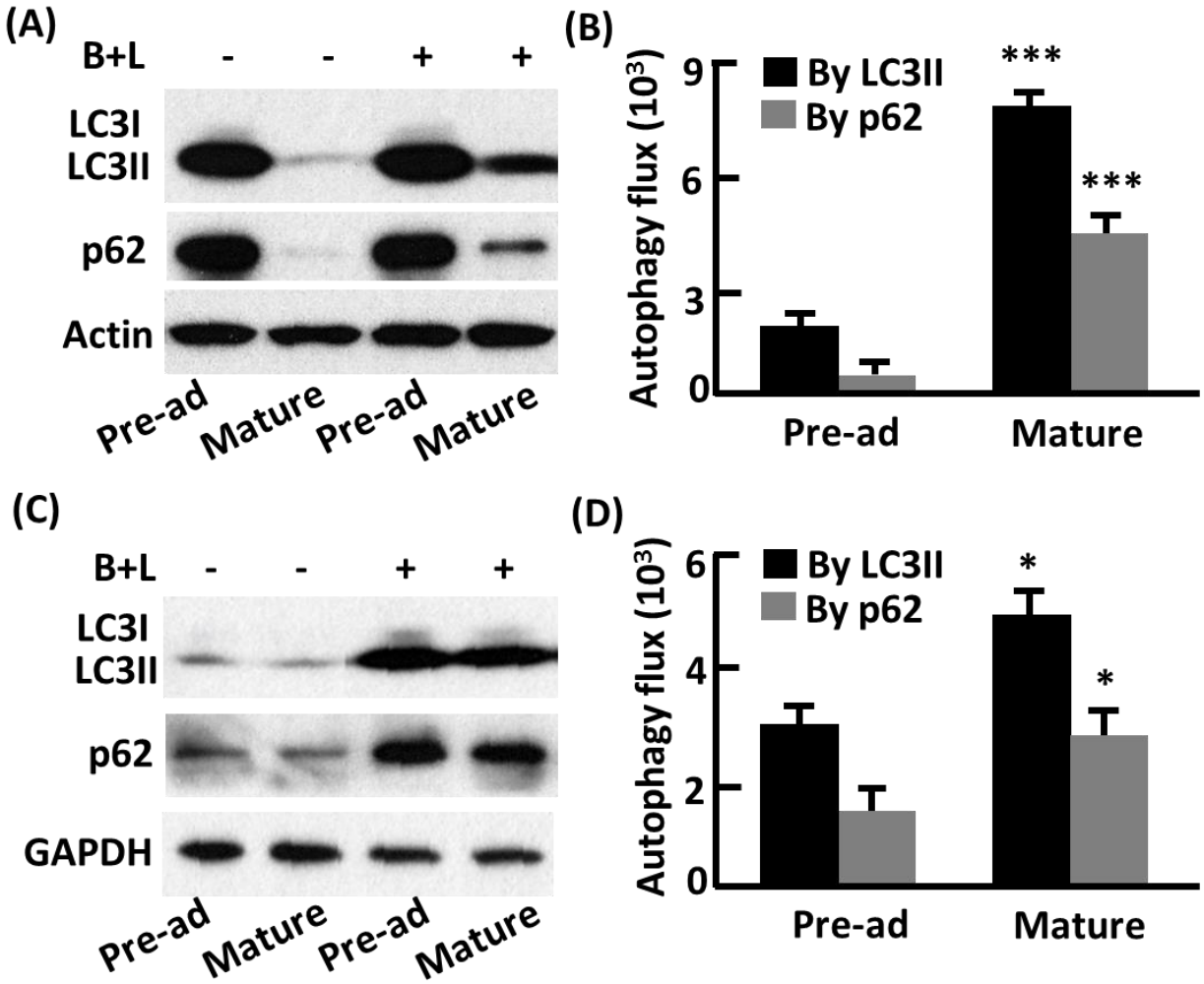
(A)
B+L - - + +
LC3I
LC3II
p62
Actin
Pre-ad
Mature
Pre-ad
Mature
(B)
Autophagy flux (10^3)
By LC3II
By p62
***
***
Pre-ad
Mature
(C)
B+L - - + +
LC3I
LC3II
p62
GAPDH
Pre-ad
Mature
Pre-ad
Mature
(D)
Autophagy flux (10^3)
By LC3II
By p62
*
*
Pre-ad
Mature

Chapter 4 Estradiol signaling mediates gender difference in visceral adiposity via autophagy

Zhipeng Tao,[1] Louise D. Zheng,[1] Cayleen Smith,[1] Jing Luo,[1] Alex Robinson,[1] Fabio A. Almeida,[2] Zongwei Wang,[3] Aria F. Olumi,[3] Dongmin Liu,[1*] Zhiyong Cheng[1*]

[1] Department of Human Nutrition, Foods, and Exercise, Fralin Life Science Institute, College of Agriculture and Life Science, Virginia Tech, Blacksburg, VA 24061, USA

[2] Department of Health Promotion, Social & Behavioral Health, College of Public Health, University of Nebraska Medical Center, Omaha, NE, USA

[3] Department of Urology, Massachusetts General Hospital, Harvard Medical School, Boston, MA, USA

* Correspondence:

Dr. Zhiyong Cheng, 1981 Kraft Drive, Blacksburg, VA 24061, USA. Phone: (540) 231 9445; Fax: (540) 231 5522; email: zcheng@vt.edu.

Dr. Dongmin Liu, 1981 Kraft Drive, Blacksburg, VA 24061, USA. Phone: (540) 231 3402; Fax: (540) 231 5522; email: doliu@vt.edu.

This chapter has been published in Cell Death and Disease. 2018; 22;9(3):309.

ABSTRACT: Excessive adiposity (particularly visceral fat mass) increases the risks of developing metabolic syndrome. Women have lower deposit of visceral fat than men, and this pattern becomes diminished postmenopausally, but the underlying mechanism remains largely unknown. Here we show that the gender difference in visceral fat distribution is controlled by an estradiol-autophagy axis. In C57BL/6J and wild type control mice, a higher visceral fat mass was detected in the males than in the females, which was associated with lower expression of estrogen receptor α (ERα) and more active autophagy in males vs. females. However, deletion of ERα normalized autophagy activity and abolished the gender difference in visceral adiposity. In line with the adiposity-reducing effect of the ERα-autophagy axis, we found that downregulation of ERα and increased autophagy activity were required for adipogenesis, while induction of estradiol signaling dampened autophagy and drastically prevented adipogenesis. Mechanistically, the estradiol-ERα signaling activated mTOR, which phosphorylated and inhibited ULK1, thereby suppressing autophagy and adipogenesis. Together, our study suggests that the lower visceral adiposity in the females (vs. the males) arises from a more active estradiol-ERα signaling, which tunes down autophagy and adipogenesis.

KEYWORDS: adipogenesis, autophagy, estradiol signaling, gender difference, metabolic syndrome, visceral adiposity

ABBREVIATIONS

Atg5, autophagy related 5; Atg7, autophagy related 7; Atg12, autophagy related 12; BL, bafilomycin-A1 and leupeptin; BMI, body mass index; DI, differentiation induction; E2, estradiol; ERα, estrogen receptor α; ERβ, estrogen receptor β; FBS, fetal bovine serum; GAPDH, glyceraldehyde 3-phosphate dehydrogenase; LC3, microtubule-associated protein 1A/1B-light chain 3-phosphatidylethanolamine conjugate; mTOR, the mechanistic target of rapamycin; p62, sequestosome 1 (SQSTM1); SVF, stromal vascular fraction; sWAT, subcutaneous white adipose tissue; ULK1, Unc-51 Like Autophagy Activating Kinase; vWAT, visceral white adipose tissue; WAT, white adipose tissue.

INTRODUCTION

White adipose (or fat) tissues (WAT) play a central role in metabolic homeostasis through energy storage and endocrine functions.[1, 2] It has been shown that fat depots at distinct anatomical (e.g., subcutaneous versus visceral) locations have intrinsic differences in hormone response, gene expression, remodeling, and metabolism.[3-9] Excessive visceral fat is associated with metabolic syndrome development (e.g., insulin resistance) in animal models and humans, whereas subcutaneous fat is benign or protective. [9-13] Compared with women, men have more visceral fat.[14, 15] Intriguingly, visceral fat mass increases in post-menopausal women (characteristic of reduced estrogen (E2) secretion), which can be prevented by E2 replacement therapy.[16, 17] These findings underscored an important role of estrogen or E2 signaling in the regulation of fat development and distribution, yet the molecular mechanism remains largely elusive.

WAT mass development and maintenance are dependent on adipocyte turnover. It was estimated that the rate of adipocyte turnover was 10% per year in humans and 1–5% per day in mice.[18, 19] The overall adipocyte number in WAT is balanced by adipogenesis (i.e., the differentiation of preadipocyte into adipocytes) and adipocyte apoptosis.[18-20] Emerging evidence suggests that autophagy, the major intracellular degradation and remodeling system, regulates both adipocyte differentiation and apoptosis.[21-23] Blockage of autophagy through ablation of Atg5 or Atg7 substantially prevents adipocyte differentiation and promotes adipocyte apoptosis, which significantly reduces fat mass in mice.[21-23] We and others have showed that autophagy is required to maintain PPARγ and FSP27, the key regulators of adipocyte differentiation and lipid droplet formation in fat cells.[24, 25] Suppression of autophagy downregulates PPARγ and FSP27, concomitant with dampened adipocyte differentiation and marginal lipid accumulation in the cells.[24, 25] Therefore, autophagy acts as a critical regulator of WAT remodeling and maintenance.

Given the above-mentioned evidence that implies E2 and autophagy in WAT regulation, we asked the question whether autophagy might interact with E2 signaling, and how it might link to the gender difference in visceral adiposity. Here we show that male mice had higher visceral fat mass than the females, which was associated with lower expression of estrogen receptors (ERα) in the visceral adipose tissue. Activation of E2 signaling suppressed autophagy via an mTOR-ULK pathway, which inhibited adipogenesis and was associated with a lower visceral adiposity in the mice. However, deletion of ERα normalized autophagy activity and gender-dependent difference in visceral adiposity. Our data reveals for the first time an E2-ERα-autophagy axis that contributes to the gender difference in visceral fat distribution.

RESULTS

Female mice had lower visceral WAT mass than male mice. A higher visceral WAT (vWAT) volume in men than women has been observed across races.[14, 15] To determine if mice have a similar pattern of fat distribution, we examined C57BL/6J at the age of 6-7 weeks (Figure 1). As expected, the female mice had lower body weight than males (average 15.4 g vs. 17.5 g, $p<0.05$; Figure 1A). The net weights of gonadal WAT (the largest visceral fat depots in mice) and subcutaneous WAT (inguinal fat depots, sWAT) were both lower in female mice than in the males (Figure 1, B-C). However, after normalization against the body weight only the vWAT mass remained lower in females than in males (average 0.87% vs 1.21%, $p<0.05$; Figure 1D), while the differences in sWAT mass became indiscernible between the males and females (average 0.45% vs 0.49%, $p=0.14$; Figure 1E). Therefore, the ratios of visceral fat to body weight (or vWAT percentage) reveal a gender-dependent phenotype in mice as observed previously in human subjects.

Autophagy activity in vWAT was lower in female than male mice. Autophagosome formation is characterized by lipidation of LC3 to form LC3-phospholipid conjugate (LC3-II), which can be degraded by lysosomal hydrolase in autolysosome.[26, 27] In sWAT, steady state LC3-II levels did not differ between female and male mice (Figure 2, A-B). However, a significantly lower (50%, $p<0.01$) steady state LC3-II was detected in vWAT from male mice vs. that from female mice (Figure 2, C-D), suggesting that autophagic degradation of LC3-II in vWAT was more active in the males than in the females. To test this, we detected LC3-II turnover (or autophagy flux),[25, 27, 28] by detecting the accumulation of LC3-II after treating WAT explant cultures with autophagy inhibitors bafilomycin A1 and leupeptin (BL) for 4 hours. In line with the steady-state levels of LC3-II in sWAT being indiscernible between the males and females (Figure 2 A-B), autophagy flux in sWAT did not show significant difference between the males and females (Figure 2 E-F). However, the autophagy flux in vWAT was significantly higher in the males (1.6-fold upregulated, $p<0.05$) than in the females (Figure 2 E-F). The turnover of p62, which is selectively degraded by autophagy, further validated the higher autophagy activity in vWAT from male mice than that from female mice (Figure 2 G-H). These data support the notion that increased LC3-II turnover results in a reduced steady-state level of LC3-II (Figure 2 C-D).[26, 29] Together, female mice had lower autophagy activity in vWAT than the males.

Estrogen receptors were upregulated in vWAT from females vs. males. E2 signaling is primarily funneled through ERα and ERβ.[30] Compared with the males, the female mice had similar expression of ERα and ERβ in sWAT (Figure 3, A-B). However, vWAT had significant lower protein levels of ERα and ERβ in male mice than in female mice (Figure 3, C-D), being 40% for ERα ($p<0.01$) and 54% for ERβ ($p<0.05$). Interestingly, the overall protein levels of

ERβ in vWAT appeared to be much lower than that of ERα for both genders (Figure 3, C-D), suggesting that ERα might play a dominant role in mediating E2 actions in vWAT.

Adipogenesis was associated with downregulation of estrogen receptors but upregulation of autophagy activity. The observation of lower expression of ER but higher autophagy activity in the males vs. females (Figures 2 and 3) prompted us to examine whether this reciprocal relation exists in adipogenesis, the process that is critical for adipose tissue development and maintenance.[31, 32] As shown in Figure 4 A-B, ERα was downregulated by 80% ($p<0.01$) and ERβ by 54% ($p<0.05$) during adipogenesis, which was characterized by drastic accumulation of lipid in the cells (Figure 4C). In addition, the downregulation of ERs was associated with 81% ($p<0.0001$) reduction in the steady state level of LC3-II (Figure 4, D-E). Autophagy flux assays by LC3-II turnover suggested that the differentiated adipocytes had an autophagy activity 2.6-fold ($p<0.0001$) higher than the preadipocytes, which was further verified by the turnover of p62 (Figure 4, F-G). These results recapitulated the pattern observed in vWAT, where steady-state level of LC3-II was reduced due to increased autophagy activity (Figure 2).[26, 29] Importantly, the *in vitro* and *in vivo* data work in concert to reveal a reciprocal relationship between autophagy activity and ER levels.

Estradiol signaling suppressed autophagy and adipogenesis. To examine whether E2 signaling *per se* regulate adipocyte autophagy and adipogenesis, we treated 3T3L1 preadipocytes with or without E2 (0.1 μM) on day 0 through day 12, during which adipogenesis was induced according to an established protocol (see *Materials and Methods*).[25, 33-35] E2 treatment substantially increased the accumulation of LC3-II (2.8 folds, $p<0.0001$), as well as p62 (1.6 fold, $p<0.05$), the selective substrate of autophagy for degradation (Figure 5, A-B).[25, 33, 36] The E2-enhanced accumulation of LC3-II and p62 was associated with reduced autophagy flux

(Figure 5, C-D), suggesting that E2 dampens autophagy activity. In addition, the E2-treated cells were barely differentiated into mature adipocytes and showed marginal lipid accumulation compared with vehicle-treated cells (Figure 5E). Likewise, treatment of 3T3L1 preadipocytes with the established autophagy inhibitor BL almost completely prevented adipogenesis (Figure 5F). In addition, the presence of E2 or autophagy inhibitor BL similarly inhibited autophagy and adipogenesis in primary stromal vascular cells isolated from vWAT (Figure 1s). Thus, E2 signaling suppresses adipogen esis at least in part via autophagy inhibition.

Estradiol signaling suppressed autophagy via mTOR-ULK1. To explore the mechanism of E2 regulating autophagy, we analyzed the interactions of E2 signaling and proteins that are known to control autophagy, including ULK1, beclin 1, Atg5, Atg7, and Atg12.[37-39] We found that beclin 1 was upregulated during adipocyte differentiation, but E2 treatment had marginal effect on beclin 1 level (Figure 2s, A-B). ULK1 was activated during adipogenesis, because the mTOR-mediated inhibitory phosphorylation of ULK1 at Ser 757 (p-ULK1^{Ser757}) was significantly reduced.[37-39] However, E2 treatment suppressed ULK1 by increasing p-ULK1^{Ser757}, concomitant with the activation of mTOR indicated by phosphorylation at Ser2448 (p-mTOR^{Ser2448}) (Figure 6, A-B).[37-41] These data suggest that E2 signaling acts on ULK1 but not beclin 1, although both proteins participate in autophagy initiation (i.e., formation of the isolation membrane).[37-39] Moreover, no discernible change was detected in Atg5, Atg7, and Atg12-Atg5 conjugate, the proteins or components that regulate membrane elongation,[37, 39] during adipocyte differentiation or during E2 treatment (Figure 2s, A-B). These results, along with the above observation that E2 suppressed autophagy in adipocytes (Figures 4-5), suggest that E2 may regulate autophagy via the mTOR-ULK1 cascade.

To validate the E2/ER signaling-mTOR-ULK1 pathway *in vivo*, we examined adipose tissues from male and female C57BL/6J mice (Figure 6, C-D). In line with the females having higher ER levels in vWAT than the males (Figure 3), the activating phosphorylation of mTOR (p-mTOR^{Ser2448}) was enhanced by 4.8-fold ($p<0.0001$), and the mTOR-mediated inhibition of ULK1 (p-ULK1^{Ser757}) was 2.1-fold stronger ($p<0.05$; Figure 6, E-F). In sWAT, however, no statistically significant difference was detected (Figure 6, C-D), consistent with the male and the females showing comparable levels of ER in sWAT (Figure 3). Notably, we did not detect significant difference in beclin 1, Atg5, Atg7, or Atg12-Atg5 conjugate, between the male and the females (Figure 2s, C-D). Together, our *in vitro* and *in vivo* results support the hypothesis that E2/ER signaling regulates adipose autophagy via the mTOR-ULK1 pathway.

Ablation of ERα normalized autophagy activity and abolished gender difference in visceral adiposity. ERα and ERβ have been shown to suppress or enhance autophagy in different cancer cells.[42-46] To determine the primary role player in the regulation of autophagy and adipocyte differentiation, we treated 3T3L1 cells with selective agonists of ERα (PPT) and ERβ (DPN).[47, 48] PPT reduced autophagy activity and suppressed adipogenesis but DPN had marginal effect, suggesting that ERα played the dominant role (Figure 3s). To validate this, we examined autophagy and visceral adiposity in ERα knockout mice (Figure 7).[49] As observed in the C57BL/6J mice, the control (or wild type, WT) females had higher expression of ERα and stronger inhibition of ULK1 (p-ULK1^{Ser757}) in vWAT than the WT males, although sWAT showed no gender difference in ERα and p-ULK1^{Ser757} (Figure 7, A-B). However, knockout (KO) of ERα reduced the inhibitory phosphorylation of ULK1 (p-ULK1^{Ser757}) in both sWAT and vWAT, and most importantly, it abolished the gender difference in vWAT (Figure 7, A-B). Consistently, the gender-dependent difference in autophagy flux was diminished by the KO of

ERα in vWAT (Figure 7, C-D; Figures 4s-5s). In line with the enhanced autophagy (Figure 7, A-D; Figures 4s-5s), which was found to promote adipogenesis (Figures 4-5; Figure 1s), the loss of ERα increased both sWAT and vWAT masses in the ERα KO mice compared with the WT mice (Figure 7, E-H). Furthermore, the gender difference in vWAT mass was abolished by the ablation of ERα (Figure 7, F and H). Therefore, the E2-ERα signaling cascade plays the central role in the gender difference in visceral adiposity via regulating autophagy.

DISCUSSION

Increased visceral adiposity has been strongly associated with higher risks of developing metabolic disorders.[9-13] Females have lower visceral fat mass than males, but this gender difference is diminished in older age groups because post-menopausal women have increased visceral adiposity; the age-related accumulation of visceral fat in post-menopausal women is likely due to drastically reduced E2 levels.[14-17, 50, 51] Indeed, E2 replacement therapy prevents post-menopausal women from excessive visceral adiposity, underlining E2 signaling as an important regulator of visceral distribution.[16, 17] To understand the underlying mechanism, we investigated the interaction between E2 signaling and autophagy, and its relation with adipogenesis and visceral adiposity in mice. We found that female mice had lower vWAT mass than males (Figure 1), which was associated with higher expression of ERs but lower activity of cell remodeling via autophagy in females (Figures 2-3). The lower vWAT mass in females seemed to arise from E2-signaling suppressed autophagy and adipogenesis (Figures 4-5, and 1s). Adipogenesis was associated with downregulation of ERs and increased autophagy activity (Figures 4 and 1s). However, induction of E2 signaling dampened autophagy and adipogenesis, and use of established autophagy inhibitor BL recapitulated the effects of E2 on adipogenesis (Figures 5 and 1s). These findings suggest that the lower visceral adiposity in females is due to a

stronger E2 signaling that inhibits autophagy and adipogenesis to a greater extent than in males. Indeed, ablation of ERα normalized autophagy activity and diminished the gender difference in visceral adiposity (Figures 7 and 3s). Of note, the sWAT mass in female mice was indiscernible from that in the males, although in humans females have higher sWAT adiposity than males.[52-54] The species similarity and disparity between mice and humans highlights the importance of carefully considering the strengths and limitations of rodents as physiological models for humans.[55]

The role of E2 signaling in metabolism and adiposity has been extensively investigated.[56-62] However, this is the first study of E2 signaling in the regulation of adipocyte autophagy. Our data suggests that E2 signaling served as a suppressor of adipocyte autophagy (Figures 4-7). In particular, E2 induced the activation of mTOR, which phosphorylated (p-ULK1^{Ser757}) and thus deactivated ULK1, the key components of autophagy initiation complex (Figure 6).[37-39] In line with males showing lower levels of ERs in vWAT, the inhibitory phosphorylation of ULK1 by mTOR was significantly lower (2.1-fold, $p<0.05$) than that in females (Figure 6). Moreover, ablation of ERα significantly mitigated (p-ULK1^{Ser757}) and normalized the gender difference in p-ULK1^{Ser757}. Both *in vitro* and *in vivo* evidence supports the existence of the E2/ER-mTOR-ULK1 signaling cascade. However, further studies are warranted to determine how E2 signaling activates mTOR. In breast cancer cells it was shown that E2 might activate mTOR via small GTPase Ras homologue enriched in brain (Rheb), and it is still unclear how E2/ER signaling interacts with Rheb.[63]

Our findings may shed light on the increased visceral adiposity and metabolic syndrome (e.g., fatty liver) in breast cancer patients receiving anti-estrogenic treatment.[64, 65] For instance, tamoxifen, a selective ER modulator that binds to ERs and suppresses E2 action, was found to

significantly increase body mass index (BMI of 30.9 on average, indicative of obesity), visceral fat area, and incidence of type 2 diabetes in women with breast cancer.[64] The E2-autophagy-adipogenesis axis identified in this study may account, at least in part, for the tamoxifen-induced visceral obesity in tamoxifen users. In laboratory animals, hyperplasia (i.e., increased adipogenesis) can be induced by removal of E2 (via ovariectomy) or ERα (via genetic knockout) which increases visceral fat mass and impairs metabolism; by contrast, administration of E2 reduces adiposity and improves metabolic homeostasis.[61, 62, 66, 67] Therefore, the effects of E2-autophagy axis on adiposity and metabolic homeostasis should be taken into consideration in future anti-estrogenic treatment of breast cancer.

Taken together, our study provides the first line of evidence that E2/ER signaling mediates gender difference in visceral adiposity by dampening autophagy and adipogenesis via the mTOR-ULK1 pathway. The males have distinctly lower expression of ER in visceral fat than the females, thereby enhancing autophagy and adipogenesis and leading to higher distribution of visceral fat in male mice. Although ERβ cannot be excluded from the regulating process, ERα appears to play the dominant role because deletion of ERα alone normalized the gender differences in autophagy activity and visceral adiposity. This study adds to the importance of considering the gender perspective on the role of autophagy in human diseases.[68] Given that nutrient signal also regulates mTOR activity,[38] it would be of interest for future investigation to depict how E2/ER interacts with nutrient statuses (e.g., fasting or feeding with high-energy diet) in the regulation of autophagy and adiposity.

MATERIALS AND METHODS

Mice. C57BL6/J mice were housed in plastic cages on a 12-hour light–dark photocycle and with free access to water and regular chow diet as described previously;[25, 34] at the age of 6–7 week

old, the mice were weighed and sacrificed for tissue collection. The WT and global ERα knockout mice were obtained by breeding heterozygous males to females as described previously;[49] at the age of 12-16 weeks old, the WT and ERα knockout mice were weighed and sacrificed for tissue collection. The WAT pads were collected and weighed quickly before SVF isolation, explant culture for autophagy flux analysis, or snap freezing in liquid nitrogen. Animal use procedures followed the National Institutes of Health guidelines and were approved by the Virginia Tech Institutional Animal Care and Use Committee.

3T3L1 cell culture, differentiation, and treatment. 3T3L1 preadipocytes (ATCC CL-173, Manassas, VA, USA) were cultured in basal media (DMEM media containing 10% FBS, 100 units/ml penicillin and 100 μg/ml streptomycin (1 × P/S)), at 37 °C in a humidified atmosphere of 5% CO2.[33-35] The media were replaced every 2 days until the cells became confluent (day 0), and after 2 more days (day 2) the medium was changed to differentiation medium I (DMEM with 10% FBS, P/S (1 ×), IBMX (0.5 mM), dexamethasone (1 μM), insulin (1 μg/ml), and rosiglitazone (2 μM)). At the end of day 4, the medium was changed to differentiation medium II (DMEM with 10% FBS, P/S (1 ×), and insulin (1 μg/ml)). At the end of day 6, the medium was changed to basal media and the cells were maintained until day 12. Preadipocytes without differentiation induction were maintained in basal media and supplied with fresh medium every 2 days till day 12. E2 at the concentrations of 1 nM-10 μM has been used to treat adipocytes.[69-76] Our preliminary tests indicated that E2 at 1 nM, 10 nM, 0.1 μM, and 0.2 μM, imposed similar effects, but E2 at 0.1 μM (likewise 0.2 μM) was the most potent (data not shown). As such, we used E2 of 0.1 μM for the treatments starting on day 0 through day 12. Other chemicals were used at the concentrations established previously, including PPT (0.1 μM), DPN (0.1 μM), and bafilomycin A1 (4 nM), and leupeptin (0.4 ng),[25, 77, 78] to treat the cells during differentiation.

Primary stromal vascular cell culture, differentiation, and treatment. Fresh gonadal WAT from C57BL6/J mice were dissected, minced, and digested as previously described.[79] Cells were suspended in basal media (DMEM/F12 containing 10% FBS and 100 units/ml penicillin and 100 μg/ml streptomycin (1 × P/S)), and centrifuged at 500 × g for 5 minutes. The pellet was resuspended in basal media and filtered through a 40-micron cell strainer. After centrifuge (500 × g) for 5 minutes, the pellet was resuspended in basal media and plated on 10 cm dishes. After cell subculture to a 95% confluence (day 0) on 6-well plates, differentiation was induced in differentiation medium (DMEM/F12 medium with 10 % FBS, 1× Pen/Strep, dexamethasone (5 μM), insulin (0.5 μg/mL), IBMX (0.5 mM), and rosiglitazone (1 μM)) for 4 days (day 4). Then the cells were maintained in maintenance medium (DMEM/F12 medium containing 10 % FBS, 1× Pen/Strep, and insulin (0.5 μg/mL)) for 6 days (day 10). The treatments with chemicals (E2 at 0.1 μM, bafilomycin A1 at 4 nM, and leupeptin at 0.4 ng/ml) started on day 0 through day 10 to examine their effects on autophagy and adipogenesis.

Oil red O staining. The Oil Red O working solution was freshly prepared by mixing 0.35% stock solution with dH_2O (6:4) and filtered, and the staining was conducted as described.[25, 33, 35] After the media were removed, the cells were washed once with cold phosphate buffered saline, and fixed in 4% formaldehyde at room temperature for 10 minutes. The cells were then washed with dH_2O and air dried. Oil Red O working solution was added to start the staining at room temperature for 1 hour. The stained cells were washed with dH_2O for 4 times before the images were captured with a Nikon ECLIPSE Ti Inverted Microscope (Melville, NY, USA).

Autophagy flux assay. To measure autophagy flux in cultured cells, we treated 3T3L1 preadipocytes, stromal vascular cells, and mature adipocytes (day 10) with bafilomycin A1 (inhibitor of autophagosome acidification, at 0.1 μM) plus leupeptin (the inhibitor of lysosomal

proteases, at 10 μg/ml) for 4 hours. The cells were then harvested to prepare cell lysates as previously described.[25, 33, 35] To measure autophagy flux in WAT explants, freshly collected adipose tissues were minced into small tissue fragments (2–3 mm^3) and cultured for 4 hours with DMEM medium supplemented with 2 mM glutamine, 1% (vol/vol) antibiotic solution, and 10% (vol/vol) FBS in a CO_2 incubator (37°C,5% CO_2). The WAT explant cultures in the presence or absence of bafilomycin-A1 (0.1 μM) and leupeptin (10 μg/ml) were then harvested and lysed as described previously [25]. The turnover of LC3-II or p62 protein, i.e., the substrates of autophagy for degradation, was measured by western blotting and image analysis to assess autophagy flux.[25, 27, 28]

Western blotting. Tissue and cell lysates were prepared with PLC lysis buffer (30 mM Hepes, pH 7.5, 150 mM NaCl, 10% glycerol, 1% Triton X-100, 1.5 mM $MgCl_2$, 1 mM EGTA, 10 mM NaPPi, 100 mM NaF, 1 mM Na_3VO_4) supplemented with protease inhibitor cocktail (Roche), and 1 mM PMSF.[80] Total protein concentrations of the lysates were determined using a DC protein assay kits (Bio-Rad). Antibody (catalog number) information: GAPDH (MA5-15738) and β-actin (MA5-15739) antibodies were purchased from Pierce (Rockford, IL, USA); Atg5 (12994s), Atg7 (8558s), Atg12 (2011s), p62 (5114s), p-mTOR (Ser2448) antibody (5536s), and p-ULK1(Ser757) antibody (14202s) from Cell Signaling Technology (Beverly, MA, USA); beclin 1 (MABN16), ERα (04-820) and ERβ (GR39) antibodies from EMD Millipore (Billerica, MA, USA); and LC3B antibody (L7543) from Sigma.

Statistical analysis. Data are presented as mean ± SD. Differences between the groups were validated by one-way-ANOVA with the least significant difference post hoc test to detect statistical differences between groups and treatments (DI+ vs. DI-, E2+ vs. E2-, and BL+ vs. BL-

). Differences in autophagy and adipose parameters between males and females were validated by a t-test. A value of $p < 0.05$ was considered statistically significant.

DISCLOSURE OF POTENTIAL CONFLICTS OF INTEREST

None.

ACKNOWLEDGMENTS

Funding for this work was provided, in part, by USDA National Institute of Food and Agriculture Hatch Project 1007334 (ZC), NIH grant R18DK091811 (FAA), and NIH grant 1R01AT007077 (DL).

REFERENCES

1. Kershaw EE, Flier JS. Adipose tissue as an endocrine organ. *J. Clin. Endocrinol. Metab.* 2004; **89**(6)**:** 2548-56.

2. Galic S, Oakhill JS, Steinberg GR. Adipose tissue as an endocrine organ. *Mol. Cell. Endocrinol.* 2010; **316**(2)**:** 129-39.

3. Kim SN, Jung YS, Kwon HJ, Seong JK, Granneman JG, Lee YH. Sex differences in sympathetic innervation and browning of white adipose tissue of mice. *Biology of Sex Differences* 2016; **7:** 67.

4. Jeffery E, Church CD, Holtrup B, Colman L, Rodeheffer MS. Rapid depot-specific activation of adipocyte precursor cells at the onset of obesity. *Nat Cell Biol* 2015; **17**(4)**:** 376-85.

5. Tchoukalova YD, Votruba SB, Tchkonia T, Giorgadze N, Kirkland JL, Jensen MD. Regional differences in cellular mechanisms of adipose tissue gain with overfeeding. *Proc. Natl. Acad. Sci. U. S. A.* 2010; **107**(42)**:** 18226-31.

6. Gesta S, Bluher M, Yamamoto Y, Norris AW, Berndt J, Kralisch S *et al.* Evidence for a role of developmental genes in the origin of obesity and body fat distribution. *Proc. Natl. Acad. Sci. U. S. A.* 2006; **103**(17)**:** 6676-81.

7. Macotela Y, Emanuelli B, Mori MA, Gesta S, Schulz TJ, Tseng YH *et al.* Intrinsic differences in adipocyte precursor cells from different white fat depots. *Diabetes* 2012; **61**(7)**:** 1691-9.

8. Macotela Y, Boucher J, Tran TT, Kahn CR. Sex and depot differences in adipocyte insulin sensitivity and glucose metabolism. *Diabetes* 2009; **58**(4)**:** 803-12.

9. Shi H, Strader AD, Woods SC, Seeley RJ. The effect of fat removal on glucose tolerance is depot specific in male and female mice. *American journal of physiology. Endocrinology and Metabolism* 2007; **293**(4)**:** E1012-20.

10. Cohen P, Levy JD, Zhang Y, Frontini A, Kolodin DP, Svensson KJ *et al.* Ablation of PRDM16 and beige adipose causes metabolic dysfunction and a subcutaneous to visceral fat switch. *Cell* 2014; **156**(1-2)**:** 304-16.

11. Veilleux A, Caron-Jobin M, Noel S, Laberge PY, Tchernof A. Visceral adipocyte hypertrophy is associated with dyslipidemia independent of body composition and fat distribution in women. *Diabetes* 2011; **60**(5)**:** 1504-11.

12. Manolopoulos KN, Karpe F, Frayn KN. Gluteofemoral body fat as a determinant of metabolic health. *Int J Obes (Lond)* 2010; **34**(6)**:** 949-59.

13. Pischon T, Boeing H, Hoffmann K, Bergmann M, Schulze MB, Overvad K *et al.* General and abdominal adiposity and risk of death in Europe. *N. Engl. J. Med.* 2008; **359**(20)**:** 2105-20.

14. Demerath EW, Sun SS, Rogers N, Lee M, Reed D, Choh AC *et al.* Anatomical patterning of visceral adipose tissue: race, sex, and age variation. *Obesity (Silver Spring)* 2007; **15**(12)**:** 2984-93.

15. Despres JP, Couillard C, Gagnon J, Bergeron J, Leon AS, Rao DC *et al.* Race, visceral adipose tissue, plasma lipids, and lipoprotein lipase activity in men and women: the Health, Risk Factors, Exercise Training, and Genetics (HERITAGE) family study. *Arterioscler. Thromb. Vasc. Biol.* 2000; **20**(8)**:** 1932-8.

16. Haarbo J, Marslew U, Gotfredsen A, Christiansen C. Postmenopausal hormone replacement therapy prevents central distribution of body fat after menopause. *Metabolism.* 1991; **40**(12)**:** 1323-6.

17. Gambacciani M, Ciaponi M, Cappagli B, Piaggesi L, De Simone L, Orlandi R *et al.* Body weight, body fat distribution, and hormonal replacement therapy in early postmenopausal women. *J. Clin. Endocrinol. Metab.* 1997; **82**(2)**:** 414-7.

18. Rigamonti A, Brennand K, Lau F, Cowan CA. Rapid cellular turnover in adipose tissue. *PloS One* 2011; **6**(3)**:** e17637.

19. Spalding KL, Arner E, Westermark PO, Bernard S, Buchholz BA, Bergmann O *et al.* Dynamics of fat cell turnover in humans. *Nature* 2008; **453**(7196)**:** 783-7.

20. Prins JB, O'Rahilly S. Regulation of adipose cell number in man. *Clin Sci (Lond)* 1997; **92**(1)**:** 3-11.

21. Singh R, Xiang Y, Wang Y, Baikati K, Cuervo AM, Luu YK *et al.* Autophagy regulates adipose mass and differentiation in mice. *J. Clin. Invest.* 2009; **119**(11)**:** 3329-39.

22. Zhang Y, Goldman S, Baerga R, Zhao Y, Komatsu M, Jin S. Adipose-specific deletion of autophagy-related gene 7 (atg7) in mice reveals a role in adipogenesis. *Proc. Natl. Acad. Sci. U. S. A.* 2009; **106**(47)**:** 19860-5.

23. Baerga R, Zhang Y, Chen PH, Goldman S, Jin S. Targeted deletion of autophagy-related 5 (atg5) impairs adipogenesis in a cellular model and in mice. *Autophagy* 2009; **5**(8)**:** 1118-30.

24. Zhang C, He Y, Okutsu M, Ong LC, Jin Y, Zheng L *et al.* Autophagy is involved in adipogenic differentiation by repressesing proteasome-dependent PPARgamma2 degradation. *American journal of physiology. Endocrinology and Metabolism* 2013; **305**(4)**:** E530-9.

25. Liu L, Zheng LD, Zou P, Brooke J, Smith C, Long YC *et al.* FoxO1 antagonist suppresses autophagy and lipid droplet growth in adipocytes. *Cell Cycle* 2016; **15**(15)**:** 2033-41.

26. Zhang J. Teaching the basics of autophagy and mitophagy to redox biologists--mechanisms and experimental approaches. *Redox Biology* 2015; **4:** 242-59.

27. Mizushima N, Yoshimori T, Levine B. Methods in mammalian autophagy research. *Cell* 2010; **140**(3)**:** 313-26.

28. Yamada E, Singh R. Mapping autophagy on to your metabolic radar. *Diabetes* 2012; **61**(2)**:** 272-80.

29. Tao Z, Liu L, Zheng LD, Cheng Z. Autophagy in Adipocyte Differentiation. *Methods Mol. Biol.* 2017.

30. Heldring N, Pawson T, McDonnell D, Treuter E, Gustafsson JA, Pike AC. Structural insights into corepressor recognition by antagonist-bound estrogen receptors. *J. Biol. Chem.* 2007; **282**(14)**:** 10449-55.

31. Berry DC, Stenesen D, Zeve D, Graff JM. The developmental origins of adipose tissue. *Development* 2013; **140**(19)**:** 3939-49.

32. Rosen ED, Spiegelman BM. What we talk about when we talk about fat. *Cell* 2014; **156**(1-2)**:** 20-44.

33. Liu L, Tao Z, Zheng LD, Brooke JP, Smith CM, Liu D *et al.* FoxO1 interacts with transcription factor EB and differentially regulates mitochondrial uncoupling proteins via autophagy in adipocytes. *Cell Death Discovery* 2016; **2:** 16066.

34. Liu L, Zou P, Zheng L, Linarelli LE, Amarell S, Passaro A *et al.* Tamoxifen reduces fat mass by boosting reactive oxygen species. *Cell Death & Disease* 2015; **6:** e1586.

35. Zou P, Liu L, Zheng L, Stoneman RE, Cho A, Emery A *et al.* Targeting FoxO1 with AS1842856 suppresses adipogenesis. *Cell Cycle* 2014; **13**(23)**:** 3759-67.

36. Komatsu M, Kurokawa H, Waguri S, Taguchi K, Kobayashi A, Ichimura Y *et al.* The selective autophagy substrate p62 activates the stress responsive transcription factor Nrf2 through inactivation of Keap1. *Nat Cell Biol* 2010; **12**(3)**:** 213-23.

37. Green DR, Levine B. To be or not to be? How selective autophagy and cell death govern cell fate. *Cell* 2014; **157**(1)**:** 65-75.

38. Kim J, Kundu M, Viollet B, Guan KL. AMPK and mTOR regulate autophagy through direct phosphorylation of Ulk1. *Nat Cell Biol* 2011; **13**(2)**:** 132-41.

39. Fougeray S, Pallet N. Mechanisms and biological functions of autophagy in diseased and ageing kidneys. *Nature reviews. Nephrology* 2015; **11**(1)**:** 34-45.

40. Chiang GG, Abraham RT. Phosphorylation of mammalian target of rapamycin (mTOR) at Ser-2448 is mediated by p70S6 kinase. *J. Biol. Chem.* 2005; **280**(27)**:** 25485-90.

41. Nave BT, Ouwens M, Withers DJ, Alessi DR, Shepherd PR. Mammalian target of rapamycin is a direct target for protein kinase B: identification of a convergence point for opposing effects of insulin and amino-acid deficiency on protein translation. *Biochem. J.* 1999; **344 Pt 2:** 427-31.

42. Pierdominici M, Maselli A, Locatelli SL, Ciarlo L, Careddu G, Patrizio M *et al.* Estrogen receptor beta ligation inhibits Hodgkin lymphoma growth by inducing autophagy. *Oncotarget* 2017; **8**(5)**:** 8522-8535.

43. Ruddy SC, Lau R, Cabrita MA, McGregor C, McKay BC, Murphy LC *et al.* Preferential estrogen receptor beta ligands reduce Bcl-2 expression in hormone-resistant breast cancer cells to increase autophagy. *Molecular Cancer Therapeutics* 2014; **13**(7)**:** 1882-93.

44. Guido C, Panza S, Santoro M, Avena P, Panno ML, Perrotta I *et al.* Estrogen receptor beta (ERbeta) produces autophagy and necroptosis in human seminoma cell line through the binding of the Sp1 on the phosphatase and tensin homolog deleted from chromosome 10 (PTEN) promoter gene. *Cell Cycle* 2012; **11**(15)**:** 2911-21.

45. Pons DG, Torrens-Mas M, Nadal-Serrano M, Sastre-Serra J, Roca P, Oliver J. The presence of Estrogen Receptor beta modulates the response of breast cancer cells to therapeutic agents. *Int. J. Biochem. Cell Biol.* 2015; **66:** 85-94.

46. Hsieh DJ, Kuo WW, Lai YP, Shibu MA, Shen CY, Pai P *et al.* 17beta-Estradiol and/or Estrogen Receptor beta Attenuate the Autophagic and Apoptotic Effects Induced by Prolonged Hypoxia Through HIF-1alpha-Mediated BNIP3 and IGFBP-3 Signaling Blockage. *Cell. Physiol. Biochem.* 2015; **36**(1)**:** 274-84.

47. Stauffer SR, Coletta CJ, Tedesco R, Nishiguchi G, Carlson K, Sun J *et al.* Pyrazole ligands: structure-affinity/activity relationships and estrogen receptor-alpha-selective agonists. *J. Med. Chem.* 2000; **43**(26)**:** 4934-47.

48. Meyers MJ, Sun J, Carlson KE, Marriner GA, Katzenellenbogen BS, Katzenellenbogen JA. Estrogen receptor-beta potency-selective ligands: structure-activity relationship studies of diarylpropionitriles and their acetylene and polar analogues. *J. Med. Chem.* 2001; **44**(24)**:** 4230-51.

49. Lubahn DB, Moyer JS, Golding TS, Couse JF, Korach KS, Smithies O. Alteration of reproductive function but not prenatal sexual development after insertional disruption of the mouse estrogen receptor gene. *Proc. Natl. Acad. Sci. U. S. A.* 1993; **90**(23)**:** 11162-6.

50. Goodman-Gruen D, Barrett-Connor E. Sex differences in measures of body fat and body fat distribution in the elderly. *Am. J. Epidemiol.* 1996; **143**(9)**:** 898-906.

51. Camhi SM, Bray GA, Bouchard C, Greenway FL, Johnson WD, Newton RL *et al.* The relationship of waist circumference and BMI to visceral, subcutaneous, and total body fat: sex and race differences. *Obesity (Silver Spring)* 2011; **19**(2)**:** 402-8.

52. White UA, Tchoukalova YD. Sex dimorphism and depot differences in adipose tissue function. *Biochim. Biophys. Acta* 2014; **1842**(3)**:** 377-92.

53. Karastergiou K, Smith SR, Greenberg AS, Fried SK. Sex differences in human adipose tissues - the biology of pear shape. *Biology of Sex Differences* 2012; **3**(1)**:** 13.

54. Fuente-Martin E, Argente-Arizon P, Ros P, Argente J, Chowen JA. Sex differences in adipose tissue: It is not only a question of quantity and distribution. *Adipocyte* 2013; **2**(3)**:** 128-34.

55. Chusyd DE, Wang D, Huffman DM, Nagy TR. Relationships between Rodent White Adipose Fat Pads and Human White Adipose Fat Depots. *Frontiers in Nutrition* 2016; **3:** 10.

56. Barros RP, Gustafsson JA. Estrogen receptors and the metabolic network. *Cell Metab* 2011; **14**(3)**:** 289-99.

57. Clegg DJ. Minireview: the year in review of estrogen regulation of metabolism. *Mol. Endocrinol.* 2012; **26**(12)**:** 1957-60.

58. Kim JH, Cho HT, Kim YJ. The role of estrogen in adipose tissue metabolism: insights into glucose homeostasis regulation. *Endocr. J.* 2014; **61**(11)**:** 1055-67.

59. Bluher M. Importance of estrogen receptors in adipose tissue function. *Molecular Metabolism* 2013; **2**(3)**:** 130-2.

60. Wang A, Luo J, Moore W, Alkhalidy H, Wu L, Zhang J *et al.* GPR30 regulates diet-induced adiposity in female mice and adipogenesis in vitro. *Scientific Reports* 2016; **6:** 34302.

61. D'Eon TM, Souza SC, Aronovitz M, Obin MS, Fried SK, Greenberg AS. Estrogen regulation of adiposity and fuel partitioning. Evidence of genomic and non-genomic regulation of lipogenic and oxidative pathways. *J. Biol. Chem.* 2005; **280**(43)**:** 35983-91.

62. Davis KE, M DN, Sun K, W MS, J DB, J AZ *et al.* The sexually dimorphic role of adipose and adipocyte estrogen receptors in modulating adipose tissue expansion, inflammation, and fibrosis. *Molecular Metabolism* 2013; **2**(3)**:** 227-42.

63. Yu J, Henske EP. Estrogen-induced activation of mammalian target of rapamycin is mediated via tuberin and the small GTPase Ras homologue enriched in brain. *Cancer Res.* 2006; **66**(19)**:** 9461-6.

64. Nguyen MC, Stewart RB, Banerji MA, Gordon DH, Kral JG. Relationships between tamoxifen use, liver fat and body fat distribution in women with breast cancer. *Int. J. Obes. Relat. Metab. Disord.* 2001; **25**(2)**:** 296-8.

65. Sheean PM, Hoskins K, Stolley M. Body composition changes in females treated for breast cancer: a review of the evidence. *Breast Cancer Res. Treat.* 2012; **135**(3)**:** 663-80.

66. Clegg DJ, Brown LM, Woods SC, Benoit SC. Gonadal hormones determine sensitivity to central leptin and insulin. *Diabetes* 2006; **55**(4)**:** 978-87.

67. Heine PA, Taylor JA, Iwamoto GA, Lubahn DB, Cooke PS. Increased adipose tissue in male and female estrogen receptor-alpha knockout mice. *Proc. Natl. Acad. Sci. U. S. A.* 2000; **97**(23)**:** 12729-34.

68. Lista P, Straface E, Brunelleschi S, Franconi F, Malorni W. On the role of autophagy in human diseases: a gender perspective. *Journal of Cellular and Molecular Medicine* 2011; **15**(7)**:** 1443-57.

69. Pektas M, Kurt AH, Un I, Tiftik RN, Buyukafsar K. Effects of 17beta-estradiol and progesterone on the production of adipokines in differentiating 3T3-L1 adipocytes: Role of Rho-kinase. *Cytokine* 2015; **72**(2)**:** 130-4.

70. Capllonch-Amer G, Llado I, Proenza AM, Garcia-Palmer FJ, Gianotti M. Opposite effects of 17-beta estradiol and testosterone on mitochondrial biogenesis and adiponectin synthesis in white adipocytes. *J. Mol. Endocrinol.* 2014; **52**(2)**:** 203-14.

71. Chen YH, Lee MJ, Chang HH, Hung PF, Kao YH. 17 beta-estradiol stimulates resistin gene expression in 3T3-L1 adipocytes via the estrogen receptor, extracellularly regulated kinase, and CCAAT/enhancer binding protein-alpha pathways. *Endocrinology* 2006; **147**(9)**:** 4496-504.

72. Collison M, Campbell IW, Salt IP, Dominiczak AF, Connell JM, Lyall H *et al.* Sex hormones induce insulin resistance in 3T3-L1 adipocytes by reducing cellular content of IRS proteins. *Diabetologia* 2000; **43**(11)**:** 1374-80.

73. Luo F, Huang WY, Guo Y, Ruan GY, Peng R, Li XP. 17beta-estradiol lowers triglycerides in adipocytes via estrogen receptor alpha and it may be attenuated by inflammation. *Lipids in Health and Disease* 2017; **16**(1)**:** 182.

74. Jeong S, Yoon M. 17beta-Estradiol inhibition of PPARgamma-induced adipogenesis and adipocyte-specific gene expression. *Acta pharmacologica Sinica* 2011; **32**(2)**:** 230-8.

75. Jenks MZ, Fairfield HE, Johnson EC, Morrison RF, Muday GK. Sex Steroid Hormones Regulate Leptin Transcript Accumulation and Protein Secretion in 3T3-L1 Cells. *Scientific Reports* 2017; **7**(1)**:** 8232.

76. Fatima LA, Campello RS, Santos RS, Freitas HS, Frank AP, Machado UF *et al.* Estrogen receptor 1 (ESR1) regulates VEGFA in adipose tissue. *Scientific Reports* 2017; **7**(1)**:** 16716.

77. Harrington WR, Sheng S, Barnett DH, Petz LN, Katzenellenbogen JA, Katzenellenbogen BS. Activities of estrogen receptor alpha- and beta-selective ligands at diverse estrogen responsive gene sites mediating transactivation or transrepression. *Mol. Cell. Endocrinol.* 2003; **206**(1-2)**:** 13-22.

78. Harris HA, Katzenellenbogen JA, Katzenellenbogen BS. Characterization of the biological roles of the estrogen receptors, ERalpha and ERbeta, in estrogen target tissues in vivo through the use of an ERalpha-selective ligand. *Endocrinology* 2002; **143**(11)**:** 4172-7.

79. Liu L, Zheng LD, Donnelly SR, Emont MP, Wu J, Cheng Z. Isolation of Mouse Stromal Vascular Cells for Monolayer Culture. *Methods Mol. Biol.* 2017; **1566:** 9-16.

80. Cheng Z, Guo S, Copps K, Dong X, Kollipara R, Rodgers JT *et al.* Foxo1 integrates insulin signaling with mitochondrial function in the liver. *Nat. Med.* 2009; **15**(11)**:** 1307-11.

Figure 1. Gender difference existed in the percentage of visceral but not subcutaneous fat. (A) The body weights of male and female mice at the age of 6-7 weeks. (B) The net weights of visceral WAT from male and female mice. (C) The net weights of subcutaneous WAT from male and female mice. (D) The percentage of visceral WAT from male and female mice, normalized against the body weights. (E) The percentage of subcutaneous WAT from male and female mice, normalized by body weights. *, $p<0.05$; **, $p<0.01$; n.s., not significant; n=4-6.

Figure 2. Autophagy activities showed gender difference in visceral but not subcutaneous fat. (A-B) The steady-state protein levels of LC3 in subcutaneous WAT, analyzed by western blotting (A) and densitometry (B). (C-D) The steady-state protein levels of LC3 in visceral WAT, analyzed by western blotting (C) and densitometry (D). (E-H) Measurement of autophagy flux in subcutaneous and visceral WAT. The WAT explant cultures were incubated with and without autophagy inhibitor bafilomycin A1 (0.1 μM) and leupeptin (10 μg/ml) for 4 hours, and the turnovers of LC3-II and p62 were examined by western blot (E, G) and densitometry (F, H). In densitometric analyses, the band densities of investigated proteins were normalized against that of GAPDH or β-actin, and the fold changes were calculated by taking the normalized density of female group as "1". For autophagy flux, we first normalized the band densities of LC3-II and p62 against that of GAPDH, then calculated the differences of normalized densities in the presence vs. the absence of autophagy inhibitor; lastly, the differences were shown as fold changes by taking the female group as "1". BL, bafilomycin A1 and leupeptin; M, male; F, female; *, $p<0.05$; **, $p<0.01$; n.s., not significant; n=3-4.

Figure 3. The expression of estrogen receptors (ER) showed gender difference in visceral but not subcutaneous fat. (A-B) The protein levels of ERα and ERβ in subcutaneous WAT, analyzed by western blotting (A) and densitometry (B). (C-D) The protein levels of ERα and ERβ in

visceral WAT, analyzed by western blotting (C) and densitometry (D). In densitometric analysis, the band densities of investigated proteins were normalized against that of β-actin, and the fold changes were calculated by taking the normalized density of female group as "1". *, $p<0.05$; **, $p<0.01$; n.s., not significant; n=3-4.

Figure 4. Adipogenesis was associated with downregulation of ER but upregulation of autophagy activity. (A-B) The protein levels of ERα and ERβ in preadipocytes and mature (or differentiated) adipocytes, analyzed by western blotting (A) and densitometry (B). DI, differentiation induction. DI+ represents differentiated 3T3L1 cells (mature adipocytes) harvested on day 12; DI- represents 3T3L1 cells without differentiation induction (i.e., preadipocytes) harvested on day 12. (C) Oil red O staining to detect the differentiation of preadipocytes into mature adipocytes. On day 12, massive lipid accumulation was detected in mature adipocytes but not in preadipocytes. (D-E) The steady-state protein levels of LC3 in preadipocytes and mature adipocytes, analyzed by western blotting (D) and densitometry (E) on day 12. (F-G) Measurement of autophagy flux in preadipocytes and mature adipocytes. On day 12, the cells were incubated in the presence or absence of autophagy inhibitor BL (bafilomycin A1 at 0.1 μM and leupeptin at 10 μg/ml) for 4 hours, and the turnovers of LC3-II and p62 were examined by Western blotting (F) and densitometry (G). In densitometric analysis, the band densities of investigated proteins were normalized against that of GAPDH or β-actin, and the fold changes were calculated by taking the normalized density of DI- group as "1". For autophagy flux analysis, we first normalized the band densities of LC3-II and p62 against that of β-actin, then calculated the differences of normalized densities in the presence vs. the absence of autophagy inhibitor; lastly, the differences were shown as fold changes by taking the DI- group as "1". BL, bafilomycin A1 and leupeptin. *, $p<0.05$; **, $p<0.01$; ***, $p<0.0001$; n=3-4.

Figure 5. Activation of estrogen signaling suppressed autophagy and adipogenesis. (A-B) Estradiol (0.1 μM, days 0-12) increased the steady-state protein levels of LC3 and p62 during 3T3L1 preadipocyte differentiation, analyzed by western blotting (A) and densitometry (B). DI+ represents 3T3L1 cells with differentiation induction and harvested on day 12. (C-D) The presence of E2 (0.1 μM, days 0-12) reduced autophagy activity during preadipocyte differentiation. On day 12, autophagy flux was analyzed by western blotting (C) and densitometry (D) after the cells were incubated with and without autophagy inhibitor BL (bafilomycin A1 at 0.1 μM and leupeptin at 10 μg/ml) for 4 hours. In densitometric analysis, the band densities of investigated proteins were normalized against that of β-actin, and the fold changes were calculated by taking the normalized density of E2- group as "1". For autophagy flux analysis, we first normalized the band densities of LC3-II and p62 against that of β-actin, then calculated the differences of normalized densities in the presence vs. the absence of autophagy inhibitor; lastly, the differences were shown as fold changes by taking the E2- group as "1". (E) The presence of E2 (0.1 μM, days 0-12) suppressed the differentiation of 3T3L1 preadipocytes, analyzed by oil red O staining on day 12. (F) The presence of autophagy inhibitor bafilomycin A1 (4 nM) and leupeptin (0.4 ng) during days 0-12 recapitulated the effects of E2 on adipogenesis, analyzed by oil red O staining on day 12. n=3-4; *, $p<0.05$; **, $p<0.01$; ***, $p<0.0001$ (with E2 vs. without E2).

Figure 6. Estradiol-ER signaling regulated autophagy via mTOR-ULK1 pathway. (A-B) E2 (0.1 μM, days 0-12) induced the activating phosphorylation of mTOR (Ser2448) and the mTOR-catalyzed inhibitory phosphorylation of ULK1 (Ser757), analyzed by western blotting (A) and densitometry (B). DI+ represents 3T3L1 cells with differentiation induction and harvested on day 12, and DI- represents 3T3L1 cells without differentiation and harvested on day 12. (C-D)

The females and males showed comparable phosphorylation of mTOR (Ser2448) and ULK1 (Ser757), analyzed by western blotting (C) and densitometry (D). (E-F) The females showed significantly stronger phosphorylation of mTOR (Ser2448) and ULK1 (Ser757) than the males, analyzed by western blotting (E) and densitometry (F). In densitometric analysis, the band densities of investigated proteins were normalized against that of GAPDH or β-actin, and the fold changes were calculated by taking the normalized density of DI-E2- group (panels A and B) or female group (panels C-F) as "1". *, $p<0.05$; **, $p<0.01$; ***, $p<0.0001$; n.s., not significant; n=3-4.

Figure 7. Ablation of ERα normalized gender difference in autophagy and visceral adiposity. (A) Knockout (KO) of ERα in sWAT activated ULK1 by de-phosphorylation at Ser757. (B) KO of ERα in vWAT activated ULK1 by de-phosphorylation at Ser757, which diminished the gender difference in ERα expression and p-ULK1 observed in the WT mice. (C-D) The vWAT in WT females had lower autophagy activity (LC-3II and p62 turnover) than that in WT males (C), but KO of ERα abolished the gender difference (D). The representative western blotting images were presented in Figures 4s and 5s. In densitometric analysis, the band densities of investigated proteins were normalized against that of GAPDH, and the fold changes were calculated by taking the normalized density of male group as "1". For autophagy flux, we first normalized the band densities of LC3-II and p62 against that of GAPDH, then calculated the differences of normalized densities in the presence vs. the absence of autophagy inhibitor; lastly, the differences were shown as fold changes by taking the male group as "1". (E-H) WT males had higher vWAT mass than the WT females (F), but KO of ERα abolished the gender difference (H). Overall, KO of ERα increased adiposity in both sWAT and vWAT, presumably due to the enhanced autophagy that promotes adipogenesis. WT, wild type; KO, knockout of

ERα; M, male; F, female; WT/M, wild type males; WT/F, wild type females; KO/M, knockout males; KO/F, knockout females; *, $p<0.05$; **, $p<0.01$; n.s., not significant; n=5-8.

Figure 1

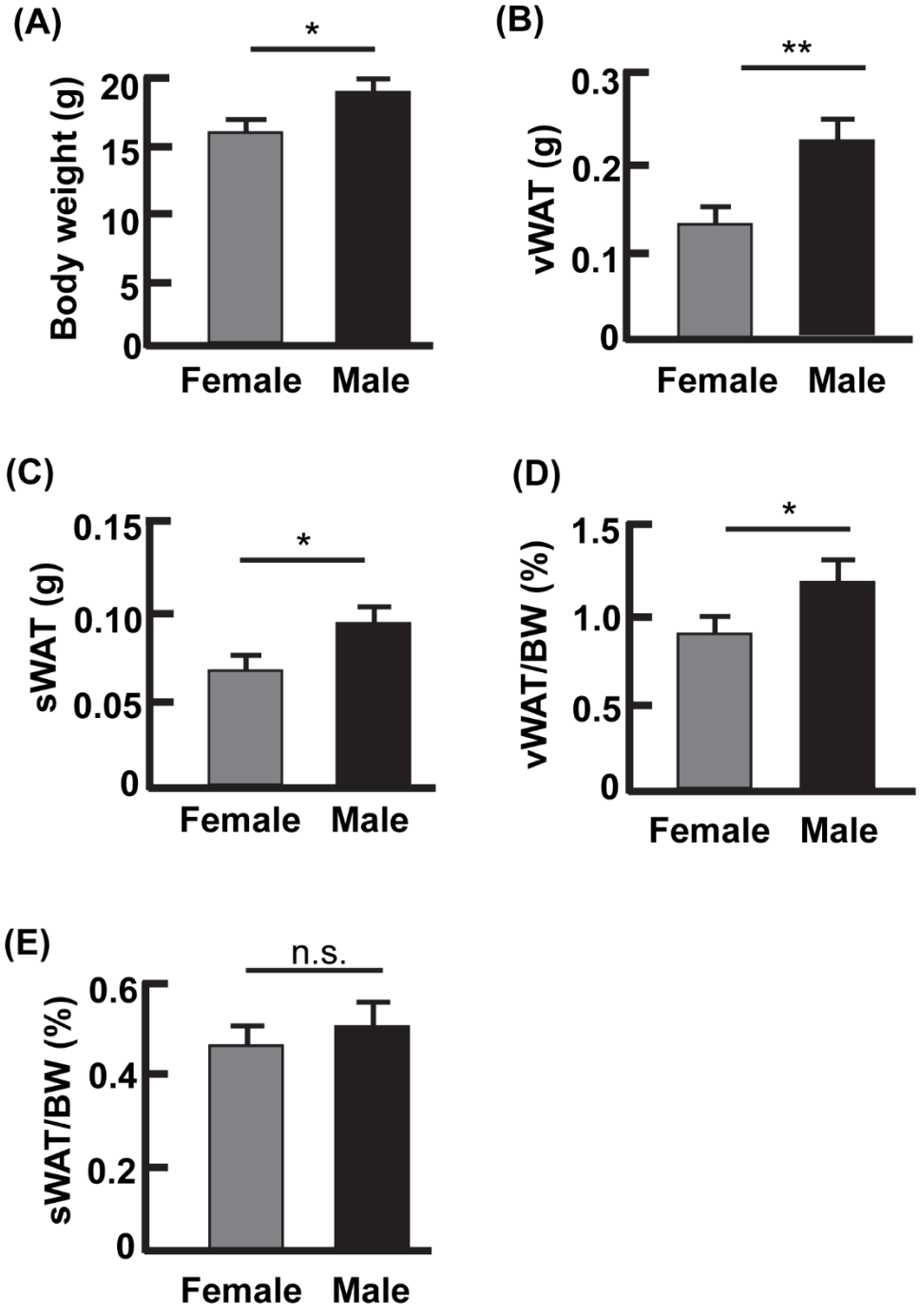
(A)
*
Body weight (g)
20
15
10
5
0
Female
Male
(B)
**
vWAT (g)
0.3
0.2
0.1
0
Female
Male
(C)
*
sWAT (g)
0.15
0.10
0.05
0
Female
Male
(D)
*
vWAT/BW (%)
1.5
1.0
0.5
0
Female
Male
(E)
n.s.
sWAT/BW (%)
0.6
0.4
0.2
0
Female
Male

Figure 2

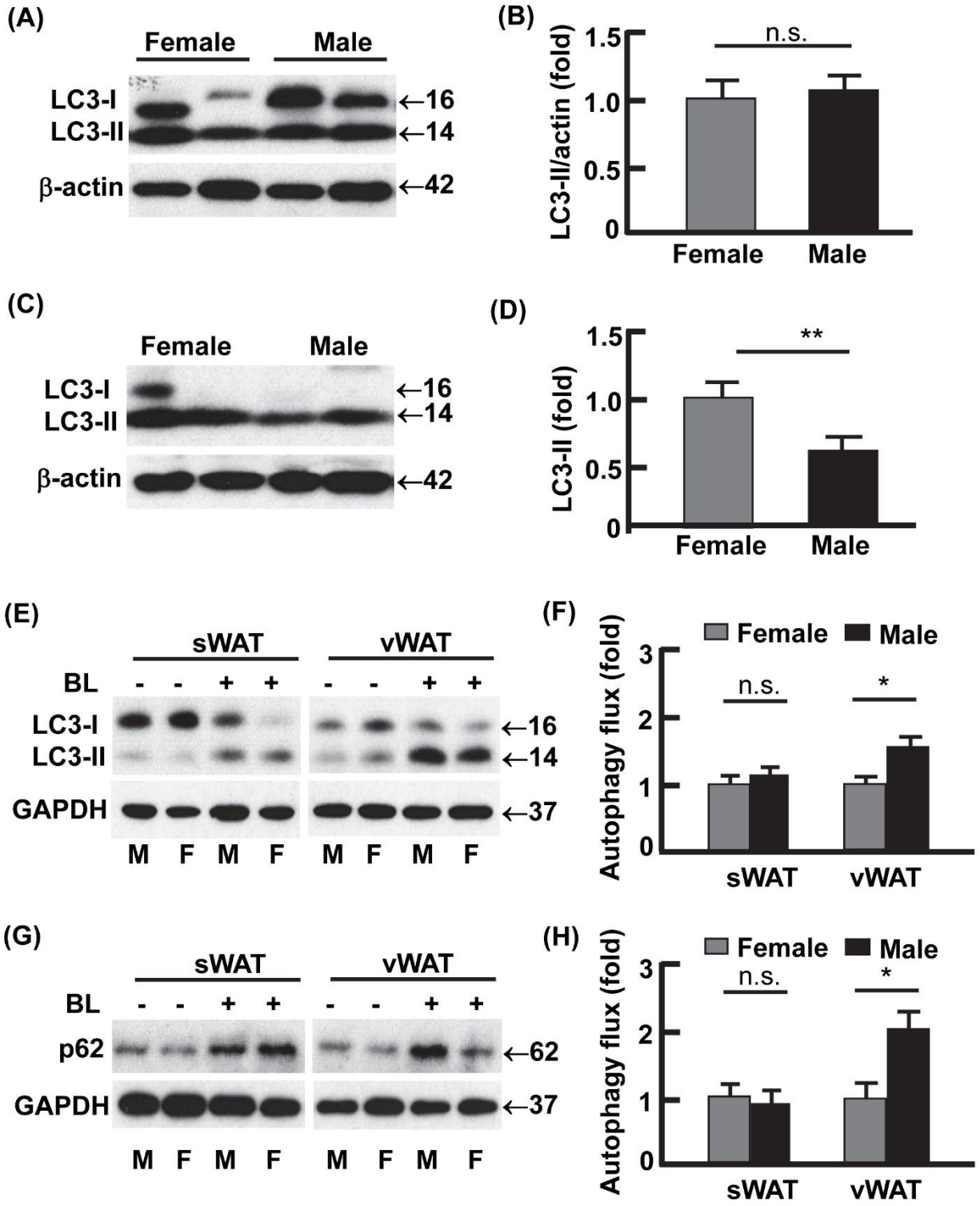
(A)
Female
Male
LC3-I
LC3-II
β-actin
←16
←14
←42
(B)
n.s.
LC3-II/actin (fold)
1.5
1.0
0.5
0
Female
Male
(C)
Female
Male
LC3-I
LC3-II
β-actin
←16
←14
←42
(D)
**
LC3-II (fold)
1.5
1.0
0.5
0
Female
Male
(E)
sWAT
vWAT
BL
- - + + - - + +
LC3-I
LC3-II
GAPDH
←16
←14
←37
M F M F M F M F
(F)
Female
Male
n.s.
*
Autophagy flux (fold)
3
2
1
0
sWAT
vWAT
(G)
sWAT
vWAT
BL
- - + + - - + +
p62
GAPDH
←62
←37
M F M F M F M F
(H)
Female
Male
n.s.
*
Autophagy flux (fold)
3
2
1
0
sWAT
vWAT

Figure 3

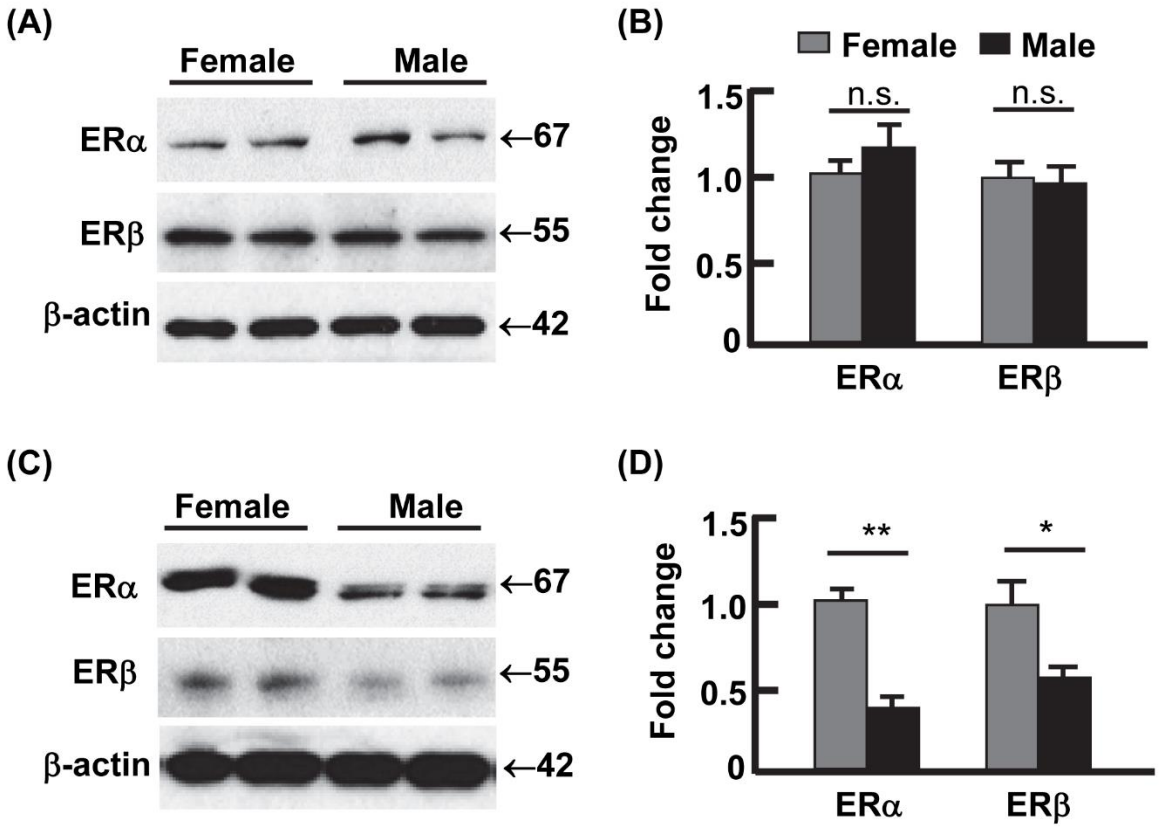
(A)
Female
Male
ERα
←67
ERβ
←55
β-actin
←42
(B)
Female
Male
n.s.
n.s.
Fold change
1.5
1.0
0.5
0
ERα
ERβ
(C)
Female
Male
ERα
←67
ERβ
←55
β-actin
←42
(D)
**
*
Fold change
1.5
1.0
0.5
0
ERα
ERβ

Figure 4

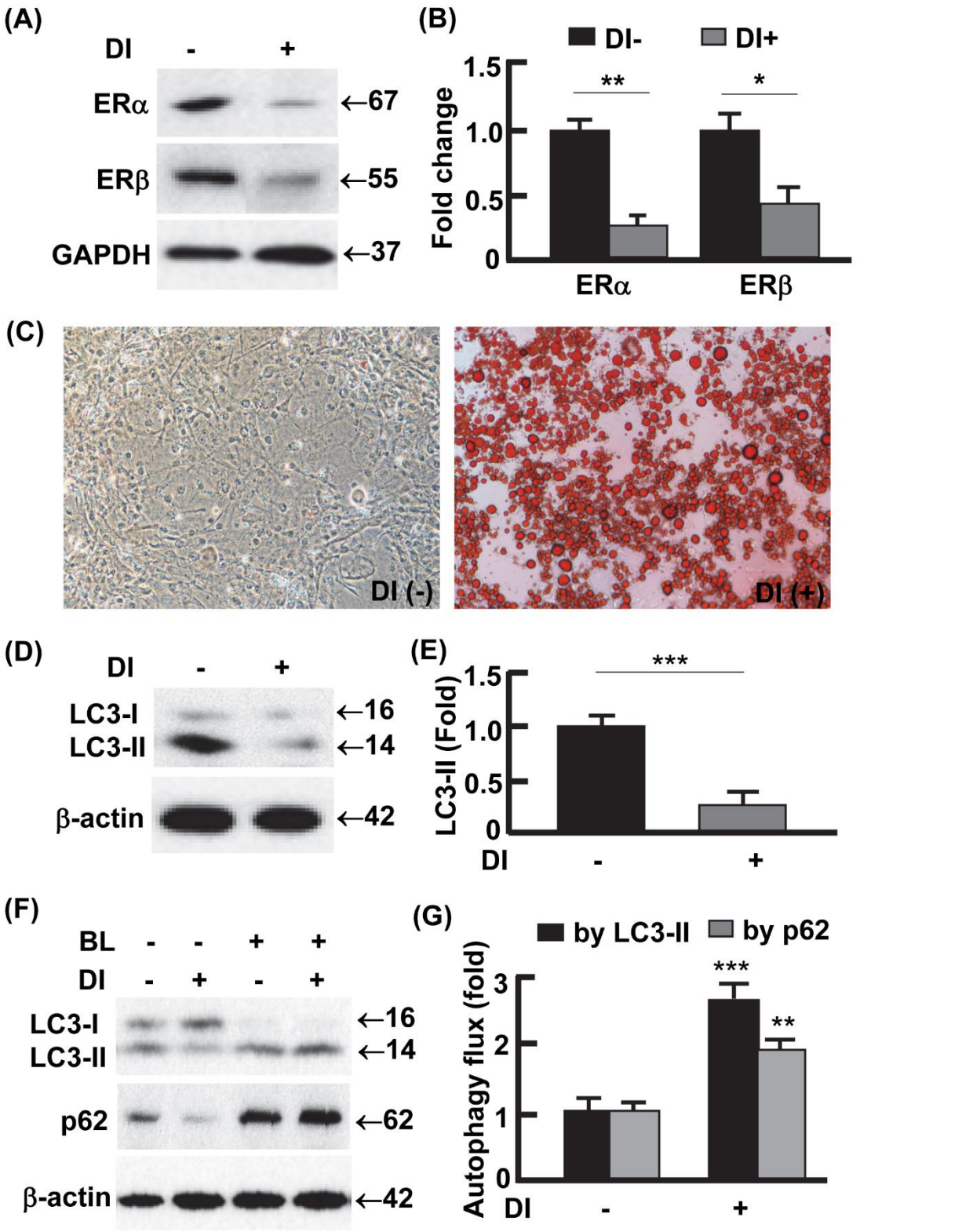
(A)
DI - +
ERα ←67
ERβ ←55
GAPDH ←37
(B)
DI- DI+
Fold change
1.5
1.0
0.5
0
**
*
ERα ERβ
(C)
DI (-)
DI (+)
(D)
DI - +
LC3-I ←16
LC3-II ←14
β-actin ←42
(E)
LC3-II (Fold)
1.5
1.0
0.5
0
***
DI - +
(F)
BL - - + +
DI - + - +
LC3-I ←16
LC3-II ←14
p62 ←62
β-actin ←42
(G)
by LC3-II by p62
Autophagy flux (fold)
3
2
1
0
***
**
DI - +

Figure 5

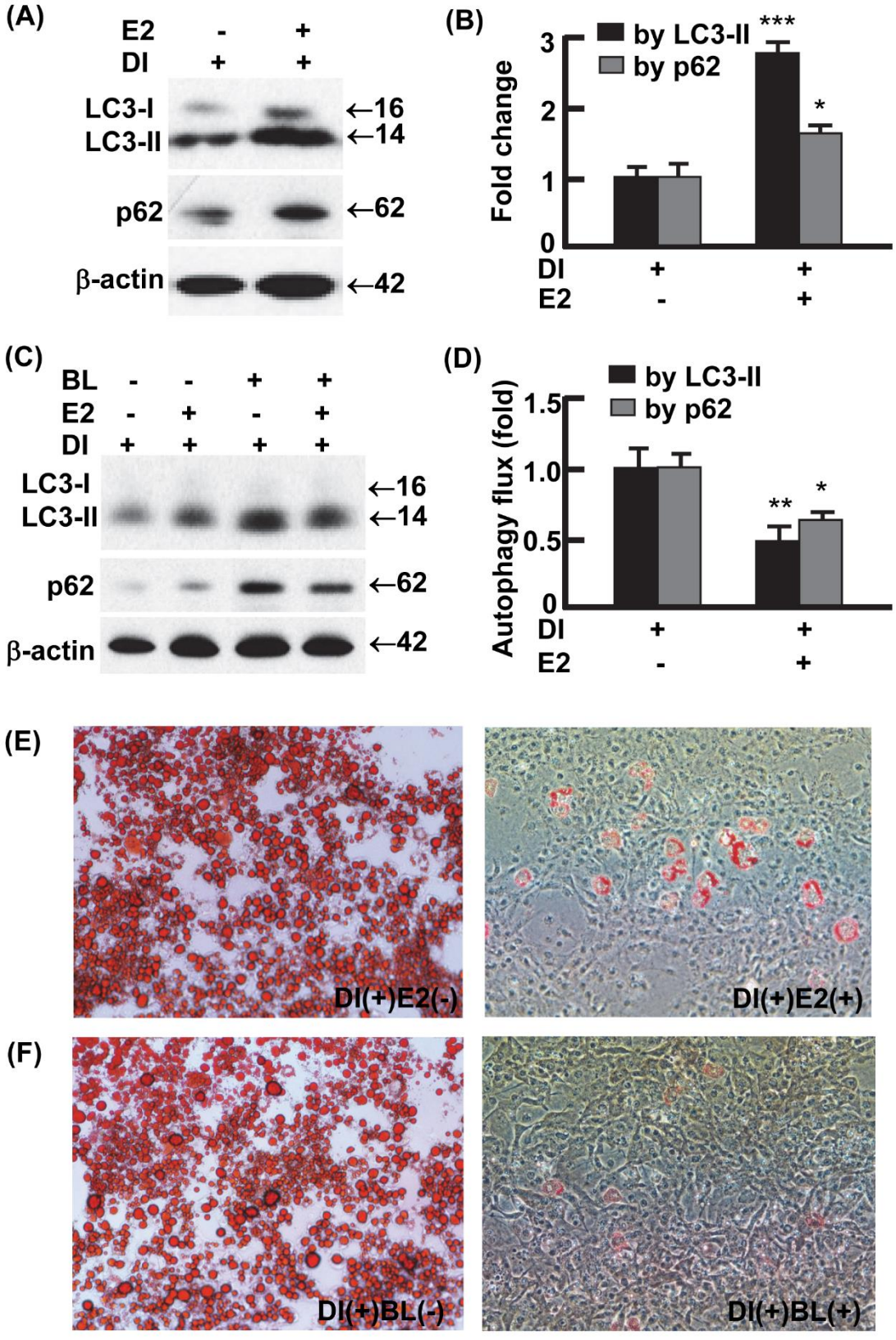
(A)
E2 - +
DI + +
LC3-I
LC3-II
←16
←14
p62
←62
β-actin
←42
(B)
by LC3-II
by p62
Fold change
***
*
DI + +
E2 - +
(C)
BL - - + +
E2 - + - +
DI + + + +
LC3-I
LC3-II
←16
←14
p62
←62
β-actin
←42
(D)
by LC3-II
by p62
Autophagy flux (fold)
**
*
DI + +
E2 - +
(E)
DI(+)E2(-)
DI(+)E2(+)
(F)
DI(+)BL(-)
DI(+)BL(+)

Figure 6

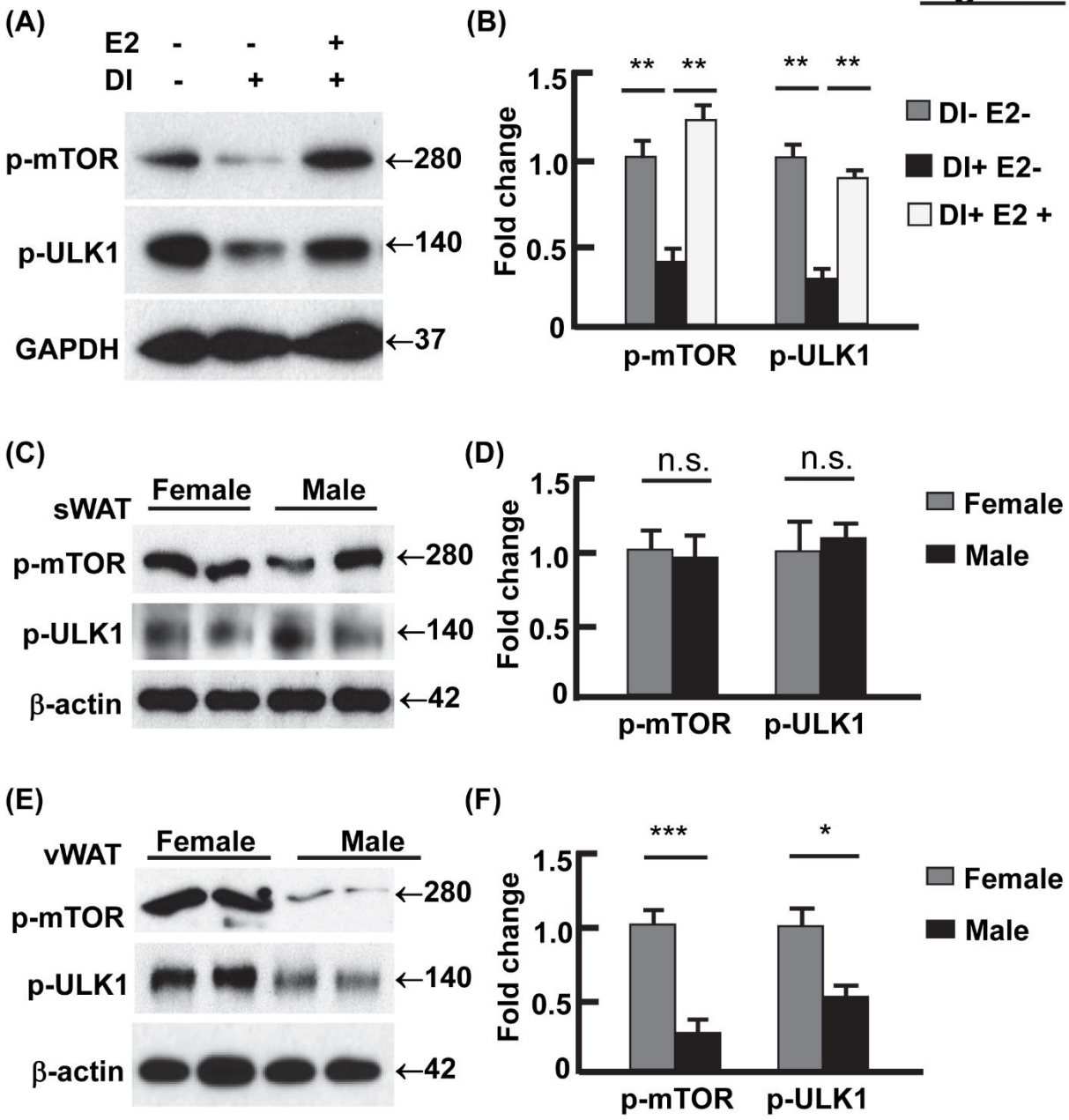
(A)
E2 - - +
DI - + +
p-mTOR
p-ULK1
GAPDH
←280
←140
←37
(B)
Fold change
1.5
1.0
0.5
0
** ** ** **
p-mTOR
p-ULK1
DI- E2-
DI+ E2-
DI+ E2 +
(C)
sWAT
Female
Male
p-mTOR
p-ULK1
β-actin
←280
←140
←42
(D)
n.s. n.s.
Fold change
p-mTOR
p-ULK1
Female
Male
(E)
vWAT
Female
Male
p-mTOR
p-ULK1
β-actin
←280
←140
←42
(F)
*** *
Fold change
p-mTOR
p-ULK1
Female
Male

Figure 7

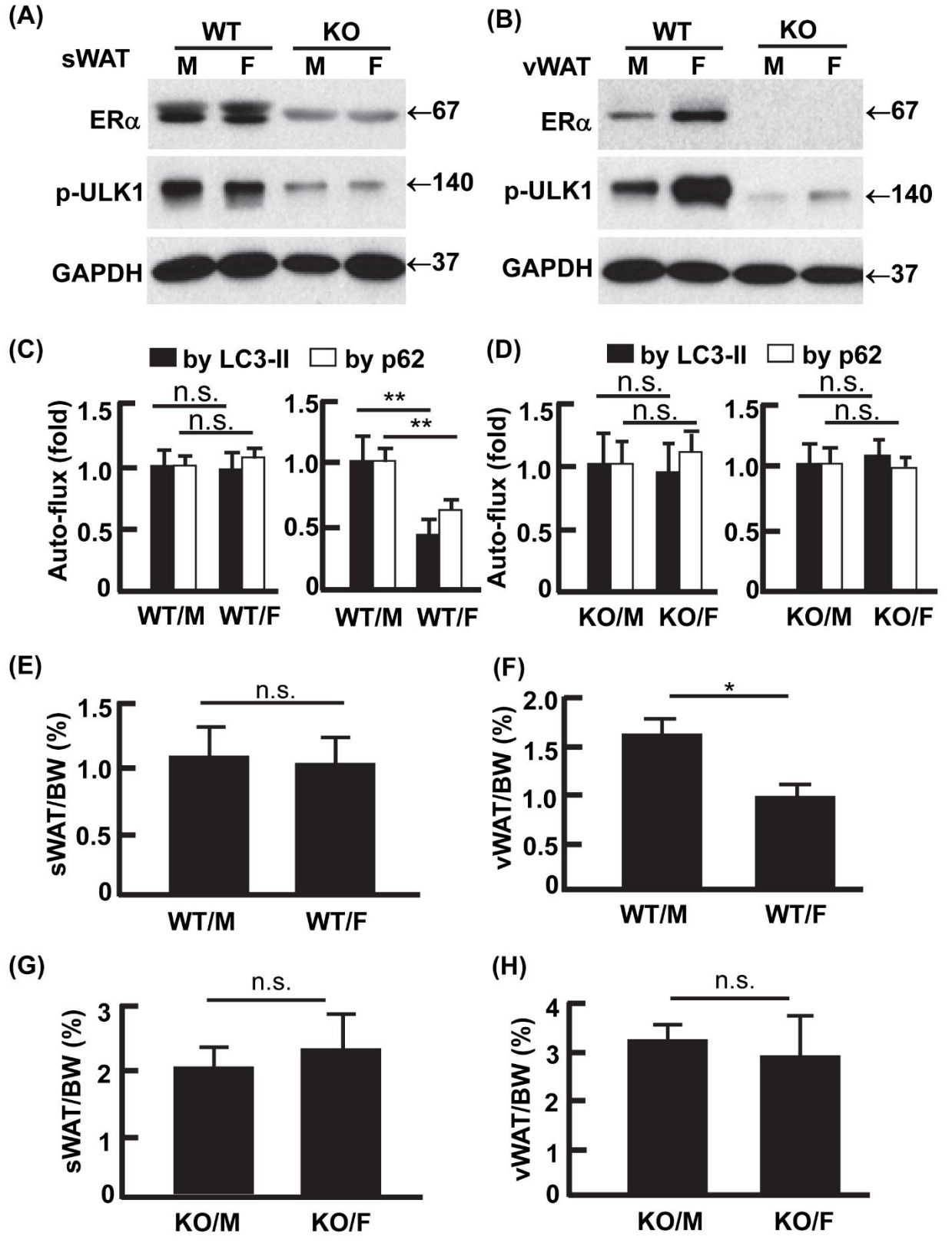
(A)
sWAT
WT
KO
M
F
M
F
ERα
←67
p-ULK1
←140
GAPDH
←37
(B)
vWAT
WT
KO
M
F
M
F
ERα
←67
p-ULK1
←140
GAPDH
←37
(C)
by LC3-II
by p62
Auto-flux (fold)
n.s.
n.s.
**
**
WT/M
WT/F
WT/M
WT/F
(D)
by LC3-II
by p62
Auto-flux (fold)
n.s.
n.s.
n.s.
n.s.
KO/M
KO/F
KO/M
KO/F
(E)
sWAT/BW (%)
n.s.
WT/M
WT/F
(F)
vWAT/BW (%)
*
WT/M
WT/F
(G)
sWAT/BW (%)
n.s.
KO/M
KO/F
(H)
vWAT/BW (%)
n.s.
KO/M
KO/F

Figure 1s. Estradiol dampened autophagy and differentiation of primary stromal vascular cells. (A-B) The presence of E2 (0.1 μM, days 0-10) suppressed autophagy activity during differentiation of primary stromal vascular cells. The autophagy flux was analyzed by Western blotting (A) and densitometry (B) after the cells were incubated with and without autophagy inhibitor BL (bafilomycin A1 at 0.1 μM and leupeptin at 10 μg/ml) for 4 hours on day 10. DI+ represents stromal vascular cells with differentiation induction and harvested on day 10; DI- represents stromal vascular cells without differentiation induction and harvested on day 10. For autophagy flux analysis, we first normalized the band densities of p62 against that of β-actin, then calculated the differences of normalized densities in the presence vs. the absence of autophagy inhibitor; lastly, the differences were shown as fold changes by taking the DI-E2- group as "1". (C) Estradiol (0.1 μM, days 0-10) suppressed the differentiation of primary stromal vascular cells, which was phenocopied by the treatment with autophagy inhibitor bafilomycin A1 (4 nM) and leupeptin (0.4 ng) during day 0 through day 10. Oil red O staining was conducted on day 10. *, $p<0.05$; **, $p<0.01$; n=3-4.

Figure 2s. Effects of the estradiol-ER signaling on autophagy proteins. (A-B) E2 (0.1 μM, days 0-12) had marginal effects on beclin 1, Atg5, Atg7, and Atg12-Atg5 conjugate, analyzed by Western blotting (A) and densitometry (B). DI+ represents 3T3L1 cells with differentiation induction and harvested on day 12; DI- represents 3T3L1 cells without differentiation induction and harvested on day 12. (C-D) The females and males showed similar patterns of beclin 1, Atg5, Atg7, and Atg12-Atg5 conjugate, analyzed by Western blotting (C) and densitometry (D). In densitometric analysis, the band densities of investigated proteins were normalized against that of GAPDH, and the fold changes were calculated by taking the normalized density of DI-

E2- group (panels A and B) or the female group (panels C and D) as "1". **, $p<0.01$; n.s., not significant; n=3-4.

Figure 3s. Effects of PPT and DPN on autophagy and adipogenesis. PPT (0.1 μM) or DPN (0.1 μM) was used at the established concentrations[76, 77] during 3T3L1 preadipocyte differentiation (days 0-12). DI+ represents 3T3L1 cells with differentiation induction and harvested on day 12. Autophagy flux (i.e., the turnover of LC3-II or p62) was analyzed by Western blotting (A) and densitometry (B) after the cells were incubated with and without autophagy inhibitor BL (bafilomycin A1 at 0.1 μM and leupeptin at 10 μg/ml) for 4 hours. For autophagy flux analysis, we first normalized the band densities of LC3-II and p62 against that of GAPDH, then calculated the differences of normalized densities in the presence vs. the absence of autophagy inhibitor; lastly, the differences in autophagy flux were shown as fold changes by taking the DI+ group as "1". n= 4; *, $p<0.05$; **, $p<0.01$. (C) The presence of PPT but not DPN (days 0-12) suppressed the differentiation of 3T3L1 preadipocytes, validated by oil red O staining on day 12.

Figure 4s. Measurements of autophagy flux by LC3-II turnover in wild type (WT) and ERα knockout (KO) mice. (A) Representative images of Western blotting assay for autophagy flux in sWAT from WT mice. (B) Representative images of Western blotting assay for autophagy flux in vWAT from WT mice. (C) Representative images of Western blotting assay for autophagy flux in sWAT from KO mice. (B) Representative images of Western blotting assay for autophagy flux in vWAT from KO mice. The results of densitometric analysis were shown in Figure 7. BL, bafilomycin A1 and leupeptin; M, male; F, female.

Figure 5s. Measurements of autophagy flux by p62 turnover in wild type (WT) and ERα knockout (KO) mice. (A) Representative images of Western blotting assay for autophagy flux in sWAT from WT mice. (B) Representative images of Western blotting assay for autophagy flux

in vWAT from WT mice. (C) Representative images of Western blotting assay for autophagy flux in sWAT from KO mice. (B) Representative images of Western blotting assay for autophagy flux in vWAT from KO mice. The results of densitometric analysis were shown in Figure 7. BL, bafilomycin A1 and leupeptin; M, male; F, female.

Figure 1s

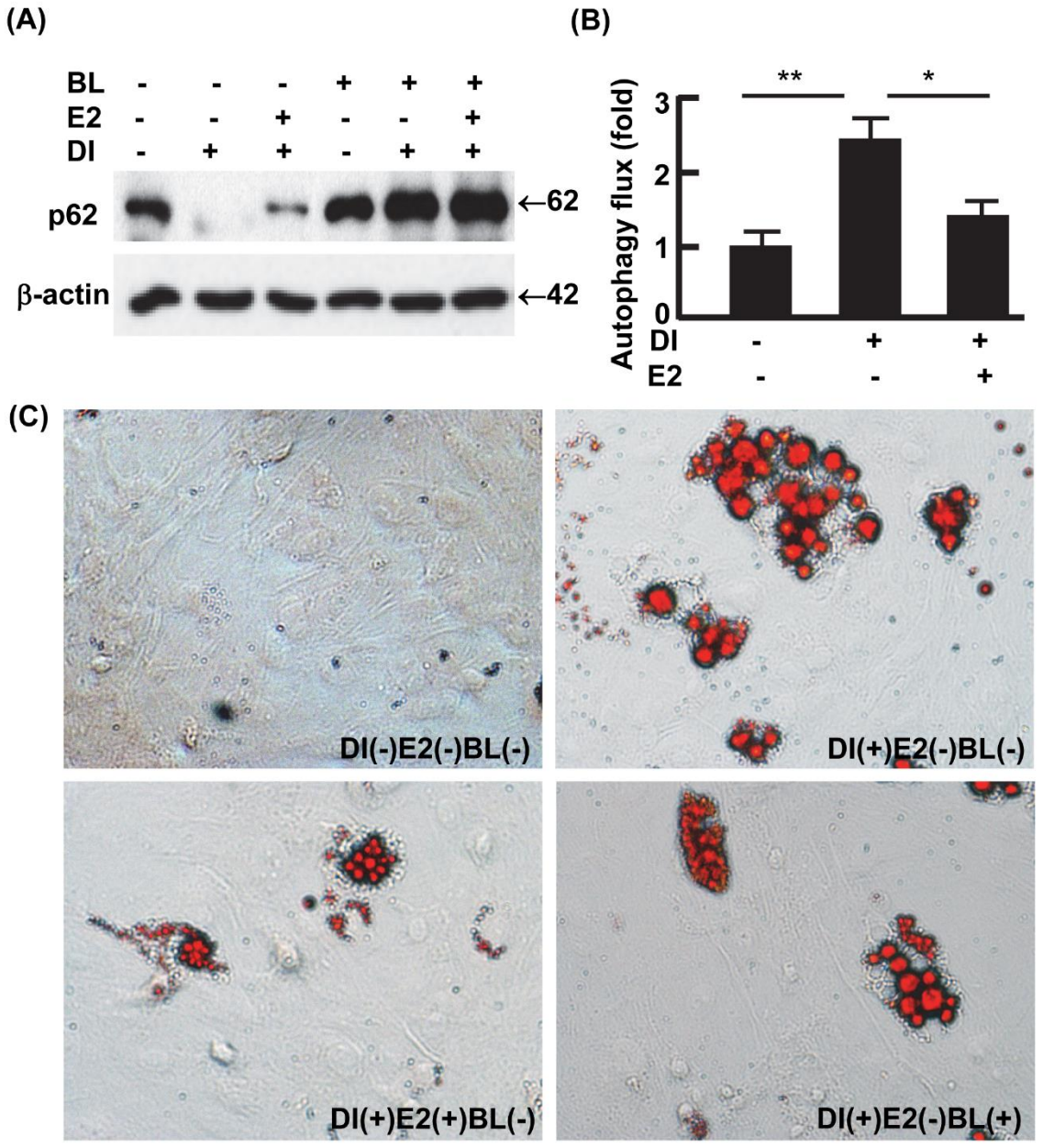

Figure 2s

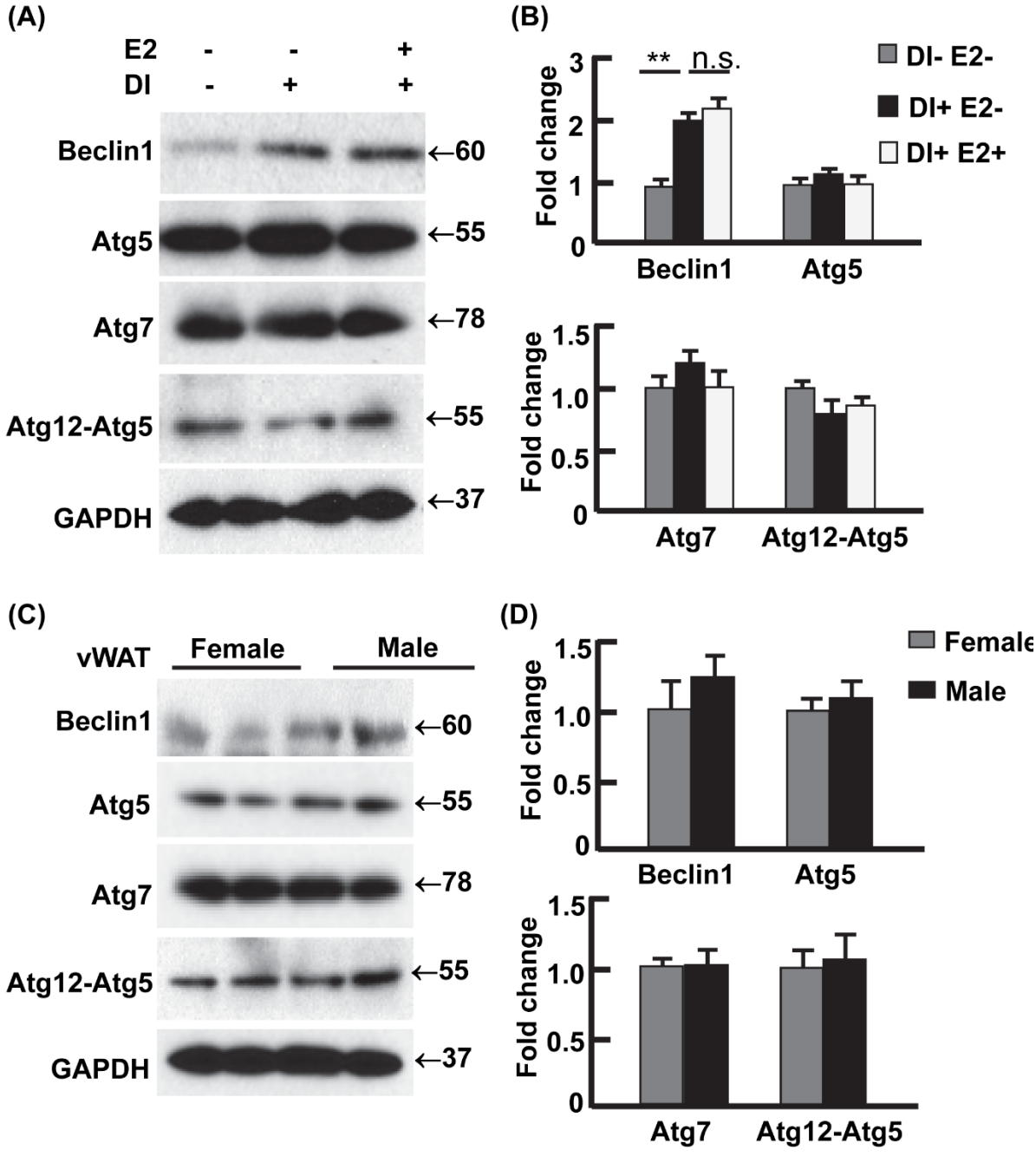
(A)
E2 - - +
DI - + +
Beclin1
←60
Atg5
←55
Atg7
←78
Atg12-Atg5
←55
GAPDH
←37
(B)
** n.s.
DI- E2-
DI+ E2-
DI+ E2+
Fold change
3
2
1
0
Beclin1
Atg5
Fold change
1.5
1.0
0.5
0
Atg7
Atg12-Atg5
(C)
vWAT
Female
Male
Beclin1
←60
Atg5
←55
Atg7
←78
Atg12-Atg5
←55
GAPDH
←37
(D)
Female
Male
Fold change
1.5
1.0
0.5
0
Beclin1
Atg5
Fold change
1.5
1.0
0.5
0
Atg7
Atg12-Atg5

Figure 3s

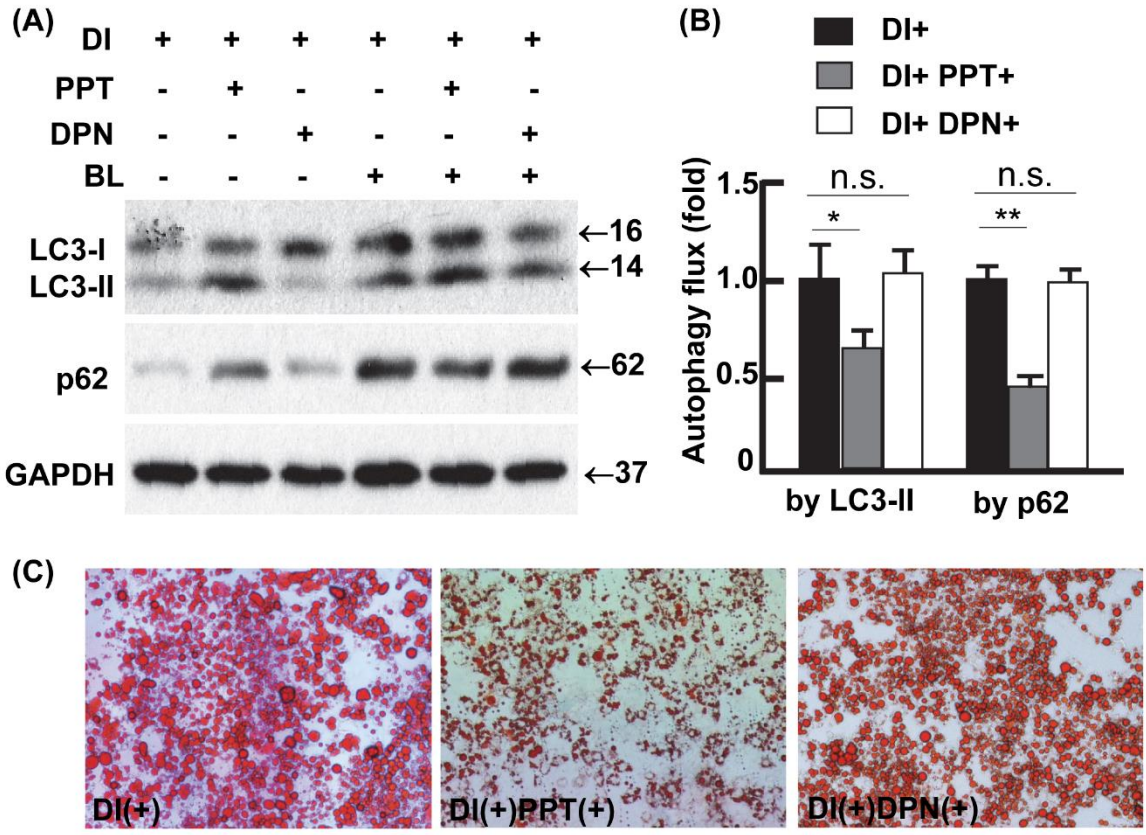
(A)
DI + + + + + +
PPT - + - - + -
DPN - - + - - +
BL - - - + + +
LC3-I
LC3-II
←16
←14
p62
←62
GAPDH
←37
(B)
DI+
DI+ PPT+
DI+ DPN+
Autophagy flux (fold)
1.5
1.0
0.5
0
n.s.
*
n.s.
**
by LC3-II
by p62
(C)
DI(+)
DI(+)PPT(+)
DI(+)DPN(+)

Figure 4s

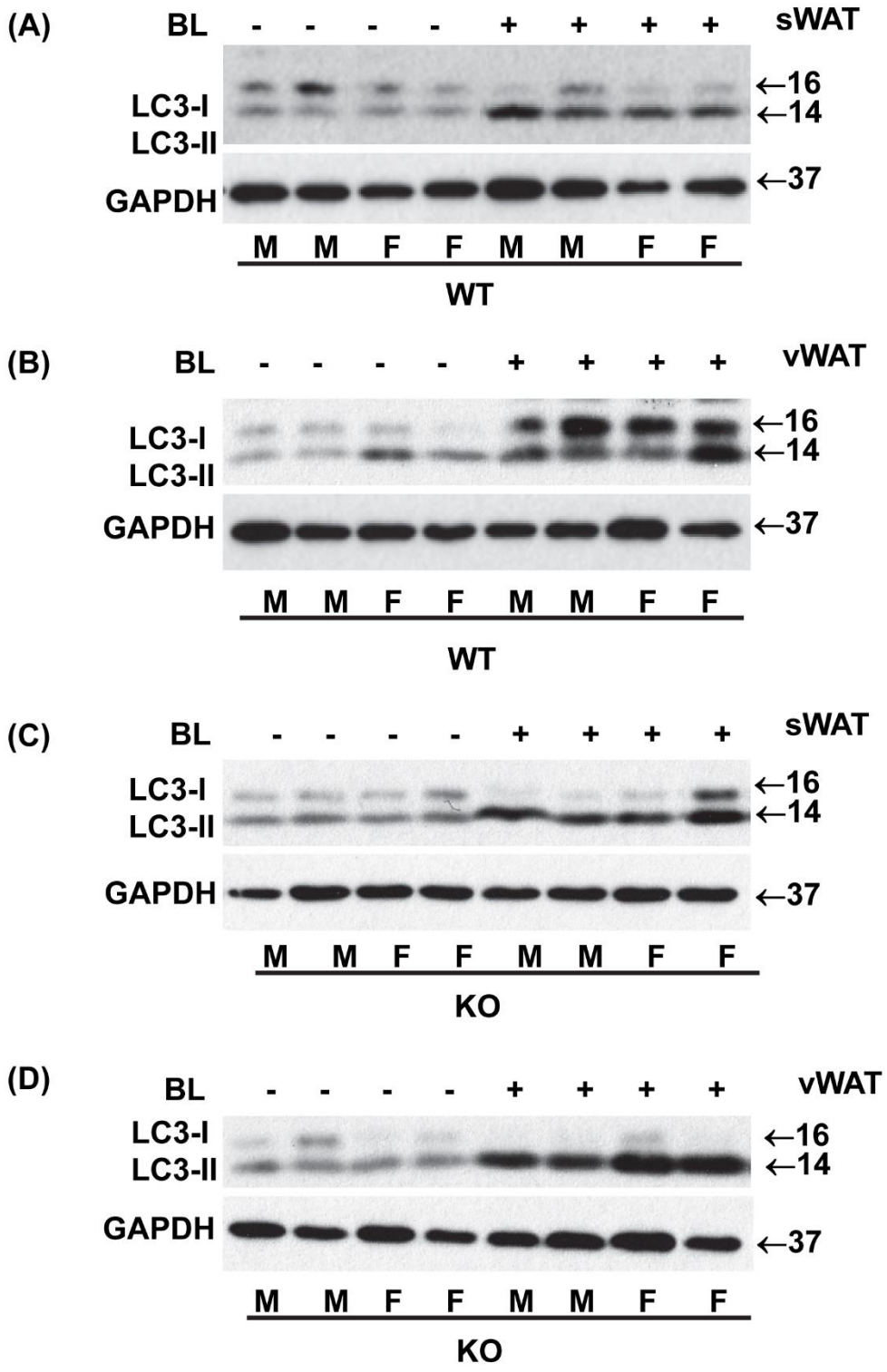
(A)
BL - - - - + + + +
sWAT
LC3-I
LC3-II
←16
←14
GAPDH
←37
M M F F M M F F
WT
(B)
BL - - - - + + + +
vWAT
LC3-I
LC3-II
←16
←14
GAPDH
←37
M M F F M M F F
WT
(C)
BL - - - - + + + +
sWAT
LC3-I
LC3-II
←16
←14
GAPDH
←37
M M F F M M F F
KO
(D)
BL - - - - + + + +
vWAT
LC3-I
LC3-II
←16
←14
GAPDH
←37
M M F F M M F F
KO

Figure 5s

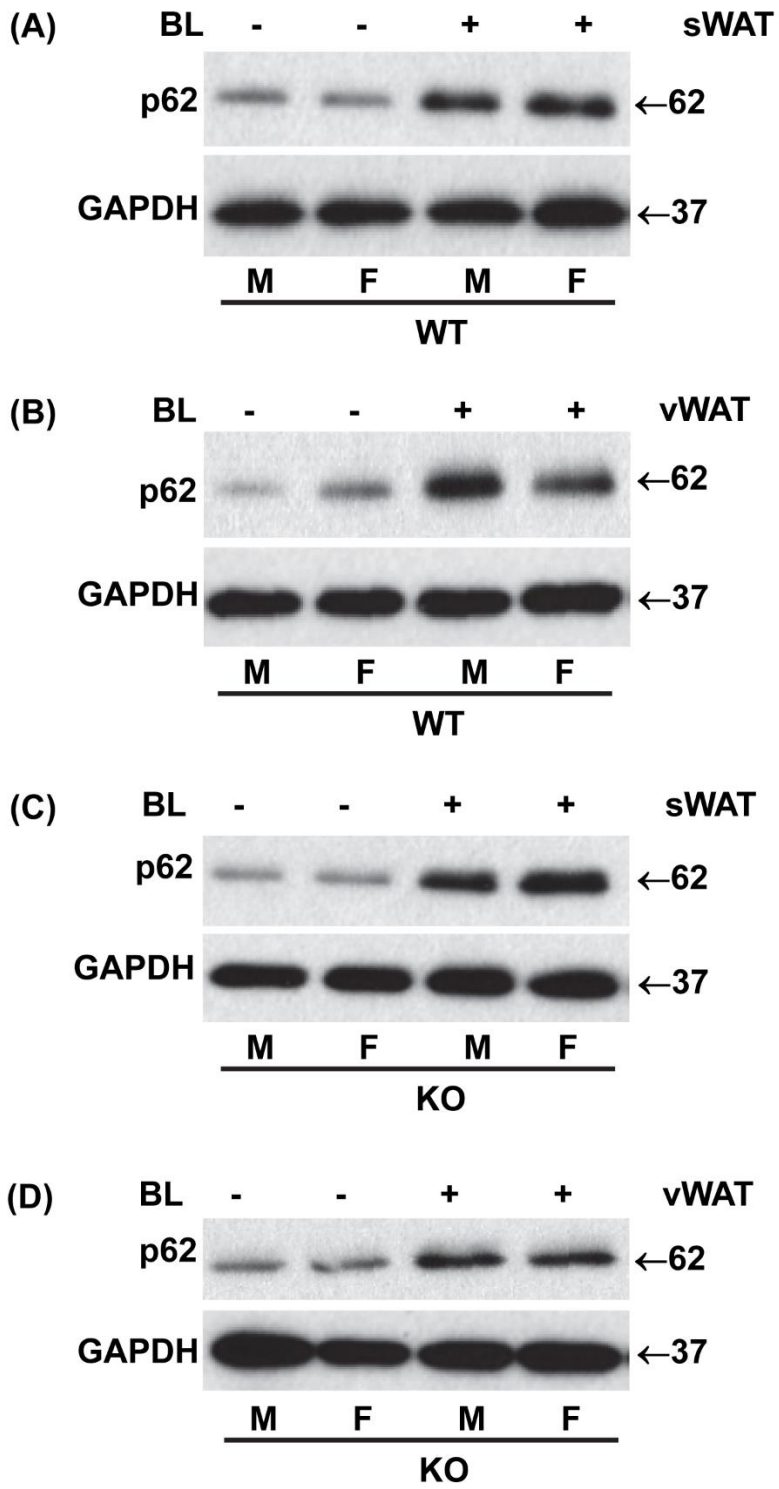
(A)
BL - - + + sWAT
p62
←62
GAPDH
←37
M F M F
WT
(B)
BL - - + + vWAT
p62
←62
GAPDH
←37
M F M F
WT
(C)
BL - - + + sWAT
p62
←62
GAPDH
←37
M F M F
KO
(D)
BL - - + + vWAT
p62
←62
GAPDH
←37
M F M F
KO

Chapter 5 Sirt1 suppressed adipocyte autophagy as downstream of ERα

ABSTRACT

Obesity is a growing epidemic, which is characterized by aberrant white adipose tissue (WAT) expansion. Sirt1 and autophagy are both closely related with adipogenesis and adipose remodeling. But how Sirt1 interacts with autophagy to modulate adipogenesis and adiposity is unknown. Here we showed that activation and overexpression of Sirt1 suppressed autophagy, while knockdown of Sirt1 induced autophagy. Mechanistically, Sirt1 induced phosphorylation of mTOR, and promoted the phosphorylation of a downstream target protein ULK1, which acts as a negative regulator of autophagy both *in vitro* and in *vivo*. Furthermore, Sirt1 was found to mediate ERα signaling in the regulatory events of autophagy and adipogenesis. Specially, E2 induced Sirt1 expression during adipogenesis, while ERα knockout mice reduced Sirt1 expression in WAT. Knockdown of Sirt1 abolished the effects of E2 on mTOR-ULK1 signaling cascade, autophagy and adipogenesis. Together, Sirt1 suppressed autophagy and adipogenesis via mTOR-ULK1cascade, which plays an important role in ERα regulation of adipogenesis.

KEYWORDS

Sirt1, adipogenesis, adiposity, autophagy, estradiol, mTOR, ULK1

ABBREVIATIONS

Sirt1, sirtuin 1; PPARγ, peroxisome proliferator-activated receptor gamma; Atg5, autophagy related 5; Atg7, autophagy related 7; BL, bafilomycin-A1 and leupeptin; DI, differentiation induction; RSV, resveratrol; E2, estradiol; ERα, estrogen receptor α; ERβ, estrogen receptor β; FBS, fetal bovine serum; GAPDH, glyceraldehyde 3-phosphate dehydrogenase; LC3, microtubule-associated protein 1A/1B-light chain 3-phosphatidylethanolamine conjugate; mTOR, the mechanistic target of rapamycin; p62, sequestosome 1 (SQSTM1); ULK1, Unc-51

like autophagy activating kinase; WAT, white adipose tissue; GFP, green fluorescent protein; shRNA, small hairpin RNA.

INTRODUCTION

Sirt1 (a NAD-dependent deacetylase) is downregulated in both genetic obesity and high fat diet (HFD) induced obesity and it is negatively correlated with adiposity and insulin resistance[1, 2]. As an energy sensor, it is involved in white adipose tissue (WAT) development, maintenance and remodeling.[1, 3] In 3T3L1 cells, it has been documented that Sirt1 acts as a negative modulator of adipogenesis by inhibiting peroxisome proliferator-activated receptor gamma (PPARγ), thus sensing energy availability in WAT and suppressing corresponding fat accumulation.[1, 4] Importantly, specific Sirt1 activator protects rodents from diet-induced obesity and insulin resistance.[5] Furthermore, Sirt1 promotes browning of subcutaneous WAT following acute cold exposure, leading to higher energy expenditure over energy intake and improved insulin sensitivity.[3] However, specific knockdown of Sirt1 in WAT promotes PPARγ upregulation and adipogenesis.[6] Moreover, knockdown of Sirt1 in WAT results in elevated macrophage recruitment to adipose tissue and adipose tissue inflammation.[7] Therefore, Sirt1 plays a significant role in controlling adipogenesis and adiposity, yet the mechanism is incompletely understood.

Autophagy, a cellular self-digestive process, is involved in cell differentiation, survival, development and remodeling.[8] Emerging evidence shows that autophagy is required for adipogenesis and normal adipose development. In preadipocyte and adipose tissue, specific deletion of an essential protein (Atg5) for autophagy abolishes adipogenesis and results in less subcutaneous mature adipocytes.[9] Likewise, adipose specific deletion of autophagy gene Atg7 improves metabolism, leading to a leanness phenotype and protection from diet-induced

obesity.[10, 11] Our previous studies indicated that both transcriptional factor FoxO1 and estrogen signaling regulated autophagy and adipogenesis. Specifically, FoxO1 specific antagonist (AS1842856) dampened autophagy through directly suppressing transcription factor EB (Tfeb), a key regulator of autophagy, which thus suppressed adipogenesis and lipid droplets formation.[12, 13, 14] Also, we found that E2 signaling suppressed autophagy, which ameliorated adipogenesis and adiposity in mice.[15] And an estradiol (E2)-ERα-autophagy axis contributes to the gender difference in visceral fat distribution.[15] These findings suggest that autophagy undergoes complex regulation in the control of adipogenesis and adiposity.

Given the regulatory role of both Sirt1 and autophagy in adipogenesis and adiposity, we ask the question whether and how Sirt1 interacts with autophagy to suppress adipogenesis and adiposity. Here we showed that specific activating or overexpressing Sirt1 suppressed autophagy through mTOR-ULK1 signaling pathway, which inhibited adipogenesis and adiposity, while knockdown of Sirt1 had opposite effects. Also, our further study found that Sirt1 may act as a downstream of ERα in autophagy and adipogenesis regulation. Out data unraveled a new mechanism where Sirt1 may inhibit adipogenesis and adiposity via suppressing autophagy, and also revealed the interaction and regulatory order of Sirt1 and ERα in adipocyte autophagy regulation.

RESULTS

Sirt1 expression is negatively correlated with autophagy and adipogenesis

During adipogenesis, lipid accumulation was significantly increased (Figure 1A). Compared with preadipocyte, Sirt1 expression was dramatically reduced in mature adipocyte, and steady state levels of p62 and LC3-II were both reduced (Figure 1B, C). it is known that p62 and LC3-II are selectively degraded by lysosomal hydrolase in autolysosome.[16] Compared with preadipocyte, the removal of p62 and LC3-II in mature adipocyte increased, suggesting autophagy flux activity

was significantly increased.[17] All of these data indicated that Sirt1 expression is negatively correlated with adipogenesis and autophagy activity.

Resveratrol (RSV) suppressed autophagy and adipogenesis

In 3T3L1 cells, after treatment with 10 μM, 25 μM and 50 μM resveratrol (RSV), p62 expression was gradually increased, as well as LC3-II (Figure 2A). To test autophagy flux activity, the cells were treated with autophagy inhibitors bafilomycin A1 and leupeptin (BL) for 4 hours.[15, 17, 18, 19] In line with steady state of p62 and LC3-II, RSV suppressed autophagy flux activity in a dose-dependent manner (Figure 2A). Previous studies indicated that suppressing autophagy blocked adipogenesis process.[13, 14, 15] Then we would ask if RSV suppressed adipogenesis in a dose-dependent manner. As shown in Figure 2B, RSV suppressed lipid accumulation in a dose-dependent manner, and 50 μM RSV almost completely blocked lipid accumulation. These data suggested that RSV suppressed autophagy and adipogenesis in a dose-dependent manner. But RSV has several targets other than Sirt1,[20, 21] we would ask if direct modulation of Sirt1 would have effects on autophagy and adipogenesis.

The effects of Sirt1 overexpression and downregulation on autophagy and adipogenesis

As shown in Figure 3A, compared with control GFP, Sirt1 overexpression was significantly increased by adenoviral vectors Mouse Sirt1 (Sirt1-GFP) transfection. And Sirt1 overexpression induced p62 and LC3-II accumulation, suggesting the autophagic degradation of p62 and LC3-II was blocked. Consistently, Sirt1 overexpression significantly suppressed autophagy flux activity (Figure 3A). As shown in Figure 3B, compared with control shRNA, Sirt1 expression was significantly decreased by Mouse Sirt1 shRNA treatment. And Sirt1 knockdown reduced p62 accumulation. Also, Sirt1 knockdown significantly induced autophagy flux activity (Figure 3B). These data suggested that Sirt1 is a suppressor of autophagy.

Based on the notion that suppressing autophagy blocks adipogenesis,[13, 14, 15] we asked what's the effects of Sirt1 overexpression and knockdown on adipogenesis. As shown in Figure 3C, Sirt1 overexpression significantly suppressed lipid accumulation. In contrast, Sirt1 knockdown promoted lipid accumulation (Figure 3C). Our data suggests that Sirt1 is a suppressor of adipogenesis and lipid accumulation.

Sirt1 suppressed autophagy via mTOR-ULK1 signaling pathway

Autophagy is a multi-step process and every step is regulated by complex signaling pathway.[8] Our study indicated that Sirt1 suppressed autophagy, but it is unknown in which step and through which signaling pathway Sirt1 suppressed autophagy. In our study, we found out that Sirt1 suppressed autophagy via mTOR-ULK1 signaling. Compared with preadipocytes, mature adipocytes showed decrease in both pmTOR and pULK1-757 (Figure 4A). Phosphorylation of ULK1 at serine757 by mTOR is a negative regulator of autophagy,[22] reduction of which further confirmed autophagy activation after differentiation. To test if Sirt1 per se regulate mTOR-ULK1 signaling, we overexpressed or knock down Sirt1 and examined pmTOR and pULK1-757 levels. Sirt1 overexpression significantly induced pmTOR and pULK1-757 levels (Figure 4A). In contrast, Sirt1 knockdown significantly suppressed pmTOR and pULK1-757 levels (Figure 4B). To confirm the effects of Sirt1 on autophagy *in vivo*, we examined the adipose tissue in Sirt1 transgenic mice (S1tg)[23]. Compared with wild type (WT) mice, S1tg mice have significantly higher Sirt1 expression in WAT (Figure 4C). Also, the expressions of pmTOR and pULK1-757 are both higher in S1tg mice than WT mice, suggesting Sirt1 is an inducer of mTOR-ULK1 signaling and a suppressor of autophagy. Downstream of mTOR, phosphorylation of p70S6 and 4EBP1 were both increased in S1tg mice, further confirming that Sirt1 induced phosphorylation of mTOR.[24, 25]

ERα signaling positively regulated Sirt1

Our previous study indicated that ERα signaling activated mTOR, which then phosphorylated and inhibited ULK1, thereby suppressing autophagy and adipogenesis.[15] Both of ERα and Sirt1 promoted mTOR-ULK1 signaling cascade, promoting us to speculate that ERα may act as upstream or downstream of Sirt1. In breast cancer MCF-7 cells Sirt1 was shown to be upstream of ERα and its deacetylase activity is responsible for promoting ERα expression.[26] However, in breast cancer ZR75.1 cells ERα was shown to be upstream of Sirt1 and it bound to with Sirt1 promoter to induce Sirt1 gene expression.[27] As indicated in Figure 1B and our previous study, both ERα and Sirt1 expression significantly reduced during adipogenesis.[15] After activation of ERα signaling by E2, Sirt1 expression was significantly increased (Figure 5A). E2 signaling recruited both ERα and ERβ to function.[28] To determine if the effect of E2 on Sirt1 expression may be due to ER pathway, we then looked at Sirt1 expression in WAT from ERα knockout mice. Compared with WT, ERα knockout mice showed no detectable ERα (Figure 5B). And ERα knockout significantly reduced Sirt1 expression, suggesting ERα may act as an upstream of Sirt1 (Figure 5B).

ERα is an upstream of Sirt1 in autophagy and adipogenesis regulations

To further confirm if ERα is upstream of Sirt1, we used E2 and Sirt1 shRNA to co-treat 3T3L1 cells during differentiation. Compared with control, E2 significantly induced LC3-II accumulation, which is consistent with our previous study that E2 suppressed autophagy during adipogenesis.[15] And Sirt1 knockdown significantly decreased LC3-II accumulation, which is consistent with the notion that Sirt1 is a suppressor of autophagy. However, after silencing Sirt1, the effect of E2 on autophagy was ameliorated (Figure 6A). Similarly, E2 significantly induced phosphorylation of mTOR and phosphorylation on ULK1-757 (Figure 6B). However, after

knockdown of Sirt1, E2 did not show significant effect on pmTOR and pULK1-757 (Figure 6B), suggesting that Sirt1 is located at downstream of ERα signaling in autophagy regulation. In adipogenesis, E2 significantly suppressed lipid accumulation (Figure 6C). However, after knockdown of Sirt1, the effect of E2 on lipid accumulation was significantly abolished (Figure 6C), further confirming that Sirt1 acts as a downstream of ERα signaling. The results in Figure 5 and Figure 6 unravel ERα as an upstream regulator of Sirt1 in autophagy and adipogenesis.

DISCUSSION

Sirt1 expression is reduced in both genetic and HFD induced obesity, which is accompanied by insulin resistance.[1, 2] Specific activation of Sirt1 prevents mice from diet-induced obesity and subsequent insulin resistance.[5] Mechanistically, Sirt1 blocked adipogenesis by inhibiting PPARγ, thus sensing energy availability in WAT and suppressing fat accumulation,[1] and specific knockdown of Sirt1 in WAT promotes PPARγ and adipogenesis.[6] However, the role of Sirt1 in adipose homeostasis is complex in nature. For instance, specific knockdown of Sirt1 in WAT promoted macrophage recruitment to adipose tissue and subsequent adipose tissue inflammation.[7] All of these underlines an important role of Sirt1 in adipogenesis and adiposity regulation. To understand the molecular mechanism of how Sirt1 regulates adipogenesis, we investigated the interaction between Sirt1 and autophagy, and its relation with adipogenesis and adiposity. We found that Sirt1 expression is negatively related with autophagy flux activity and lipid accumulation during adipogenesis (Figure 1). Specific activation and overexpression of Sirt1 suppressed autophagy and adipogenesis, while knockdown Sirt1 promoted autophagy and adipogenesis (Figure 2-3), indicating Sirt1 is a suppressor of autophagy and adipogenesis. Previous studies proposed Sirt1 as a promotor of autophagy since overexpression of Sirt1 promoted the conversion of LC3-I to LC3-II in colon cancer HCT116 cells.[29] However, steady

state marker of autophagy is insufficient to reflect autophagy flux activity.[30, 31] The increase of LC-3II may due to induced conversion of LC3-I to LC3-II and suppressed degradation of LC3-II by lysosomal hydrolase in autolysosome.[31, 32]

Autophagy machinery contained multiple steps and each step is regulated by complex signaling.[8] We elucidated that Sirt1 suppressed autophagy via mTOR-ULK1 signaling cascade. Specifically, activation or overexpression of Sirt1 induced phosphorylation of mTOR and phosphorylation of ULK1 at serine757, which is a negative regulator of autophagy (Figure 4).[22] This phenotype was recapitulated in Sirt1 transgenic mice, indicating that Sirt1 suppressed autophagy via mTOR-ULK1 cascade both *in vitro* and *in vivo*. The role of Sirt1 in adipogenesis and adiposity has been extensively explored.[1, 3, 5, 6, 7, 23] The present study for the first time elucidate the mechanism that Sirt1 interacts with autophagy to regulate adipogenesis and adiposity via mTOR-ULK1 cascade. However, how Sirt1 induced the phosphorylation and activation of mTOR is unknown. Sirt1 deacetylates FoxO1 and FoxO3 to deactivate its transcriptional activity.[33, 34] And FoxO1 and FoxO3 regulates Sestrins gene expressions,[35] which are negative regulator of mTOR.[36, 37] On the other hand, during tumorigenesis and axonogenesis Sirt1 deacetylates Akt to induce its activity,[38, 39] which activates of mTOR signaling and suppresses autophagy.[40]

Our previous study also found that ERα signaling activated mTOR, which phosphorylated and inhibited ULK1, thereby suppressing autophagy and adipogenesis.[15] The same targets of ERα and Sirt1 on autophagy regulation potentiates their interaction during this process. Our further study indicated ERα expression is positively correlated with Sirt1 *in vitro* and *in vivo* (Figure 5). And Sirt1 knockdown abolished the effects of E2 on autophagy and adipogenesis regulations, indicating Sirt1 is a downstream of E2 signaling. But how ERα regulated Sirt1 transcriptionally

or post-transcriptionally is of interest in our future study. In breast cancer cells, ERα bind with Sirt1 promoter to induce its gene expression.[27]

Our findings may shed light on estrogen deficiency induced adiposity and related diseases.[41, 42, 43, 44] For example, the unraveled interaction between ERα and Sirt1 might lead to new therapeutic approach to adiposity and metabolic dysfunction in post-menopausal women or individuals with abnormal estrogen secretion. For example, dietary intervention or exercise challenge to activate Sirt1 may partially compensate estrogen deficiency.

To sum up, our study elucidated for the first time the mechanism of Sirt1 on adipocyte autophagy regulation via mTOR-ULK1 cascade. Sirt1 acted as downstream of ERα to suppress autophagy and adipogenesis. Sirt1 knockdown abolished the effects of ERα on autophagy and adipogenesis regulation. This study pointed out the importance to consider interaction of hormone signaling (e.g., ERα) and energy signaling (e.g., Sirt1) in future metabolic disease study, and provide alternatively therapeutic approaches for individuals with estrogen deficiency by activating Sirt1.

MATERIALS AND METHODS

Mice. The wild type (WT) and Sirt1 transgenic mice were bred and housed according to breeding instruction as described previously.[15, 23] In details, WT and Sirt1 transgenic mice were housed in plastic cages on a 12-hour light–dark photocycle and with free access to both water and regular chow diet as described previously.[15, 45] At the age of 8–10 week old, the mice were weighed with scale, and fat mass and fat percentage were measured with a Bruker Minispec LF90 NMR Analyzer (Bruker Optics, Billerica, MA, USA). And mice were sacrificed for tissue collection. The WAT pads were collected and weighed quickly, explant culture for autophagy flux analysis, or snap freezing in liquid nitrogen. Animal use procedures followed the National

Institutes of Health guidelines and were approved by the Virginia Tech Institutional Animal Care and Use Committee.

3T3L1 cell culture, differentiation, and treatment. 3T3L1 preadipocytes (ATCC CL-173, Manassas, VA, USA) were cultured in basal media (DMEM media containing 10% FBS, 100 units/ml penicillin and 100 μg/ml streptomycin (1 × P/S)), at 37 °C in a humidified atmosphere of 5% CO2.[12, 17] The media were replaced every 2 days until the cells became confluent (day 0), and after 2 more days (day 2) the medium was changed to differentiation medium I (DMEM with 10% FBS, P/S (1 ×), IBMX (0.5 mM), dexamethasone (1 μM), insulin (1 μg/ml), and rosiglitazone (2 μM)). At the end of day 4, the medium was switched to differentiation medium II (DMEM with 10% FBS, P/S (1 ×), and insulin (1 μg/ml)). At the end of day 6, the medium was changed to basal media and the cells were maintained until day 12. Preadipocytes without differentiation induction were maintained in basal media and supplied with fresh medium every 2 days till day 12. Resveratrol (RSV) at the concentrations of 10 μM, 25 μM and 50 μM were used to treat cells from day 0 to day 12. Sirt1 activator II (374922-43-7) (SA) purchased from EMD Millipore (Billerica, MA, USA) at concentration of 10 μM was used to treat cells from day 0 to day 12. β-Estradiol (E2) of 0.1 μM was used to treat the cells during differentiation. Other chemicals were used at the concentrations established previously, including bafilomycin A1 (4 nM), and leupeptin (0.4 ng/ml),[13] to treat the cells during differentiation.

Cell transfection. After cells reached 80-90% confluent, specific overexpression and knockdown of Sirt1 were achieved by incubating the cells with adenoviral vectors Mouse Sirt1 (Sirt1-GFP), Mouse Sirt1 shRNA (Indiana University School of Medicine) (Sirt1-shRNA) at concentration of 5×10^6 pfu/ml until day 2. Then, cell differentiation was induced and cells were grown to day 9 and harvested. Corresponding control GFP and shRNA (Indiana University

School of Medicine) were used as controls. After harvesting the cells, efficiency of Sirt1 overexpression and knockdown was examined by western blotting.

Oil red O staining. The Oil Red O working solution was freshly prepared by mixing 0.35% stock solution with dH_2O (6:4) and filtered, and the staining was conducted as described.[46, 47, 48] After the media were removed, the cells were washed once with cold phosphate buffered saline, and fixed in 4% formaldehyde at room temperature for 10 minutes. The cells were then washed with dH_2O and air dried. Oil Red O working solution was added to start the staining at room temperature for 30 min. The stained cells were washed with dH_2O for 4 times before the images were captured with a Nikon ECLIPSE Ti Inverted Microscope (Melville, NY, USA).

Autophagy flux assay. To measure autophagy flux in cultured cells, we treated 3T3L1 preadipocytes and mature adipocytes with bafilomycin A1 (inhibitor of autophagosome acidification, at 0.1 μM) plus leupeptin (the inhibitor of lysosomal proteases, at 10 μg/ml) for 4 hours. The cells were then harvested to prepare cell lysates as previously described.[46, 47, 48] To measure autophagy flux in WAT explants, freshly collected adipose tissues were minced into small tissue fragments (2–3 mm^3) and cultured for 4 hours with DMEM medium supplemented with 2 mM glutamine, 1% (vol/vol) antibiotic solution, and 10% (vol/vol) FBS in a CO_2 incubator (37°C, 5% CO_2). The turnover of LC3-II or p62 protein, i.e., the substrates of autophagy for degradation, was measured by western blotting and image analysis to assess autophagy flux.[47, 49, 50]

Western blotting. Tissue and cell lysates were prepared with PLC lysis buffer (30 mM Hepes, pH 7.5, 150 mM NaCl, 10% glycerol, 1% Triton X-100, 1.5 mM $MgCl_2$, 1 mM EGTA, 10 mM NaPPi, 100 mM NaF, 1 mM Na_3VO_4) supplemented with protease inhibitor cocktail (Roche), and 1 mM PMSF.[51] Total protein concentrations of the cell and tissue lysates were determined by

using a DC protein assay kits (Bio-Rad). Antibody (catalog number) information: GAPDH (MA5-15738) and β-actin (MA5-15739) antibodies were purchased from Pierce (Rockford, IL, USA); p-mTOR (Ser2448) antibody (5536s) and p-ULK1(Ser757) antibody (14202s) from Cell Signaling Technology (Beverly, MA, USA); ERα (04-820) and Sirt1 (07-131) antibodies from EMD Millipore (Billerica, MA, USA); p62 (ab56416) from abcam (Cambridge, MA, USA) and LC3B antibody (L7543) from Sigma (Billerica, MA, USA).

Statistical analysis. Data are presented as mean ± SD. Differences between the groups were validated by one-way-ANOVA with the least significant difference post hoc test to detect statistical differences between groups and treatments (DI+ vs. DI-, RSV+ vs. RSV-, SA+ vs. SA-, Sirt1-GFP vs. control GFP, Sirt1-shRNA vs. control shRNA, and BL+ vs. BL-). Differences in autophagy and adipose parameters between WT and Sirt1 transgenic were validated by a t-test. A value of $p < 0.05$ was considered statistically significant.

Reference

1. Picard F, Kurtev M, Chung N, Topark-Ngarm A, Senawong T, De Oliveira RM, *et al.* Sirt1 promotes fat mobilization in white adipocytes by repressing PPAR-γ. *Nature* 2004, **429**(6993)**:** 771.

2. Chalkiadaki A, Guarente L. High-fat diet triggers inflammation-induced cleavage of SIRT1 in adipose tissue to promote metabolic dysfunction. *Cell Metabolism* 2012, **16**(2)**:** 180-188.

3. Qiang L, Wang L, Kon N, Zhao W, Lee S, Zhang Y, *et al.* Brown remodeling of white adipose tissue by SirT1-dependent deacetylation of Pparγ. *Cell* 2012, **150**(3)**:** 620-632.

4. dos Santos Costa C, Rohden F, Hammes TO, Margis R, Bortolotto JW, Padoin AV, *et al.* Resveratrol upregulated SIRT1, FOXO1, and adiponectin and downregulated PPARγ1–3 mRNA expression in human visceral adipocytes. *Obesity Surgery* 2011, **21**(3)**:** 356-361.

5. Feige JN, Lagouge M, Canto C, Strehle A, Houten SM, Milne JC, *et al.* Specific SIRT1 activation mimics low energy levels and protects against diet-induced metabolic disorders by enhancing fat oxidation. *Cell Metabolism* 2008, **8**(5)**:** 347-358.

6. Mayoral R, Osborn O, McNelis J, Johnson AM, Izquierdo CL, Chung H, *et al.* Adipocyte SIRT1 knockout promotes PPARγ activity, adipogenesis and insulin sensitivity in chronic-HFD and obesity. *Molecular Metabolism* 2015, **4**(5)**:** 378-391.

7. Gillum MP, Kotas ME, Erion DM, Kursawe R, Chatterjee P, Nead KT, *et al.* SirT1 regulates adipose tissue inflammation. *Diabetes* 2011, **60**(12)**:** 3235-3245.

8. Levine B, Kroemer G. Autophagy in the pathogenesis of disease. *Cell* 2008, **132**(1)**:** 27-42.

9. Baerga R, Zhang Y, Chen P-H, Goldman S, Jin SV. Targeted deletion of autophagy-related 5 (atg5) impairs adipogenesis in a cellular model and in mice. *Autophagy* 2009, **5**(8)**:** 1118-1130.

10. Singh R, Xiang Y, Wang Y, Baikati K, Cuervo AM, Luu YK, *et al.* Autophagy regulates adipose mass and differentiation in mice. *The Journal of Clinical Investigation* 2009, **119**(11)**:** 3329-3339.

11. Zhang Y, Goldman S, Baerga R, Zhao Y, Komatsu M, Jin S. Adipose-specific deletion of autophagy-related gene 7 (atg7) in mice reveals a role in adipogenesis. *Proceedings of the National Academy of Sciences* 2009, **106**(47)**:** 19860-19865.

12. Zou P, Liu L, Zheng L, Liu L, Stoneman RE, Cho A, *et al.* Targeting FoxO1 with AS1842856 suppresses adipogenesis. *Cell Cycle* 2014, **13**(23)**:** 3759-3767.

13. Liu L, Zheng LD, Zou P, Brooke J, Smith C, Long YC, *et al.* FoxO1 antagonist suppresses autophagy and lipid droplet growth in adipocytes. *Cell Cycle* 2016, **15**(15)**:** 2033-2041.

14. Liu L, Tao Z, Zheng LD, Brooke JP, Smith CM, Liu D, *et al.* FoxO1 interacts with transcription factor EB and differentially regulates mitochondrial uncoupling proteins via autophagy in adipocytes. *Cell Death Discovery* 2016, **2:** 16066.

15. Tao Z, Zheng LD, Smith C, Luo J, Robinson A, Almeida FA, *et al.* Estradiol signaling mediates gender difference in visceral adiposity via autophagy. *Cell Death & Disease* 2018, **9**(3)**:** 309.

16. Bjørkøy G, Lamark T, Brech A, Outzen H, Perander M, Øvervatn A, *et al.* p62/SQSTM1 forms protein aggregates degraded by autophagy and has a protective effect on huntingtin-induced cell death. *The Journal of Cell Biology* 2005, **171**(4)**:** 603-614.

17. Tao Z, Liu L, Zheng LD, Cheng Z. Autophagy in adipocyte differentiation. *Autophagy in Differentiation and Tissue Maintenance*. Springer, 2017, pp 45-53.

18. Mizushima N, Yoshimori T, Levine B. Methods in mammalian autophagy research. *Cell* 2010, **140**(3)**:** 313-326.

19. Klionsky DJ, Abdelmohsen K, Abe A, Abedin MJ, Abeliovich H, Acevedo Arozena A, *et al.* Guidelines for the use and interpretation of assays for monitoring autophagy. *Autophagy* 2016, **12**(1)**:** 1-222.

20. Tennen RI, Michishita-Kioi E, Chua KF. Finding a target for resveratrol. *Cell* 2012, **148**(3)**:** 387-389.

21. Chen D, Guarente L. SIR2: a potential target for calorie restriction mimetics. *Trends in molecular medicine* 2007, **13**(2)**:** 64-71.

22. Kim J, Kundu M, Viollet B, Guan K-L. AMPK and mTOR regulate autophagy through direct phosphorylation of Ulk1. *Nature Cell Biology* 2011, **13**(2)**:** 132.

23. Banks AS, Kon N, Knight C, Matsumoto M, Gutiérrez-Juárez R, Rossetti L, *et al.* SirT1 gain of function increases energy efficiency and prevents diabetes in mice. *Cell Metabolism* 2008, **8**(4)**:** 333-341.

24. Hay N, Sonenberg N. Upstream and downstream of mTOR. *Genes & Development* 2004, **18**(16)**:** 1926-1945.

25. Fingar DC, Salama S, Tsou C, Harlow E, Blenis J. Mammalian cell size is controlled by mTOR and its downstream targets S6K1 and 4EBP1/eIF4E. *Genes & Development* 2002, **16**(12)**:** 1472-1487.

26. Yao Y, Li H, Gu Y, Davidson NE, Zhou Q. Inhibition of SIRT1 deacetylase suppresses estrogen receptor signaling. *Carcinogenesis* 2009, **31**(3)**:** 382-387.

27. Elangovan S, Ramachandran S, Venkatesan N, Ananth S, Gnana-Prakasam JP, Martin PM, *et al.* SIRT1 is essential for oncogenic signaling by estrogen/estrogen receptor α in breast cancer. *Cancer Research* 2011, **71**(21)**:** 6654-6664.

28. Heldring N, Pawson T, McDonnell D, Treuter E, Gustafsson J-Å, Pike AC. Structural insights into corepressor recognition by antagonist-bound estrogen receptors. *Journal of Biological Chemistry* 2007, **282**(14)**:** 10449-10455.

29. Lee IH, Cao L, Mostoslavsky R, Lombard DB, Liu J, Bruns NE, *et al.* A role for the NAD-dependent deacetylase Sirt1 in the regulation of autophagy. *Proceedings of the National Academy of Sciences* 2008, **105**(9)**:** 3374-3379.

30. Zhang X-j, Chen S, Huang K-x, Le W-d. Why should autophagic flux be assessed? *Acta Pharmacologica Sinica* 2013, **34**(5)**:** 595.

31. Tao Z, Liu L, Zheng LD, Cheng Z. Autophagy in Adipocyte Differentiation. 2019,**1854**:45-53.

32. Zhang J. Teaching the basics of autophagy and mitophagy to redox biologists—mechanisms and experimental approaches. *Redox Biology* 2015, **4:** 242-259.

33. Lee D, Goldberg AL. SIRT1 protein, by blocking the activities of transcription factors FoxO1 and FoxO3, inhibits muscle atrophy and promotes muscle growth. *Journal of Biological Chemistry* 2013, **288**(42)**:** 30515-30526.

34. Motta MC, Divecha N, Lemieux M, Kamel C, Chen D, Gu W, *et al.* Mammalian SIRT1 represses forkhead transcription factors. *Cell* 2004, **116**(4)**:** 551-563.

35. Chen C-C, Jeon S-M, Bhaskar PT, Nogueira V, Sundararajan D, Tonic I, *et al.* FoxOs inhibit mTORC1 and activate Akt by inducing the expression of Sestrin3 and Rictor. *Developmental Cell* 2010, **18**(4)**:** 592-604.

36. Parmigiani A, Nourbakhsh A, Ding B, Wang W, Kim YC, Akopiants K, *et al.* Sestrins inhibit mTORC1 kinase activation through the GATOR complex. *Cell Reports* 2014, **9**(4)**:** 1281-1291.

37. Wolfson RL, Chantranupong L, Saxton RA, Shen K, Scaria SM, Cantor JR, *et al.* Sestrin2 is a leucine sensor for the mTORC1 pathway. *Science* 2016, **351**(6268)**:** 43-48.

38. Li X-h, Chen C, Tu Y, Sun H-t, Zhao M-l, Cheng S-x, *et al.* Sirt1 promotes axonogenesis by deacetylation of Akt and inactivation of GSK3. *Molecular Neurobiology* 2013, **48**(3)**:** 490-499.

39. Sundaresan NR, Pillai VB, Wolfgeher D, Samant S, Vasudevan P, Parekh V, *et al.* The deacetylase SIRT1 promotes membrane localization and activation of Akt and PDK1 during tumorigenesis and cardiac hypertrophy. *Sci Signal* 2011, **4**(182)**:** ra46-ra46.

40. Mammucari C, Schiaffino S, Sandri M. Downstream of Akt: FoxO3 and mTOR in the regulation of autophagy in skeletal muscle. *Autophagy* 2008, **4**(4)**:** 524-526.

41. Calle EE, Thun MJ. Obesity and cancer. *Oncogene* 2004, **23**(38)**:** 6365.

42. Kritz-Silverstein D, Barrett-Connor E. Long-term postmenopausal hormone use, obesity, and fat distribution in older women. *Jama* 1996, **275**(1)**:** 46-49.

43. Heine P, Taylor J, Iwamoto G, Lubahn D, Cooke P. Increased adipose tissue in male and female estrogen receptor-α knockout mice. *Proceedings of the National Academy of Sciences* 2000, **97**(23)**:** 12729-12734.

44. Haarbo J, Marslew U, Gotfredsen A, Christiansen C. Postmenopausal hormone replacement therapy prevents central distribution of body fat after menopause. *Metabolism* 1991, **40**(12)**:** 1323-1326.

45. Liu L, Zou P, Zheng L, Linarelli LE, Amarell S, Passaro A, *et al.* Tamoxifen reduces fat mass by boosting reactive oxygen species. *Cell Death & Disease* 2015, **6**(1)**:** e1586.

46. Liu L, Tao Z, Zheng LD, Brooke JP, Smith CM, Liu D, *et al.* FoxO1 interacts with transcription factor EB and differentially regulates mitochondrial uncoupling proteins via autophagy in adipocytes. *Cell Death Discovery* 2016, **2:** 16066.

47. Liu L, Zheng LD, Zou P, Brooke J, Smith C, Long YC, *et al.* FoxO1 antagonist suppresses autophagy and lipid droplet growth in adipocytes. *Cell Cycle* 2016, **15**(15)**:** 2033-2041.

48. Zou P, Liu L, Zheng L, Stoneman RE, Cho A, Emery A, *et al.* Targeting FoxO1 with AS1842856 suppresses adipogenesis. *Cell Cycle* 2014, **13**(23)**:** 3759-3767.

49. Mizushima N, Yoshimori T, Levine B. Methods in mammalian autophagy research. *Cell* 2010, **140**(3)**:** 313-326.

50. Yamada E, Singh R. Mapping autophagy on to your metabolic radar. *Diabetes* 2012, **61**(2)**:** 272-280.

51. Cheng Z, Guo S, Copps K, Dong X, Kollipara R, Rodgers JT, *et al.* Foxo1 integrates insulin signaling with mitochondrial function in the liver. *Nat Med* 2009, **15**(11)**:** 1307-1311.

Figure legends

Figure 1 Adipogenesis was associated with downregulation of Sirt1 expression and activation of autophagy flux

A. ORO staining of preadipocyte and mature adipocyte. DI, differentiation induction. DI+ represents differentiated 3T3L1 cells (mature adipocytes) harvested on day 12; DI- represents 3T3L1 cells without differentiation induction (i.e., preadipocytes) harvested on day 12.

B. During differentiation, Sirt1 expression reduced. Protein expression of Sirt1 in preadipocyte and mature adipocyte was analyzed by western blotting.

C. Autophagy flux was increased in matuture adipocytes than preadipocytes and. On day 12, the cells were incubated in the presence or absence of autophagy inhibitor BL (bafilomycin A1 at 0.1 μM and leupeptin at 10 μg/ml) for 4 hours, and the turnovers of LC3-II and p62 were examined by western blotting.

Figure 2 Resveratrol (RSV) suppressed autophagy flux and adipogenesis in a dose-dependent manner

A. In 3T3L1 cells, 10 μM, 25 μM and 50 μM RSV gradually reduced autophagy flux activity. On day 12, the cells were incubated in the presence or absence of autophagy inhibitor BL (bafilomycin A1 at 0.1 μM and leupeptin at 10 μg/ml) for 4 hours, and the turnovers of LC3-II and p62 were examined by western blotting.

B. In 3T3L1 cells, 10 μM, 25 μM and 50 μM RSV gradually reduced lipid droplets accumulation.

Figure 3 The effects of overexpression and downregulation of Sirt1 on autophagy flux activity and adipogenesis

A. Sirt1 overexpression suppressed autophagy flux activity. On day 12, the cells were incubated in the presence or absence of autophagy inhibitor BL (bafilomycin A1 at 0.1 μM and leupeptin at 10 μg/ml) for 4 hours, and the turnovers of LC3-II and p62 were examined by western blotting. The expressions of Sirt1, p62, LC3 were analyzed by western blotting.

B. Sirt1 knockdown promoted autophagy flux activity. On day 9, the cells were incubated in the presence or absence of autophagy inhibitor BL (bafilomycin A1 at 0.1 μM and leupeptin at 10 μg/ml) for 4 hours, and the turnovers of LC3-II and p62 were examined by western blotting. The expressions of Sirt1, p62, LC3 were analyzed by western blotting.

C. Sirt1 overexpression reduced lipid droplets accumulation; Sirt1 knockdown promoted lipid droplets accumulation.

Figure 4 Sirt1 promoted phosphorylation of mTOR and ULK1-757

A. Sirt1 overexpression increased pmTOR, pULK-757. The expressions of pmTOR, pULK1-757 were analyzed by western blotting.

B. Sirt1 knockdown decreased pmTOR, pULK-757. The expressions of pmTOR, pULK1-757 were analyzed by western blotting.

C. Sirt1 transgenic mice increased pmTOR, pULK-757 (WB) than wt. The expressions of Sirt1, pmTOR, pULK1-757, pp70S6, p4EBP1 were analyzed by western blotting.

Figure 5 ERα signaling positively regulated Sirt1

A. In 3T3L1 cells, E2 (0.1 μM) treatment increased Sirt1 expression. The protein expression of Sirt1 was analyzed by western blotting.

B. ERα knockout mice has lower Sirt1 expression in sWAT. The protein expressions of Sirt1, ERα were analyzed by western blotting.

Figure 6 Sirt1 acted as a downstream of ERα

A. E2 suppressed autophagy flux (p62, LC3), Sirt1 knockdown blunted this effect. On day 9, the cells were incubated in the presence or absence of autophagy inhibitor BL (bafilomycin A1 at 0.1 μM and leupeptin at 10 μg/ml) for 4 hours, and the turnovers of LC3-II were examined by western blotting. The expressions of Sirt1 and LC3 were analyzed by western blotting.

B. E2 promoted pmTOR, pULK-757, Sirt1 knockdown blunted this effect. The expressions of pmTOR, pULK-757 were blunted by Sirt1 knockdown.

C. E2 treatment reduced lipid droplets accumulation, Sirt1 knockdown and Estrogen co-treatment blunted estrogen's effects. Lipid droplets in E2 treatment was lower than Sirt1 knockdown and co-treatment.

Figures
Figure 1

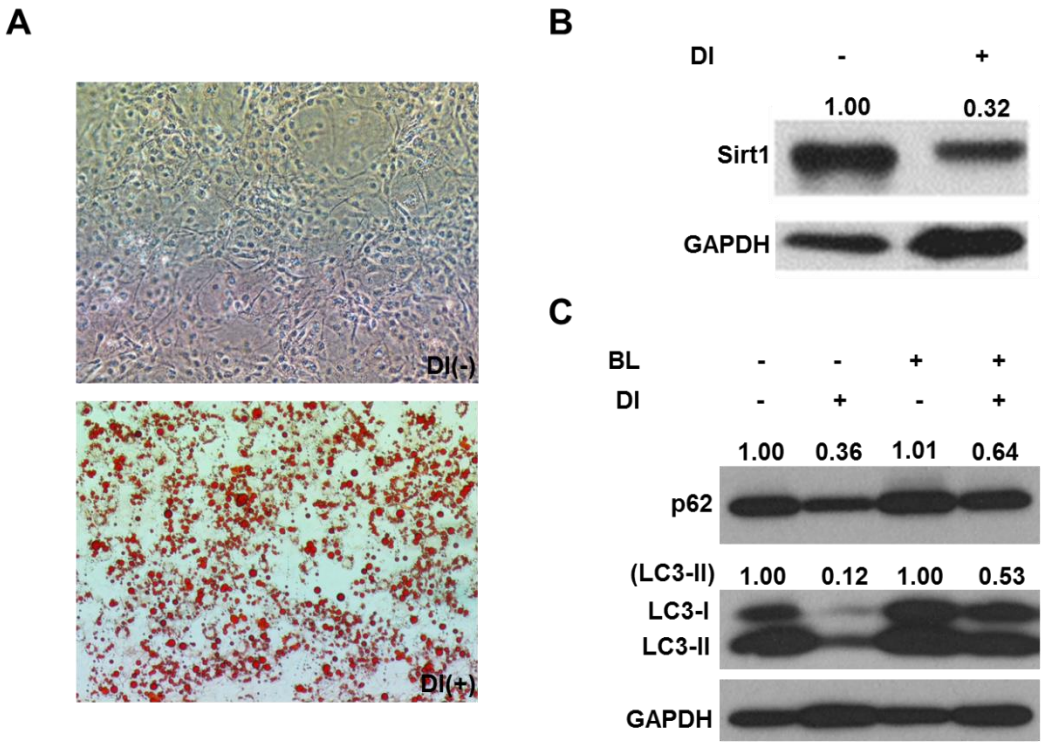

Figure 2

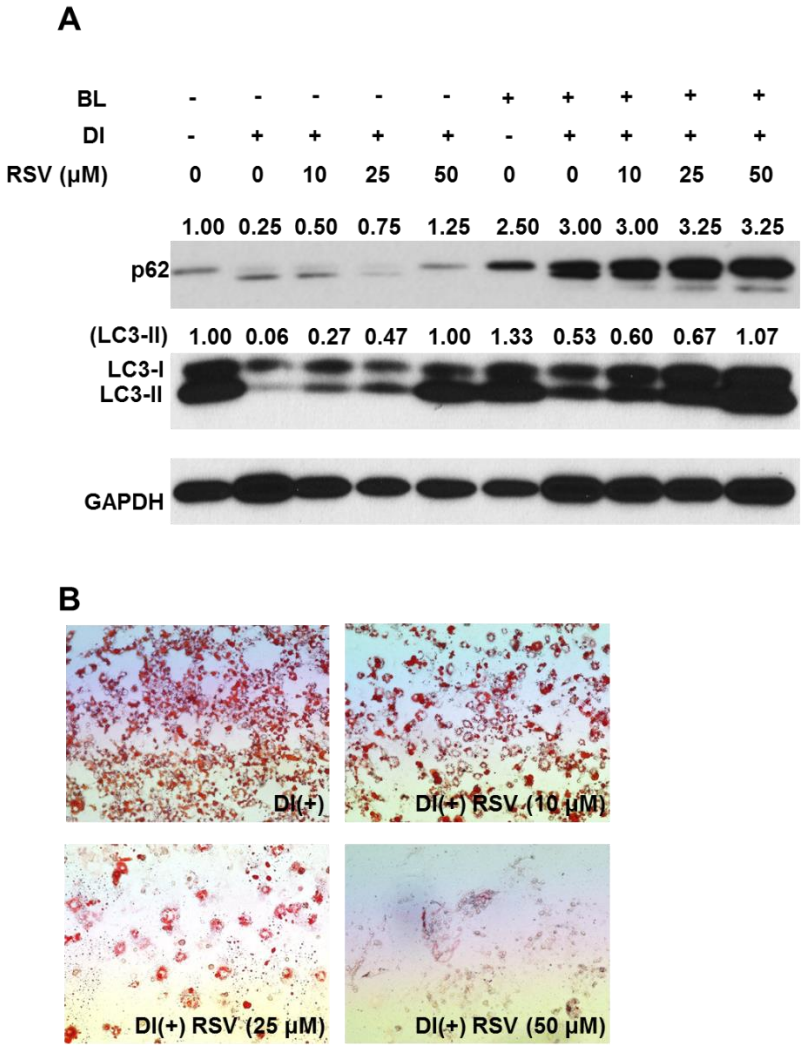
A
BL - - - - - + + + + +
DI - + + + + - + + + +
RSV (μM) 0 0 10 25 50 0 0 10 25 50
1.00 0.25 0.50 0.75 1.25 2.50 3.00 3.00 3.25 3.25
p62
(LC3-II) 1.00 0.06 0.27 0.47 1.00 1.33 0.53 0.60 0.67 1.07
LC3-I
LC3-II
GAPDH
B
DI(+)
DI(+) RSV (10 μM)
DI(+) RSV (25 μM)
DI(+) RSV (50 μM)

Figure 3

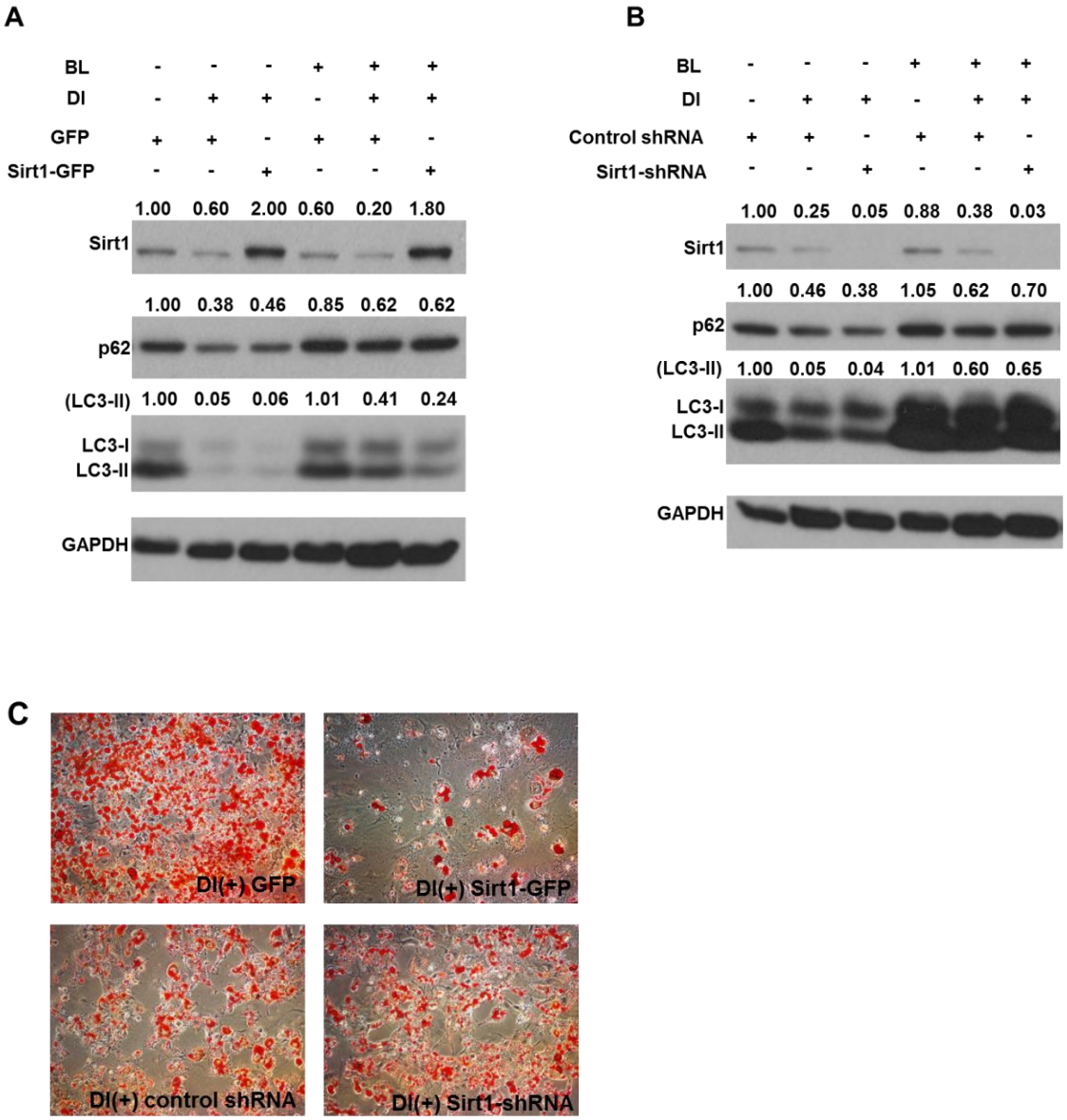
A
BL - - - + + +
DI - + + - + +
GFP + + - + + -
Sirt1-GFP - - + - - +
1.00 0.60 2.00 0.60 0.20 1.80
Sirt1
1.00 0.38 0.46 0.85 0.62 0.62
p62
(LC3-II) 1.00 0.05 0.06 1.01 0.41 0.24
LC3-I
LC3-II
GAPDH
B
BL - - - + + +
DI - + + - + +
Control shRNA + + - + + -
Sirt1-shRNA - - + - - +
1.00 0.25 0.05 0.88 0.38 0.03
Sirt1
1.00 0.46 0.38 1.05 0.62 0.70
p62
(LC3-II) 1.00 0.05 0.04 1.01 0.60 0.65
LC3-I
LC3-II
GAPDH
C
DI(+) GFP
DI(+) Sirt1-GFP
DI(+) control shRNA
DI(+) Sirt1-shRNA

Figure 4

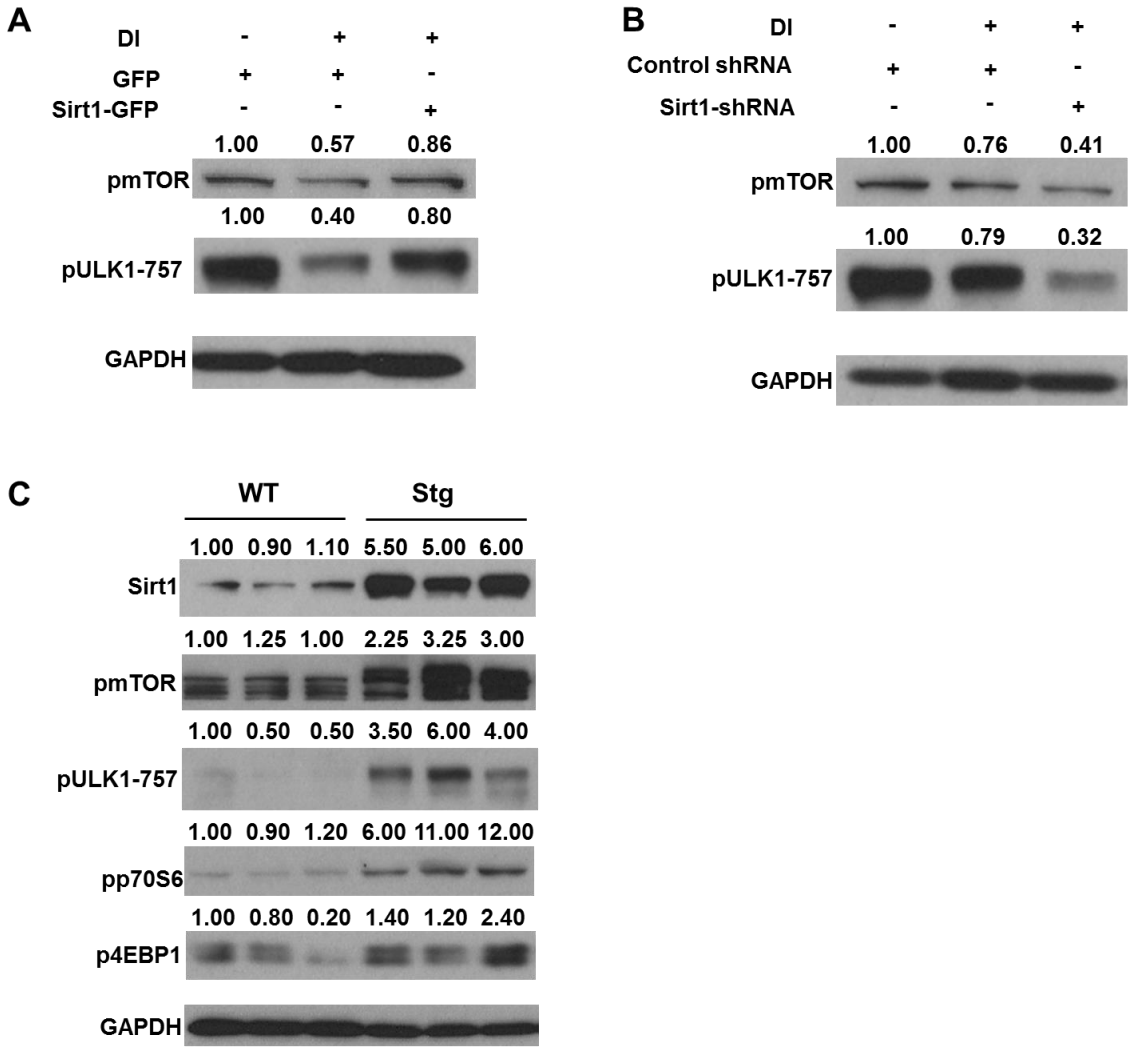
A
DI - + +
GFP + + -
Sirt1-GFP - - +
1.00 0.57 0.86
pmTOR
1.00 0.40 0.80
pULK1-757
GAPDH
B
DI - + +
Control shRNA + + -
Sirt1-shRNA - - +
1.00 0.76 0.41
pmTOR
1.00 0.79 0.32
pULK1-757
GAPDH
C
WT
Stg
1.00 0.90 1.10 5.50 5.00 6.00
Sirt1
1.00 1.25 1.00 2.25 3.25 3.00
pmTOR
1.00 0.50 0.50 3.50 6.00 4.00
pULK1-757
1.00 0.90 1.20 6.00 11.00 12.00
pp70S6
1.00 0.80 0.20 1.40 1.20 2.40
p4EBP1
GAPDH

Figure 5

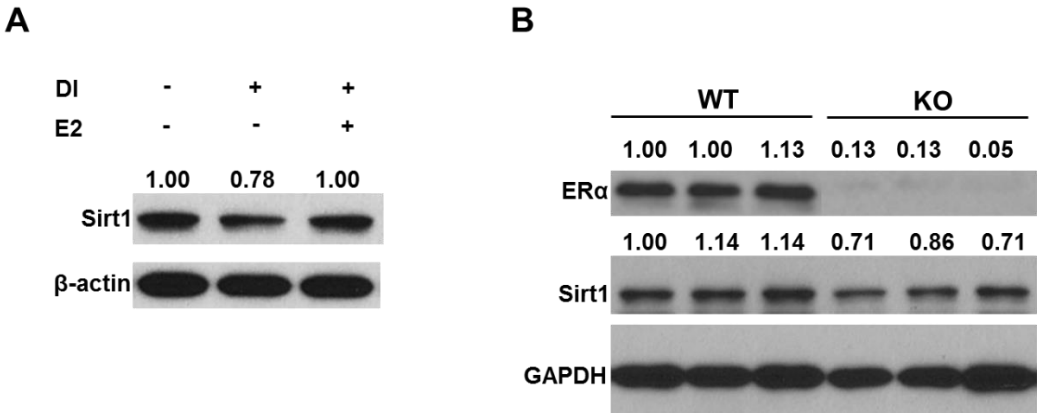
A
DI - + +
E2 - - +
1.00 0.78 1.00
Sirt1
β-actin
B
WT
KO
1.00 1.00 1.13 0.13 0.13 0.05
ERα
1.00 1.14 1.14 0.71 0.86 0.71
Sirt1
GAPDH

Figure 6

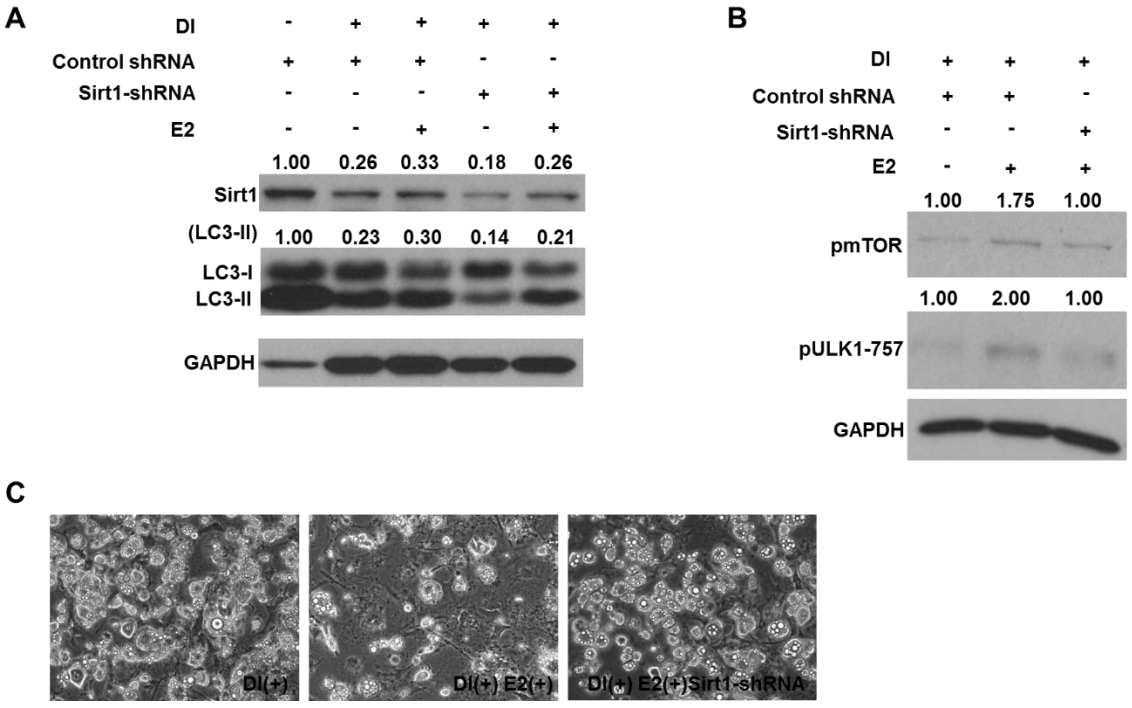
A
DI - + + + +
Control shRNA + + + - -
Sirt1-shRNA - - - + +
E2 - - + - +
1.00 0.26 0.33 0.18 0.26
Sirt1
(LC3-II) 1.00 0.23 0.30 0.14 0.21
LC3-I
LC3-II
GAPDH
B
DI + + +
Control shRNA + + -
Sirt1-shRNA - - +
E2 - + +
1.00 1.75 1.00
pmTOR
1.00 2.00 1.00
pULK1-757
GAPDH
C
DI(+)
DI(+) E2(+)
DI(+) E2(+)Sirt1-shRNA

Chapter 6 Conclusions and future direction

Conclusions

The fundamental findings in this project are summarized as follows:

(1) The protocol to monitor autophagy flux during adipocyte differentiation was developed. Autophagy is a highly dynamic machinery with multiple steps, simple steady-state assay cannot determine autophagy activity. This study provided a method to monitor autophagy flux (or substrate turnover) along with steady-state parameters of autophagy, which can better reflect autophagy activity (Tao, Liu, Zheng, & Cheng, 2017). Indeed, autophagy activity was increased after 3T3L1 cell and SVF cells differentiation compared with undifferentiated controls.

(2) In C57BL/6J and wild type control mice, a higher visceral fat mass was detected in the males than in the females, which was associated with lower expression of estrogen receptorα (ERα) and more active autophagy in males vs. females (Tao et al., 2018). However, deletion of ERα normalized autophagy activity and abolished the gender difference in visceral adiposity. Mechanistically, the estradiol-ERα signaling activated mTOR, which phosphorylated and inhibited ULK1, thereby suppressing autophagy and adipogenesis. This is the first time of elucidating the mechanism of gender difference in adiposity and discussing how E2 suppresses autophagy to prevent adiposity. In the future, the role of autophagy should be taken into consideration when discussing E2 signaling in metabolism. Also, this study may provide theoretical reference regarding how E2-autophagy axis working in other metabolic syndrome and diseases.

(3) Sirt1 expression was suppressed during adipogenesis along with autophagy elevation. Overexpression Sirt1 during adipogenesis suppressed autophagy and adipogenesis.

However, Sirt1 knockdown showed opposite effects, promotion of autophagy and adipogenesis. In line with inhibition of autophagy and adipogenesis in 3T3L1 cells by Sirt1, overexpression of Sirt1 in mouse reduced adiposity in adipose tissue, along with suppression of autophagy. Mechanistically, Sirt1 suppressed autophagy through promotion of mTOR-ULK1 cascade. This study explains the reason why Sirt1 overexpression mice has low level of adiposity and improved metabolism. It adds to new knowledge of how Sirt1 regulating autophagy and may shed light on how nutrient signaling regulating autophagy in other metabolic diseases.

(4) Sirt1 knockdown during 3T3L1 cell differentiation blunted the effect of E2 on autophagy and adipogenesis. Estrogen antagonist promoted autophagy and adipogenesis during 3T3L1 cell differentiation. However, Sirt1 overexpression reversed the effects of estrogen antagonist. Also, in ERα knockout mouse, Sirt1 expression was coinstantaneously reduced. Taken all these results together, ERα may promote Sirt1 expression to suppress autophagy through mTOR-ULK1 cascade, and then to prevent adipogenesis and adiposity.

Future directions

(1) To explore how ERα regulates upstream of mTOR-ULK1-autophagy cascades in adipocyte, potentially through p85 or Rheb (Figure 1). Previous study proposed the interaction of ERα with p85 to activate PI3K-Akt-mTOR signaling (Mannella & Brinton, 2006). In breast cancer cells it was shown that E2 might activate mTOR via small GTPase Ras homologue enriched in brain (Rheb) (Yu & Henske, 2006).

(2) To explore how Sirt1 regulates mTOR-ULK1-autophagy cascades in adipocyte, potentially through FoxO1-Sestrin (SESN) proteins signaling pathway (Figure 1).

(3) To examine how ERα transcriptionally regulates Sirt1 gene expression in adipocyte. In breast cancer MCF7 cells, ERα directly binds to the promoter for Sirt1 and increased its transcription (Elangovan et al., 2011).

(4) To test if reconstruction of Sirt1 in ERα knockout mice will prevent the mice from diet induced obesity.

Reference

Elangovan, S., Ramachandran, S., Venkatesan, N., Ananth, S., Prakasam, J. P. G., Martin, P. M., . . . Ganapathy, V. (2011). SIRT1 is essential for oncogenic signaling by estrogen/estrogen receptor α in breast cancer. *Cancer Research, 17(21); 6654–64.*

Mannella, P., & Brinton, R. D. (2006). Estrogen receptor protein interaction with phosphatidylinositol 3-kinase leads to activation of phosphorylated Akt and extracellular signal-regulated kinase 1/2 in the same population of cortical neurons: a unified mechanism of estrogen action. *Journal of Neuroscience, 26*(37), 9439-9447.

Tao, Z., Liu, L., Zheng, L. D., & Cheng, Z. (2019). Autophagy in adipocyte differentiation. *Methods in Molecular Biology, 1854*:45-53.

Tao, Z., Zheng, L. D., Smith, C., Luo, J., Robinson, A., Almeida, F. A., . . . Cheng, Z. (2018). Estradiol signaling mediates gender difference in visceral adiposity via autophagy. *Cell Death & Disease, 9*(3), 309.

Yu, J., & Henske, E. P. (2006). Estrogen-induced activation of mammalian target of rapamycin is mediated via tuberin and the small GTPase Ras homologue enriched in brain. *Cancer Research, 66*(19), 9461-9466.

Figure Legend

Figure 1 Flow chart of future directions. ①, ERα interacts with p85 to activate PI3K-Akt, then activates mTOR-ULK1 signaling; ②, ERα promotes Rheb to activate mTOR-ULK1 signaling; ③ ERα transcriptionally activates Sirt1 gene expression, and then Sirt1 inhibits FoxO1 activity and SESNs gene expression, and then promotes mTOR-ULK1 signaling.

Figure 1

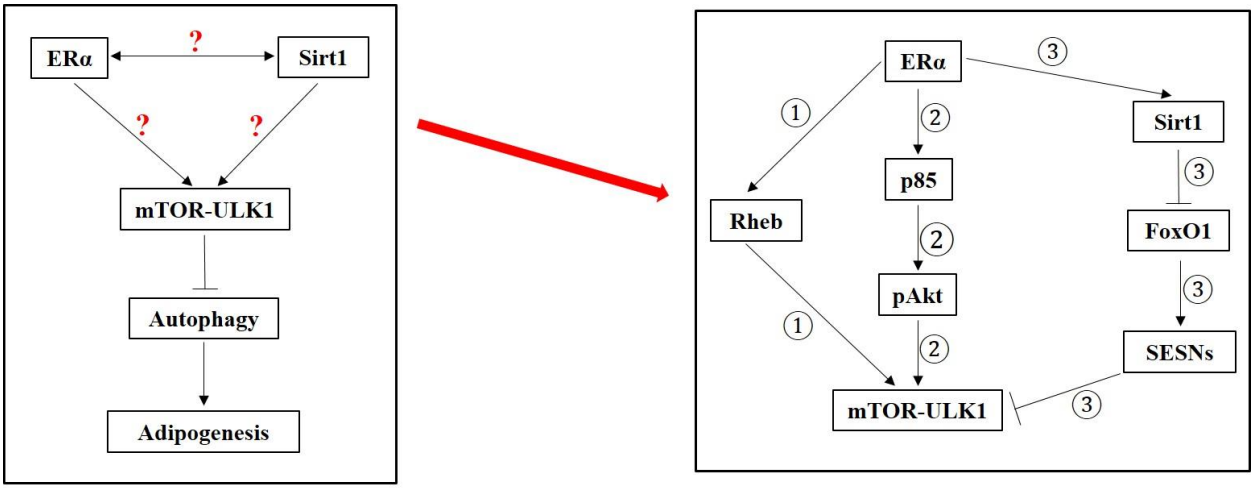

Conclusions **Future Directions**